

MASTER THESIS

PHYSIK-DEPARTMENT E62 - DENSE AND STRANGE
HADRONIC MATTER

Analyses of Anisotropic Flow with Symmetric Cumulants in ALICE at the Large Hadron Collider

Author:

Deniz KARAKOÇ

Supervisors:

Prof. Laura FABBIETTI

Dr. Ante BILANDZIC

June 12, 2017



Abstract

Ultra relativistic heavy-ion collisions at Large Hadron Collider (LHC) create strongly interacting particles. As a result of these strong interactions and initial anisotropic geometry anisotropic flow phenomena takes place: Outgoing particles are correlated with reaction plane. Analysis of the flow phenomena depends on so-called flow harmonics v_n . In this thesis two and multi-particle correlations techniques have been utilized to determine the harmonics. Since these techniques are sensitive to non-flow, we have used a precise method Q-Cumulant to suppress it. Q-Cumulant is biased even if the absence of non-flow due to flow fluctuations which are cable of creating any type of harmonics. Recently symmetric cumulants $SC(m,n)$ have been introduce to investigate the correlation between two different harmonics (v_m, v_n) , in this thesis Monte Carlo simulations of $SC(4,2)$ and $SC(3,2)$ have been presented and they were also calculated from data collected by ALICE detector in 2010 from Pb–Pb collisions at center-of-mass energy $\sqrt{s_{NN}} = 2.76 \text{ TeV}$. Finally, we generalized the symmetric cumulants to three harmonics $SC(1,2,3)$ and examined the generalization in terms of constant, independent, two and three correlated harmonics.

Contents

1	Introduction	1
1.1	Quantum Chromodynamics	1
1.2	Quark Gluon Plasma	3
1.3	Centrality Determination	5
1.4	Experimental Setup	7
2	Flow Analyses	11
2.1	Anisotropic Flow Phenomena	11
2.2	Flow Harmonics	12
2.3	Two-Particle Azimuthal Correlations Technique	15
2.3.1	Results	18
2.4	Multi-Particle Azimuthal Correlations Technique	19
2.5	Q-vector	22
2.5.1	Q-vector and Two-Particle Correlations	22
2.5.2	Q-vector and Multi-Particle Correlations	25
2.6	Q-Cumulants	30
2.6.1	Data Selection and Results	34
3	Flow Fluctuations	39
3.1	Symmetric Cumulants	39
3.1.1	Monte Carlo Simulations	41
3.1.2	Results	42
3.2	Generalized Symmetric Cumulants	44
3.2.1	Introduction	44
3.2.2	$SC(k, l, m)$	46
3.2.3	Toy Monte Carlo Studies for $SC(k, l, m)$	47
	Appendices	57
A	Four Particle Average Decomposition	59
B	Flow Fluctuation	61

C	Statistical Errors	63
D	Distributions	67
D.1	Distribution of Azimuthal Angle	67
D.2	Distribution of Multiplicity	68
E	Code Snippets	71
E.0.1	Fig. (2.9)	71
E.0.2	Fig. (3.7)	75
E.0.3	Fig. (3.11)	83

Chapter 1

Introduction

1.1 Quantum Chromodynamics

We may claim that every human being, at least once in his or her life, wonders about the edge or size of the Universe and the smallest part of the matter which can not be divided any more. The answer to the latter might be found in particle physics which is probing into fundamental constituents of matter and the interactions among them. It is very well known that atoms are composed of electrons orbiting around a nucleus consisting of neutrons and protons. Independently in '60s, it has been proposed by Zweig and Gell-Mann that protons, neutrons and all other hadrons are composed of some elementary particles which are called quark: [1]. There are six flavors of quarks up(u), down(d), strange(s), charm(c), top(t), and bottom(b). With their intrinsic properties (charge, mass and spin), they are depicted in standard model as in Fig. (1.1). For each quark, there is a corresponding antiquark with the same mass and different sign of charges. All mesons are composed of a quark and an antiquark, all baryons are composed of three quarks. Antiparticles of hadrons have constituents which own corresponding antiparticle and vice versa. Quark model in this state violates Pauli exclusion principle: two fermions can not occupy the same quantum state. Since quarks carry spin one-half, exclusion principle applies to quarks as well. At this stage it has been suggested that each quark has an additional intrinsic property: redness, greenness or blueness. When a quark owns a type of color, its antiquark carries one unit of corresponding anti-color. In this regard, there are two possibilities: either hadrons' total amount of color is zero or they possess the same amount of the colors. For instance a meson has a quark and an antiquark, let's suppose one is red the other one has to be minus/anti red; a baryon owns three quarks, all have to possess a different color and it is the same for antibaryon which has to be composed of three different and minus/anti colors. It means natural particles

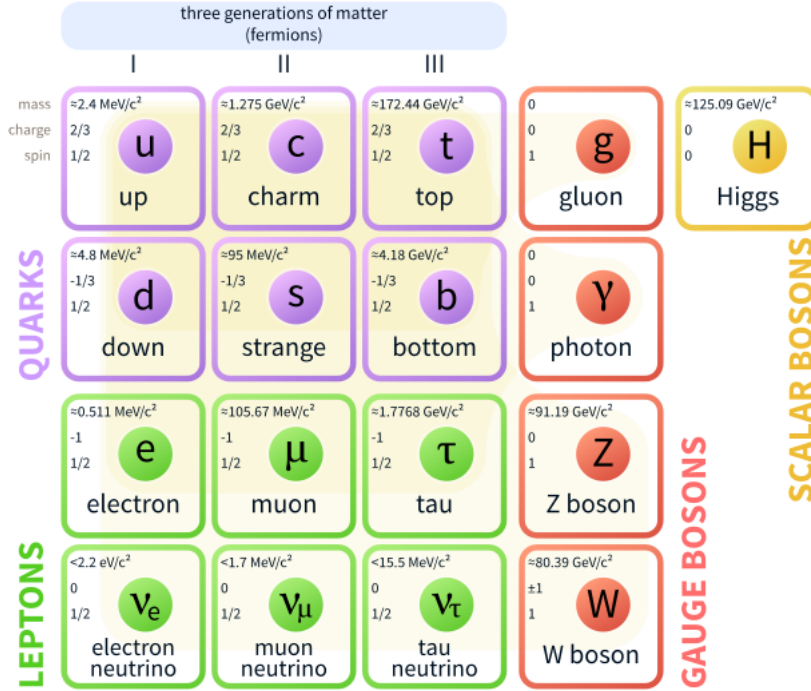


Figure 1.1: Standard model of elementary particles (Fermilab, Office of Science, United States Department of Energy).

are colorless which is corresponding to both situations which has been described and like charge, color is conserved. This phenomena is called as color confinement which explain why an isolated quark can not be observed. According to the quantum chromodynamics (QCD) strong force, which is responsible for binding quarks and keeping nucleons inside the nucleus against repulsive electromagnetic force, is mediated by gluons. Fundamental process of strong interaction is $q \rightarrow q + g$, a quark emits or absorbs a gluon. In this process color of quark might be changed, according to the color conservation incoming quark's color is equal to the total color of outgoing particles. For instance incoming quark is red and outgoing is blue, it means gluon carry red and anti blue. It is clear from this example that gluons are bicolored. Since gluons also carry color, unlike photon which is neutral, they are also subject to strong interactions as well as being mediators, this situation makes the strong interactions harder to analyze.

According to QCD, similar to color confinement, strong interaction prevents to observe an isolated quark. Potential for strong force, which is dominated by linear term at large distance, is given by

$$V(r) = -\frac{4}{3} \frac{\alpha_s}{r} + \kappa r. \quad (1.1.0.1)$$

In above equation r is the distance among a quark and an antiquark, κ the

string tension and α_s the coupling strength. Linear term in the equation shows that when distance is increased among the particles, as a result attractive force becomes stronger. As it is simply depicted in Fig. (1.2), when we exert energy to pull apart one of the quark from a hadron, at some point a quark and an antiquark pair are created from the vacuum because it is energetically favorable. At the end, the process results in two new hadrons. Whenever we try to pull

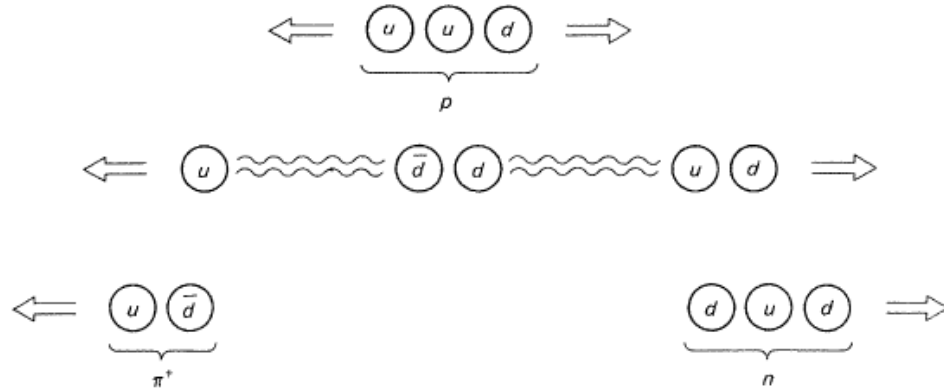


Figure 1.2: As energy is exerted to separate the quark u from proton, a quark pair (d, \bar{d}) is created. Instead of having an isolated quark we have a neutron and pion at the end [2].

away one of the quarks the same process takes place and each time we have new hadrons in which quarks are confined.

1.2 Quark Gluon Plasma

According to QCD, asymptotic freedom implies that unlike in quantum electrodynamics (QED), coupling constant is not constant but depends on distance between two interacting particles. At short distance, coupling is asymptotically weaker meaning in this case quarks within a hadron do not interact strongly. This implies that at short distance (equivalently at high energy) interaction among quarks is weak and they are nearly free. So in this regime quarks behave like free particles. Based on asymptotic freedom, it is expected that at extremely high temperature and/or densities quarks and gluons are in a different phase which is called quark-gluon plasma (QGP). In this phase quarks and gluons are deconfined.

One way of creating QGP is by increasing hadron density to a critical point which is around $0.16 \text{ GeV}/\text{fm}^3$, ten times the matter density in nuclei. We see a representation of this process in Fig. (1.3). Another way of forming QGP is reaching the critical temperature which is around 175 MeV , 100000 times higher than center of Sun temperature. In Fig. (1.4), we show both of these situations on

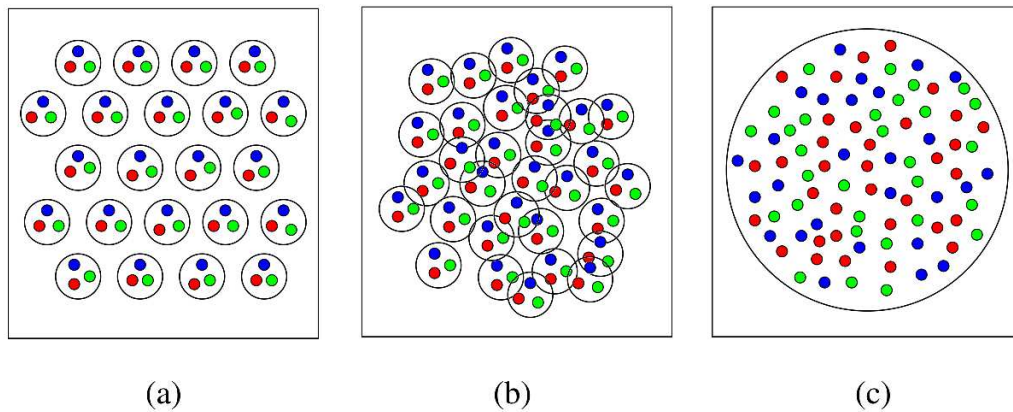


Figure 1.3: Formation of quark-gluon plasma with increment of hadron density [3].

phase-diagram expected in QCD. Vertical axis is temperature and horizontal axis is net quark density implying the difference between quarks and antiquarks. Arrow of expansion of the early Universe is showing that the Universe just after the Big Bang was in phase of quark-gluon plasma with extremely high temperature. In a short period, temperature drops sharply because of rapid expansion of the early Universe; as a result matter passes into hadronic phase where quarks and gluons are confined in baryons. Heavy ion collisions are following the opposite direction of the early Universe. We collide nucleons in which quarks and gluons are confined at high energy. If thermalization occurs at temperature which exceeds the critical point, deconfinement of partons (quarks and gluons) takes place. At this stage partons form the quark-gluon plasma for a short time; because of the fast expansion, plasma cools down rapidly and partons undergo hadronization. As we see in Fig. (1.4), in both of them; expansion of early Universe and heavy ion collisions, net baryon density do not play an important role. When early Universe was very hot, the difference among quarks and antiquarks was small. In case of heavy ion collisions, although before the collision we have a few hundreds of nucleons, this value is still small compared to the number of hadrons obtained at the end of final state [4]. QGP may exist in the core of neutron stars as it is depicted on the figure.

In Fig. (1.5), we see representation of two colliding nuclei. Vertical axis is proper time and horizontal axis is beam line. At first stage, nuclei undergo Lorentz contraction along the beam line and collide at $t = 0$ and $z = 0$. Just after the collision, a bulk quark-gluon is released which is in non-equilibrium state and has ten times higher density compared to hadrons in Pb–Pb collisions at the LHC. In later stage, if there were no interactions among partons, they would separately evolve to hadronization. But at LHC with collision of Pb–Pb, we observe the

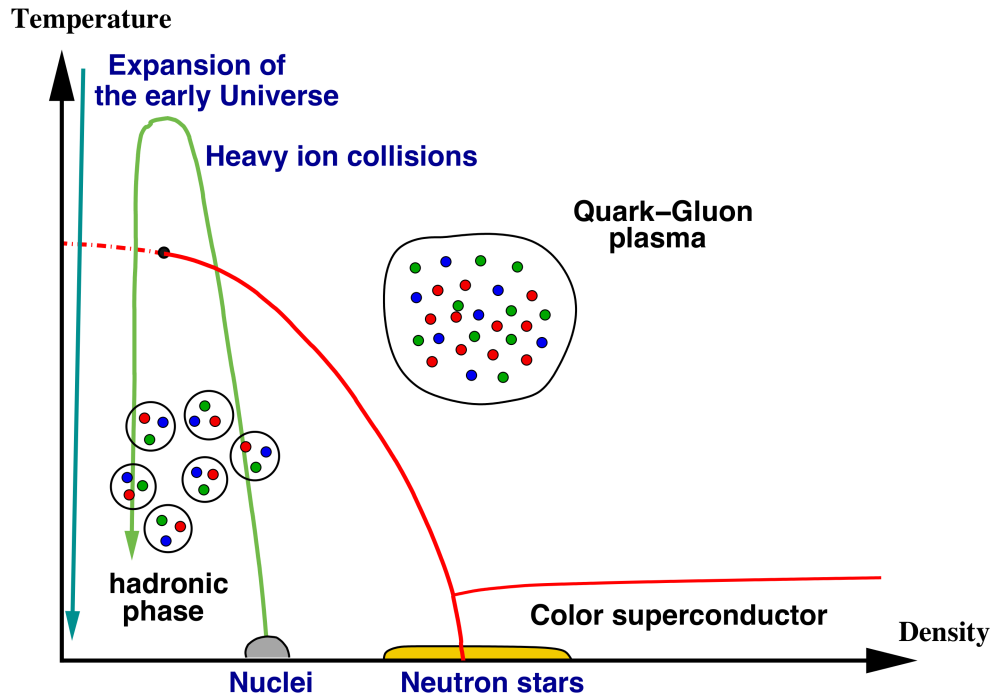


Figure 1.4: Schematic representation of the phase diagram [4].

opposite, collective flow: At this stage partons interact with each other, quite strongly. As a result of this strong interaction the partonic matter quickly reaches the thermal equilibrium. As a consequence of this thermalization, process ends up in quark-gluon plasma. With expansion of the plasma, temperature starts decreasing and partons start creating colorless hadrons after temperature drops to the critical point. At the next stage which is shown as hadrons in Fig. (1.5), we have still high density and local equilibrium. In the last stage hadrons have low density and they are no longer interacting. As a result, expansion rate becomes higher than collision rate. The transition between many interactions to the free particles is called freeze-out, at this stage particles without any interaction move towards detector.

1.3 Centrality Determination

Collective flow is sensitive to the initial geometry, that is why it is crucial to sort out all collisions in terms of initial geometries, which can be achieved with the centrality. In Fig. (1.6), there are three different collision geometries of the same type of nuclei which are depicted on transverse plane. Impact parameter b on the figures connects the centers of the nuclei, it may have value between zero and diameter of the nucleus. In Fig. (1.6A) a central collision which is

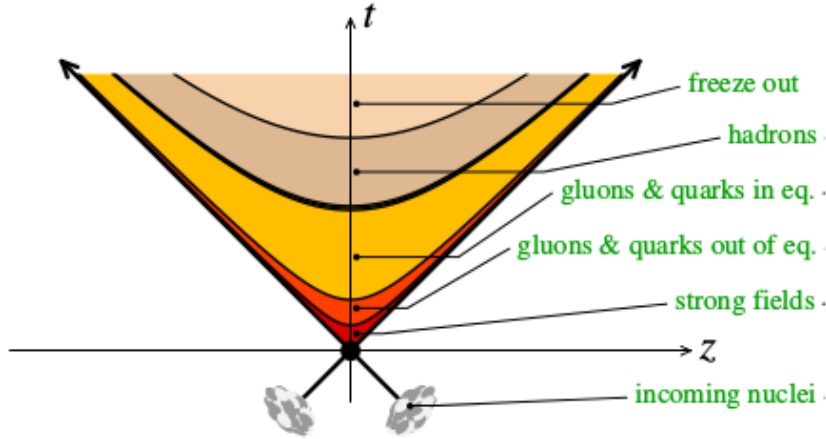


Figure 1.5: Space-time picture of heavy-ion collision for various stages [4].

represented with impact parameter nearly zero corresponds roughly to centrality class 0 – 5% and in Fig. (1.6C) a peripheral collision, which is corresponding roughly to centrality class 70 – 80%, is represented with impact parameter around diameter of the nucleus. In Fig. (1.6B), we see a representation of mid-central collision corresponding roughly to centrality class 30 – 40%, impact parameter is among the values for central and peripheral collisions. The azimuthal angle of the impact parameter in a heavy ion collision is random, any value is equally probable.

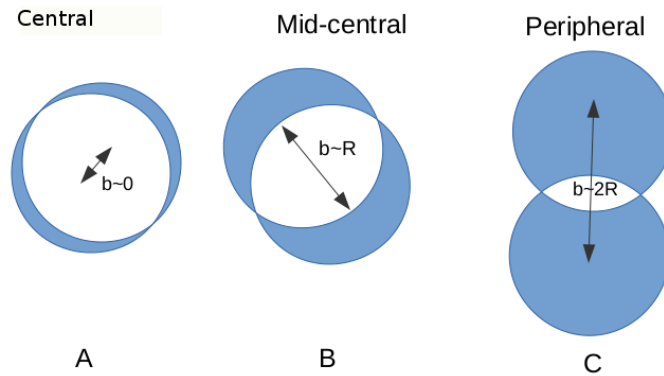


Figure 1.6: Representations of central, mid-central and peripheral collisions.

The impact parameter and the collision geometry can not be controlled by experiment and they are not recorded by detectors directly. But there is a relation between multiplicity, transverse energy, number of spectator nucleons which do not participate in the collisions and the centrality. Easily we may assume there is positive correlation between number of participating nucleons and released energy, also among the multiplicity and participating nucleons. So we can conclude

that energy released in the collision and multiplicity have a positive correlation. Central collisions result in higher values of multiplicity or transverse energy and contrarily peripheral collisions yield lower values of multiplicity and release less energy. That is why multiplicity or transverse energy distribution might be exploited to determine centrality. More precisely, Glauber-type Monte Carlo calculations, which depends on idea we just mentioned and utilize the Woods–Saxon nuclear density distributions, is used to define centralities [5].

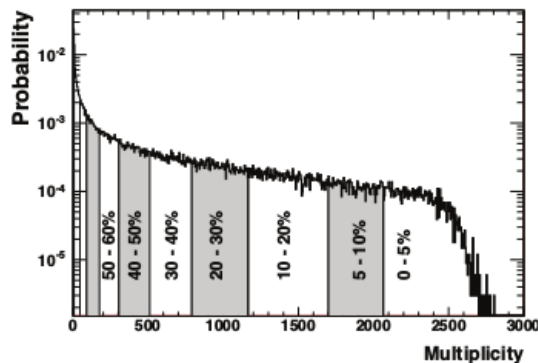


Figure 1.7: The uncorrected multiplicity distribution of charged particles in the TPC [6].

In Fig. (1.7), published by ALICE Collaboration [6], we see multiplicity distribution of charged particles in the time projection chamber (TPC) with $45K$ collisions. As it can be seen from the figure, more central collisions correspond to higher multiplicities and vice versa [7].

1.4 Experimental Setup

The Large Hadron Collider (LHC) is located at France–Switzerland border near Geneva, Switzerland and built by the European Organization for Nuclear Research (CERN). LHC’s tunnel which is buried on average $100m$ underground has 27 kilometers circumference. To be able to reach out aimed center of mass energy, which is $7 TeV$ per beam for $p - p$ collisions and $2.76 TeV$ per nucleon pair for Pb–Pb collisions, particles are accelerated very close to the speed of light.

LHC hosts seven experiments. A Toroidal LHC ApparatuS (ATLAS) is the largest detector ever built. Mainly it is probing into physics beyond the standard model and search for Higgs boson, in 2012 ATLAS collaboration has announced that a new particle consistent with Higgs boson was discovered [8]. The Compact Muon Solenoid (CMS) has similar aims as ATLAS with different technical design, discovery of Higgs boson was reported by CMS as well [9]. Both ATLAS and CMS play also an important role in the heavy-ion program. The Large Hadron

Collider beauty (LHCb) experiment is working on asymmetry between matter and antimatter in the Universe. The Large Hadron Collider forward (LHCf) experiment has a primary aim to test models used to estimate the primary energy of the ultra high-energy cosmic ray. The TOTAl Elastic and diffractive cross section Measurement (TOTEM) experiment has goal to measure the cross section of proton. Monopole and Exotics Detector at the LHC (MoEDAL) is making research on hypothetical highly ionising particles. And finally A Large Ion Collider Experiment (ALICE) which is the only dedicated heavy-ion experiment at LHC.

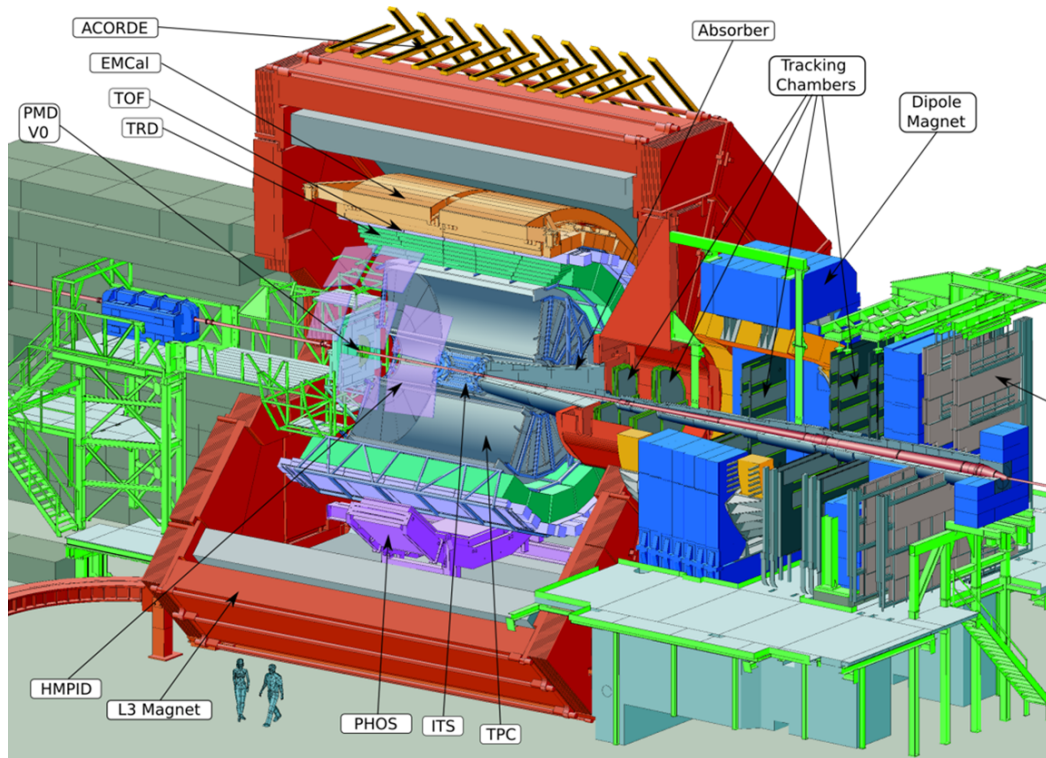


Figure 1.8: ALICE detector.

ALICE is specialized on analyzing Pb–Pb collisions at a center of mass energy of 2.76 TeV per nucleon pair in Run 1 and 5.02 TeV per nucleon pair in Run 2 to be able to understand properties of quark-gluon plasma which has been described in previous sections. As shown in Fig. (1.8), the ALICE detector owns 18 operational subdetectors, some of them are the Inner Tracking System, the cylindrical Time Projection Chamber, the Time-of-Flight, High Momentum Particle Identification Detector, the Transition Radiation detectors, the electromagnetic calorimeters which are the PHOS and the EMCal, forward muon spectrometer that examines heavy quarkonium states which are sensitive to quark-gluon plasma formation, also several smaller detectors (ACORDE, ZDC, PMD, FMD, T0, V0). For the purpose of this research four of them will be examined here.

Time Projection Chamber (TPC) is the main tracking detector, a cylinder

filled with gas, utilizing electric and magnetic field with ionized gas to determine trajectories of the particles. Gas is ionized with charged particles traversing the TPC, by releasing electrons drifting towards the end plates of the cylinder. Analysis of the process gives information about z , r and φ coordinates. The transverse momentum range $0.1 < p_T < 100 \text{ GeV}/c$ can be detected by TPC with a resolution of about 6% for $p_T < 20 \text{ GeV}/c$ in central Pb–Pb collisions. TPC azimuthal acceptance is full with exception of dead zones corresponding to about 10%. That is why TPC is an ideal detector for our analysis which is requiring full azimuthal acceptance. TPC's azimuthal resolution is about $\delta\varphi = 0.7 \text{ mrad}$ and has a pseudorapidity coverage of $\eta < |0.9|$. TPC also serves for particle identification and centrality determination with a resolution of about 0.5% in the most central collisions [7] [10].

The ALICE Inner Tracking System is located inside the inner TPC radius and it is the closest detector to beam line. With a resolution better than $100 \mu\text{m}$, it is used to determine the primary vertex. It serves as tracker to recover tracks which are not reconstructed by TPC (because of dead zones of TPC) and reconstruct low momentum particles. Also it provides particle identification and it is used as a centrality estimator with resolution 0.5% in the most central collisions. Transverse momentum is covered in the range $0.1 - 3 \text{ GeV}/c$ and pseudorapidity in $\eta < |0.9|$ [7] [10].

The VZERO detector is located inside of the main magnet and it consists of two arrays of scintillator counters VZERO-A and VZERO-C; each has different pseudorapidity ranges $2.8 < \eta < 5.1$ and $-3.7 < \eta < -1.7$, respectively. Both provide minimum bias triggers for Pb–Pb collisions and are used for centrality determination which has resolution of about 0.5% for central and 2% for peripheral collisions. The VZERO detector is capable of providing beam luminosity and the charged particle multiplicity measurement [7] [10].

Finally, the Zero Degree Calorimeter (ZDC) detects spectator protons and neutrons separately (since spectator protons are deflected slightly from the beam line) to be able to determine the centrality and it has resolution of about 1% in central collisions and around 3% in mid-central collisions [7]. Thus, mainly it is utilized to determine the centrality.

Chapter 2

Flow Analyses

2.1 Anisotropic Flow Phenomena

In Fig. (2.1), a non-central nucleus-nucleus collision is depicted in transverse plane. Blue circles represent the spectator nucleons which do not participate in collision. Red circles represent the nucleons which undergo at least one collision and which are called participants. The impact parameter b connects the centers of the nuclei. Reaction plane is spanned by vector b and beam line z . That is why projection of reaction plane corresponds to b line on transverse plane which is denoted by dashed line on the figure. Reaction plane angle is denoted by ψ_R in fixed lab frame. In this figure overlapping region has an almond shape and it is characterized to leading order by second harmonic as we will see in the next section.

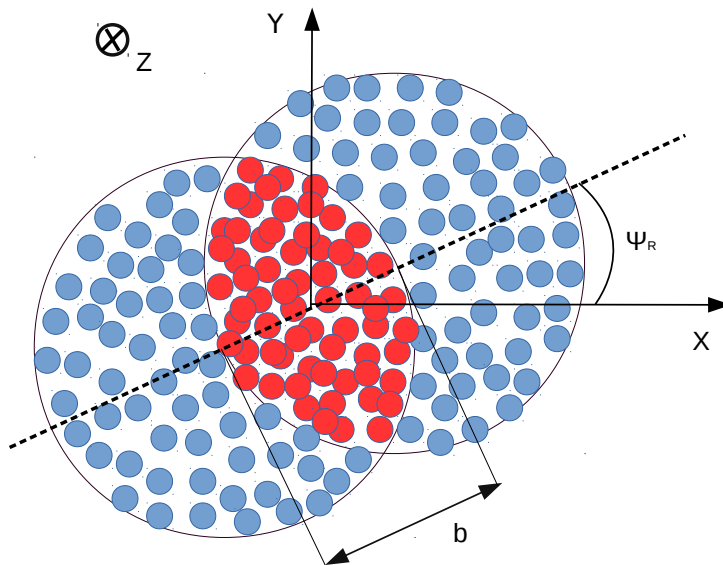


Figure 2.1: A non-central nucleus-nucleus collision on transverse plane.

If there are no mutual collisions among the outgoing particles, they separately evolve without reaching the thermalisation. On the other hand, at sufficiently high energies anisotropic collisions will create strong interactions among outgoing particles. Because of these mutual interactions, higher pressure gradient will be created along the minor axis of almond shape compared to the major axis. That is why this process results in more particles emitted along the reaction plane. In this way anisotropy of the initial geometry has been converted into anisotropic distribution of outgoing particles. At the end of the day we have a periodic function of azimuthal distribution. This process is shown in Fig. (2.2), yellow arrows are pressure gradients, black arrow represent outgoing particles which are populated more along the reaction plane.

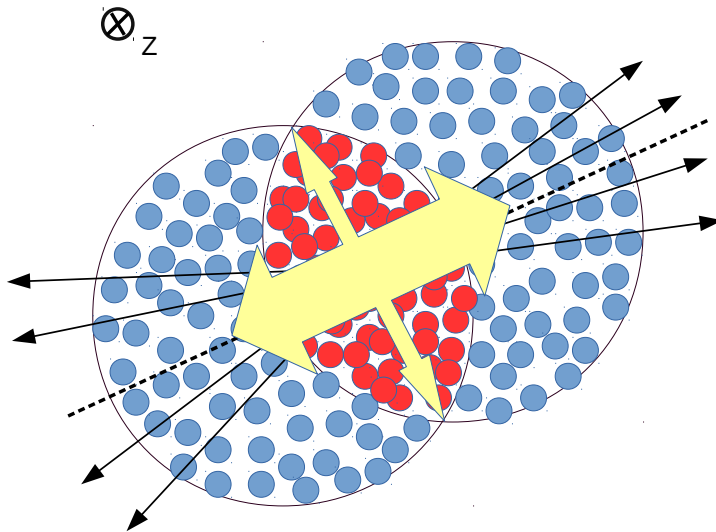


Figure 2.2: Pressure gradient and more particles emitted along minor axis of almond.

2.2 Flow Harmonics

Random observable φ is described on the transverse plane which is vertical to beam line and it is the azimuthal angle of quantity under probe, for instance it might be the total momentum of outgoing particles at the angle φ . It is clear that sample space of φ is $[0, 2\pi)$. Probability density function p.d.f of the quantity will be denoted as f . Since it is a periodic function, it can be decomposed into Fourier series as [11]:

$$f(\varphi) = \frac{1}{2\pi} \left[1 + 2 \sum_{n=1}^{\infty} (c_n \cos n\varphi + s_n \sin \varphi) \right]. \quad (2.2.0.1)$$

In Eq. (2.2.0.1) c_n and s_n are called as Fourier coefficients and c_0 was assigned to 1 to be able to normalize the probability density function, hence we can write the next equation,

$$\int_0^{2\pi} f(\varphi) d\varphi = 1. \quad (2.2.0.2)$$

We need to find out the Fourier coefficients c_n and s_n in Eq. (2.2.0.1), for this purpose the orthogonality relations of trigonometric functions which are expressed as below can be exploited.

$$\int_0^{2\pi} \sin(mx + \alpha) \sin(nx + \beta) dx = \pi \cos(\alpha - \beta) \delta_{mn}, \quad (2.2.0.3)$$

$$\int_0^{2\pi} \cos(mx + \alpha) \cos(nx + \beta) dx = \pi \cos(\alpha - \beta) \delta_{mn}, \quad (2.2.0.4)$$

$$\int_0^{2\pi} \sin(mx + \alpha) \cos(nx + \beta) dx = \pi \sin(\alpha - \beta) \delta_{mn} \quad (2.2.0.5)$$

where δ_{mn} is the Kronecker delta symbol, n and m are nonzero integers, while α and β are arbitrary numbers. By using orthogonality relations the Fourier coefficients are constructed as below:

$$\int_0^{2\pi} f(\varphi) \cos(n\varphi) dx = c_n, \quad (2.2.0.6)$$

$$\int_0^{2\pi} f(\varphi) \sin(n\varphi) dx = s_n. \quad (2.2.0.7)$$

In Eq. (2.2.0.1) p.d.f was decomposed into Fourier series, but equivalently we can also write the function in this form:

$$f(\varphi) = \frac{1}{2\pi} \left[1 + 2 \sum_{n=1}^{\infty} v_n \cos[n(\varphi - \Psi_n)] \right], \quad (2.2.0.8)$$

where v_n are anisotropic flow harmonics and Ψ_n are corresponding symmetry planes. The relationships between the coefficients in Eq. (2.2.0.1) and Eq. (2.2.0.8) can be written as $v_n = \sqrt{c_n^2 + s_n^2}$ and $\Psi_n = \left(\frac{1}{n}\right) \arctan \frac{s_n}{c_n}$.

If we multiply both sides of equation (2.2.0.8) with $\cos[m(\varphi - \Psi_m)]$ where m is non-negative integer and take integral of the both sides over sample space, the

equation becomes:

$$\int_0^{2\pi} \cos[m(\varphi - \Psi_m)]f(\varphi)d\varphi = \frac{1}{2\pi} \int_0^{2\pi} \cos[m(\varphi - \Psi_m)]d\varphi + \frac{1}{\pi} \sum_{n=1}^{\infty} \int_0^{2\pi} v_n \cos[m(\varphi - \Psi_m)] \cos[n(\varphi - \Psi_n)]d\varphi. \quad (2.2.0.9)$$

As we clearly see in Eq. (2.2.0.9), $\int_0^{2\pi} \cos[m(\varphi - \Psi_m)]d\varphi$ is equal to $\frac{1}{m}(\sin(m2\pi - m\Psi_m) - \sin(-m\Psi_m))$. In case of m being positive integer, result is obviously zero¹. In order to evaluate the second term in the right-hand side of the equation, we use orthogonality relation described at Eq. (2.2.0.4) in which $\alpha = -\Psi_m$ and $\beta = -\Psi_n$. If m is equal to n , Kronecker delta is 1, otherwise it is zero. That is why only contribution to the summation comes from equality of m and n , the remaining terms do not contribute anything. So, the argument becomes $\frac{v_m}{\pi} \pi \cos(\Psi_m - \Psi_m)$ which is equal to v_m . Now we reached out the equation below (for the sake of generality we used index n instead of m):

$$\int_0^{2\pi} \cos[n(\varphi - \Psi_n)]f(\varphi)d\varphi = v_n. \quad (2.2.0.10)$$

For continuous random variable, the mean value is calculated as $\langle x \rangle = \int_0^{2\pi} xf(x)dx$ where $f(x)$ is probability density function. In case of mean value of a function (as an example $g(x)$), the equation turns into $\int_0^{2\pi} g(x)f(x)dx$. In this regard Eq. (2.2.0.10) is mean value of $\cos[n(\varphi - \Psi_n)]$ and can be expressed as below

$$v_n = \langle \cos[n(\varphi - \Psi_n)] \rangle. \quad (2.2.0.11)$$

The harmonic v_1 is called directed flow, the harmonic v_2 elliptic flow, the harmonic v_3 triangular flow, etc. So it is clear that to be able to determine the flow harmonics (v_n) and correspondingly to quantify anisotropic flow, we need to know independently the corresponding symmetry planes Ψ_n in each event. Problem of estimating the symmetry plane is that it fluctuates from event to event. Since neither symmetry planes are recorded by detectors nor we have a reliable technique to calculate the planes, it has become the main issue in the flow analysis to estimate the amplitudes of flow harmonics v_n without knowing the symmetry planes Ψ_n . This can be achieved by utilizing two- and multi-particle

¹Where m is zero the first argument in right-hand side of the equation $\frac{1}{2\pi} \int_0^{2\pi} \cos[m(\varphi - \Psi_m)]d\varphi$ turns into $\frac{1}{2\pi} \int_0^{2\pi} d\varphi$ which is equal to 1. Left hand-side of the equation becomes $\int_0^{2\pi} f(\varphi)d\varphi$. As a result of orthogonality relation the second argument in right-hand side of the equation is zero since of inequality of $m = 0$ and $n > 0$. So in case of $m = 0$ the equation becomes $\int_0^{2\pi} f(\varphi)d\varphi = 1$ which is the normalization equation. This is what we expect, because we assigned the value of v_0 to 1 to be able to normalize the probability density function.

correlation techniques which will be explained at the following chapters.

2.3 Two-Particle Azimuthal Correlations Technique

First we will define the all-events average two-particle azimuthal correlation in the following way:

$$\langle\langle 2 \rangle\rangle = \langle\langle e^{in(\varphi_1 - \varphi_2)} \rangle\rangle = \frac{1}{\Omega} \sum_{n=1}^N \sum_{j=1}^{M_n} \sum_{\substack{k=1 \\ k \neq j}}^{M_n} e^{in(\varphi_{n,j} - \varphi_{n,k})}. \quad (2.3.0.12)$$

In the above equation, angular brackets denote the average over all events. N is the number of events and M_n is the multiplicity, i.e. the number of produced particles in the n th event. $\varphi_{j,n}$ is the azimuthal angle of j th particle from n th event measured in the fixed laboratory frame.

We have enforced the constraint $k \neq j$ in Eq. (2.3.0.12), the equality of these indices is called autocorrelation and this contribution is extracted therefore from the equation by definition. We are interested in calculation of two-particle average, by keeping autocorrelation terms in the two-particle average calculation, since two φ are the same we are not dealing with two-particle correlation any more, so in that case we would just add some $\cos(0)$ values into calculation and that would be strongly biased since $\cos(0)$ is obviously the maximum value of the function. Or more simply Eq. (2.3.0.12) is the average of two **different** particle correlations, that is why $\varphi_{j,n}$ and $\varphi_{k,n}$ angles have to belong to two **different** particles (it means the extraction of autocorrelations).

In Eq. (2.3.0.12) we are calculating the average of $e^{in(\varphi_1 - \varphi_2)}$ terms and Ω is number of such terms over all events with extraction of autocorrelations and it is the total number of permutations over all classes. ²

²As an analogy there are five students in a class (in our problem it is multiplicity) and two chairs (in our problem it is φ_1 and φ_2), what is the number of possibilities (arrangement/ordering) to make sit these students on the chairs. Any of five students can sit on the first chair, since one of them is already sitting on the first one, any of four students left can sit on the second chair (in our problem this situation is valid because of extraction of autocorrelations). The number of possible arrangements is the multiplication of five and four which is the five-permutation of two: $P(5, 2) = \frac{5!}{(5-2)!} = \frac{5 \cdot 4 \cdot 3!}{3!} = 5 \cdot 4$. We just need to remember in permutation ordering (a, b) and (b, a) are two different situations/cases. For instance in above student-chair example Jack, David sitting order is different than David, Jack order; so both are counted in permutation calculations (this corresponds to inclusion of both $e^{in(\varphi_a - \varphi_b)}$ and $e^{in(\varphi_b - \varphi_a)}$ in our average calculation). Now we extend the analogy and assume that there are some number of classes and in each of them, there are different numbers of students (this corresponds to fluctuation of multiplicity from event to event in our problem) and we want to find out what total number of arrangements of students sitting on the two chairs over all classes is. We found out that in the class which is composed of five students, the number of arrangements is the number

In case of average calculation of two-particle correlation the same phenomenon takes place. For n th event, where M_n denotes the multiplicity of the n th event, M_n different particles can take place of φ_1 ; since autocorrelations are extracted $(M_n - 1)$ particles are left to occupy the φ_2 place. As stated before $e^{in(\varphi_a - \varphi_b)}$ and $e^{in(\varphi_b - \varphi_a)}$ are both included in the calculation. As a result of these, the number of terms (arrangements) is the multiplication of these two values $M_n \cdot (M_n - 1)$ for n th event or equivalently multiplicity permutation of 2:

$$P(M_n, 2) = \frac{M_n!}{(M_n - 2)!} = M_n \cdot (M_n - 1) = \Omega_n. \quad (2.3.0.13)$$

Ω_n is the number of permutation (number of two-particle correlations) for n th event. So at each event we have Eq. (2.3.0.13) contributes to Ω as the number of two-particle correlations of the event and that is why Ω would be the addition of the permutations over all events:

$$\Omega = \sum_{n=1}^N P(M_n, 2) = \sum_{n=1}^N M_n(M_n - 1). \quad (2.3.0.14)$$

So Eq. (2.3.0.12) takes the final form:

$$\langle 2 \rangle = \langle \langle e^{in(\varphi_1 - \varphi_2)} \rangle \rangle = \frac{1}{\sum_{n=1}^N P(M_n, 2)} \sum_{n=1}^N \sum_{j=1}^M \sum_{\substack{k=1 \\ k \neq j}}^M e^{in(\varphi_{n,j} - \varphi_{n,k})}. \quad (2.3.0.15)$$

Above equation is the straight average of two-particle correlations. If we want to write it in weight-average form, we start by extending above equation over all events:

$$\langle \langle 2 \rangle \rangle = \frac{1}{\sum_{n=1}^N P(M_n, 2)} \left[\sum_{j=1}^{M_1} \sum_{\substack{k=1 \\ k \neq j}}^{M_1} e^{in(\varphi_{1,j} - \varphi_{1,k})} + \sum_{j=1}^{M_2} \sum_{\substack{k=1 \\ k \neq j}}^{M_2} e^{in(\varphi_{2,j} - \varphi_{2,k})} + \dots + \sum_{j=1}^{M_N} \sum_{\substack{k=1 \\ k \neq j}}^{M_N} e^{in(\varphi_{N,j} - \varphi_{N,k})} \right]. \quad (2.3.0.16)$$

If $\langle 2 \rangle_n$ is the average of the n th event, n th argument in the right hand side of

of permutation $P(5, 2)$, structure is the same for the other classes: for instance the number of arrangements for the class composed of seven students is $P(7, 2)$ and $P(10, 2)$ for the class with ten students etc. That is why Ω is the total number of permutations over all classes.

Eq. (2.3.0.16) can be written as

$$\sum_{j=1}^{M_n} \sum_{\substack{k=1 \\ k \neq j}}^{M_n} e^{in(\varphi_{n,j}-\varphi_{n,k})} = M_n(M_n - 1) \frac{\sum_{j=1}^{M_n} \sum_{\substack{k=1 \\ k \neq j}}^{M_n} e^{in(\varphi_{n,j}-\varphi_{n,k})}}{M_n(M_n - 1)} = M_n(M_n - 1) \langle 2 \rangle_n. \quad (2.3.0.17)$$

As it has been seen in above equation, for n th event we add all two-particle correlation terms up and divide it by the number of the permutation of the event and obviously result is two-particle average of the n th event $\langle 2 \rangle_n$.

After reminding that $M_n(M_n - 1)$ is equal to $P(M_n, 2)$, we insert Eq. (2.3.0.17) into equation Eq. (2.3.0.16) and reach the following equation:

$$\langle \langle 2 \rangle \rangle = \frac{1}{\sum_{n=1}^N P(M_n, 2)} [P(M_1, 2) \langle 2 \rangle_1 + P(M_2, 2) \langle 2 \rangle_2 + \dots + P(M_N, 2) \langle 2 \rangle_N], \quad (2.3.0.18)$$

which in a compact form can be written as

$$\langle \langle 2 \rangle \rangle = \frac{\sum_{n=1}^N P(M_n, 2) \langle 2 \rangle_n}{\sum_{n=1}^N P(M_n, 2)}. \quad (2.3.0.19)$$

Above equation is the weighted average of two-particle correlation and weight function is the number of permutations of the n th event. We have derived the weight-average from the straight average and expect to see the same results from both of them in any numerical calculations.

One of the key assumption of flow analysis is that emitted particles are independent of each other [12]. If x_1 and x_2 are two independent observables, this independency allows us to write the average of multiplication as the multiplication of the averages ($\langle x_1 x_2 \rangle = \langle x_1 \rangle \langle x_2 \rangle$). Hence we are able to write the two-particle correlations in case of ideal flow as

$$\langle \langle 2 \rangle \rangle = \langle \langle e^{in(\varphi_1 - \varphi_2)} \rangle \rangle = \langle \langle e^{in(\varphi_1 - \Psi_n)} \rangle \langle e^{-in(\varphi_2 - \Psi_n)} \rangle \rangle. \quad (2.3.0.20)$$

Due to the fact that taking average is a linear mapping (where a and b are constants; x and y are variables, $\langle ax + y \rangle = a \langle x \rangle + \langle y \rangle$) we can write single-event average in Eq. (2.3.0.20) as

$$\langle e^{in(\varphi_1 - \varphi_2)} \rangle = \langle \cos(n(\varphi_1 - \Psi_n)) \rangle + i \langle \sin(n(\varphi_2 - \Psi_n)) \rangle. \quad (2.3.0.21)$$

In a symmetric collision (beam and target particle are the same), it is equally probable of having an emitted particle with an angle $(\varphi - \Psi_n)$ and $-(\varphi - \Psi_n)$.

So the contribution to average from these particles cancel each other: $\sin(\varphi - \Psi_n) + \sin[-(\varphi - \Psi_n)] = \sin(\varphi - \Psi_n) - \sin(\varphi - \Psi_n) = 0$. Therefore the term $\langle \sin(n(\varphi_1 - \Psi_n)) \rangle$ in above equation will vanish. In that regard if we insert Eq. (2.2.0.11) into Eq. (2.3.0.20), we reached the equation which gives the relation between two-particle correlation average and flow harmonics as

$$\langle\langle 2 \rangle\rangle = \langle v_n^2 \rangle. \quad (2.3.0.22)$$

We have developed a method in order to calculate the flow harmonics. The method, as we aimed in previous section do not depend on symmetry plane Ψ_n ; but Eq. (2.3.0.22) is biased even if in only existence of ideal flow due to statistical fluctuation $\langle v_n^k \rangle \neq \langle v_n \rangle^k$.

2.3.1 Results

In Fig. (2.3), true Monte Carlo simulation, straight and weighted average of two-particle correlation technique for second harmonic is presented. For this simulation 50K events has been run, symmetry plane angles (Ψ_n) have been sampled from uniform distribution with sample space $[0, 2\pi)$ and multiplicity of an event from uniform distribution with sample space $[50, 500]$. Azimuthal angles (φ) were sampled from probability density function described in Eq. (2.2.0.8). In this function the value of v_2 was given as 0.05, the other harmonics were set to zero.

Blue circle represents the straight average of Eq. (2.3.0.15), red square denotes the weighted average with number of permutations in Eq. (2.3.0.19), purple square represent the weighted average with weight one, green square is weighted with multiplicity and black square is the result of Eq. (2.2.0.11) as a true Monte Carlo simulation.

As it can be seen from the figure, true Monte Carlo simulation is converging to initial value 0.05. As we expect straight average and weighted average with number of permutations are exactly the same since they are derived from each other and they are in agreement with initial value of $v_2 = 0.05$. Weight functions as one and multiplicity in this figure are also in agreement with initial value of second harmonic, but we will see that these weights will deviate from the initial value and from true Monte Carlo simulation for higher correlation.

An important result for this simulation, weighted average with permutation is in exact agreement with straight average. Also CPU time was recorded as 1178.6 and real time was 19:40 minutes. We will see that the time required to run the particle correlation algorithm will sharply increase for higher orders.

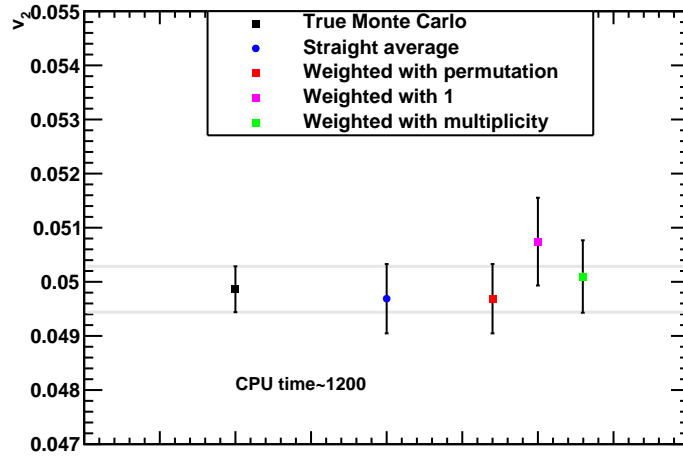


Figure 2.3: Result of straight and weighted average of two-particle correlations for second harmonic.

2.4 Multi-Particle Azimuthal Correlations Technique

In this section, we first will develop four-particle correlations technique; afterwards we generalize the technique for higher number of particles. Any correlation involving more than two particles is called multi-particle correlations. We start by defining the average of four-particle correlations over all events:

$$\langle\langle 4 \rangle\rangle = \langle\langle e^{in(\varphi_1 + \varphi_2 - \varphi_3 - \varphi_4)} \rangle\rangle = \frac{1}{\Omega_4} \sum_{n=1}^N \sum_{j=1}^{M_n} \sum_{\substack{k=1 \\ k \neq j}}^{M_n} \sum_{\substack{l=1 \\ l \neq k \\ l \neq j}}^{M_n} \sum_{\substack{s=1 \\ s \neq l \\ s \neq k \\ s \neq j}}^{M_n} e^{in(\varphi_{n,j} + \varphi_{n,k} - \varphi_{n,l} - \varphi_{n,s})}. \quad (2.4.0.1)$$

In the above equation, the notation has the same meaning as described in previous section. Again we removed out all the terms which are result of any type of equalities of the indices (autocorrelations) from the average calculation. In case of equality of two indices which does not cancel each other like j and k , three particles would remain ($j = k, l, s$) and it means we are adding three particle correlations terms into average of four-particle correlations; if they cancel each other like j and l or any three of the indexes are the same, two-particles would left and we would add two-particle correlations terms into average of four-particle correlations. If all of the indices are the same we just add some $\cos(0)$ as it is explained in previous section. So now it is clear that we need to extract autocorrelations from the average calculation, since otherwise they are biased.

Ω_4 is the number of four-particle correlations over all events. We may use

student-chair analogy which has been given in previous section. Now only difference is that, there are not two but four chairs in each classes. If there are N_n students in the n th class, N_n different students may sit on the first chair, any $N_n - 1$ students left can sit on the second chair, $N_n - 2$ students can sit on the third chair and $N_n - 3$ students may sit on the fourth chair. So the number of orderings is the multiplication: $N_n(N_n - 1)(N_n - 2)(N_n - 3)$ which is the number of permutation $P(N_n, 4)$. Over all classes where N is the number of them, the total number of orderings (arrangements) is the sum of permutations of each class $\sum_{n=1}^N P(N_n, 4)$.

We are seeking the four-particle correlations over all events. If N is the number of events and M_n is the multiplicity of the n th event, M_n particles may occupy the place of φ_1 . After extraction of autocorrelation $M_n - 1$ particles are left for φ_2 , $M_n - 2$ particles for φ_3 and $M_n - 3$ particles are left for φ_4 . So the number of the four-particle correlations for n th event is the multiplication: $M_n(M_n - 1)(M_n - 2)(M_n - 3)$ which is the number of permutations $P(M_n, 4)$. Total number of the correlations over all events is the sum of the permutations:

$$\Omega_4 = \sum_{n=1}^N P(M_n, 4). \quad (2.4.0.2)$$

By inserting Eq. (2.4.0.2) into Eq. (2.4.0.1) we reached out the straight average of four-particle correlation:

$$\langle\langle 4 \rangle\rangle = \frac{1}{\sum_{n=1}^N P(M_n, 4)} \sum_{n=1}^N \sum_{j=1}^{M_n} \sum_{\substack{k=1 \\ k \neq j}}^{M_n} \sum_{\substack{l=1 \\ l \neq k \\ l \neq j}}^{M_n} \sum_{\substack{s=1 \\ s \neq l \\ s \neq k \\ s \neq j}}^{M_n} e^{in(\varphi_{n,j} + \varphi_{n,k} - \varphi_{n,l} - \varphi_{n,s})}. \quad (2.4.0.3)$$

Now we extend the equation above over all events, for simplicity instead of four summations we use only one from now on and write it as

$$\langle\langle 4 \rangle\rangle = \frac{1}{\sum_{n=1}^N P(M_n, 4)} \left[\sum_{\substack{j,k,l,s=1 \\ j \neq k \neq l \neq s}}^{M_1} e^{in(\varphi_{1,j} + \varphi_{1,k} - \varphi_{1,l} - \varphi_{1,s})} + \dots \right. \\ \left. \dots + \sum_{\substack{j,k,l,s=1 \\ j \neq k \neq l \neq s}}^{M_N} e^{in(\varphi_{N,j} + \varphi_{N,k} - \varphi_{N,l} - \varphi_{N,s})} \right]. \quad (2.4.0.4)$$

As we proceeded for two-particle correlations before, n th argument in the right

hand side of the above equation can be written in terms of n th event average as

$$\begin{aligned} M_n(M_n - 1)(M_n - 2)(M_n - 3) & \frac{\sum_{\substack{j,k,l,s=1 \\ j \neq k \neq l \neq s}}^{M_n} e^{in(\varphi_{n,j} + \varphi_{n,k} - \varphi_{n,l} - \varphi_{n,s})}}{M_n(M_n - 1)(M_n - 2)(M_n - 3)} \\ & = M_n(M_n - 1)(M_n - 2)(M_n - 3) \langle 4 \rangle_n \\ & = P(M_n, 4) \langle 4 \rangle_n. \end{aligned} \quad (2.4.0.5)$$

After inserting the above equation into Eq. (2.4.0.4), it becomes

$$\langle \langle 4 \rangle \rangle = \frac{1}{\sum_{n=1}^N P(M_n, 4)} [P(M_1, 4) \langle 4 \rangle_1 + P(M_2, 4) \langle 4 \rangle_2 + \dots + P(M_N, 4) \langle 4 \rangle_N]. \quad (2.4.0.6)$$

Above equation is expressed in summation form as

$$\langle \langle 4 \rangle \rangle = \frac{\sum_{n=1}^N P(M_n, 4) \langle 4 \rangle_n}{\sum_{n=1}^N P(M_n, 4)}. \quad (2.4.0.7)$$

So the last equation is the weight-average of four-particle correlation where weight function is the number of permutations. The equation has been derived from the straight average. Therefore we expect to have the exactly the same result from both of them in any numerical calculations.

It is straightforward to generalize the multi-particle correlation technique for higher orders. Ω will be the total multiplicity-permutation of six for straight average of six particle correlation, multiplicity-permutation of eight for straight average of eight particle correlation etc. So in that regard straight average of six particle correlation is written as

$$\langle \langle 6 \rangle \rangle = \frac{1}{\sum_{n=1}^N P(M_n, 6)} \sum_{n=1}^N \sum_{\substack{j,k,l,s,f,t=1 \\ j \neq k \neq l \neq s \neq t \neq f}}^{M_n} e^{in(\varphi_{n,j} + \varphi_{n,k} + \varphi_{n,l} - \varphi_{n,s} - \varphi_{n,t} - \varphi_{n,f})}, \quad (2.4.0.8)$$

eight and higher order of particles correlation follow the same way. In weight average form, the weight function is permutation of six for six particles, permutation of eight for eight particles, etc. Now we write the above equation in weighted form:

$$\langle \langle 6 \rangle \rangle = \frac{\sum_{n=1}^N P(M_n, 6) \langle 6 \rangle_n}{\sum_{n=1}^N P(M_n, 6)}, \quad (2.4.0.9)$$

eight and higher orders of particle correlations follow the same structure.

In previous section we exploited independency of the emitted particles and related the harmonics with average of two-particle correlations. By using the

same assumption it is also possible to show the relations of average of multi-particle correlation with harmonics. We start with four-particle:

$$\begin{aligned} \langle\langle 4 \rangle\rangle &= \langle\langle e^{in(\varphi_1+\varphi_2-\varphi_3-\varphi_4)} \rangle\rangle \\ &= \langle\langle e^{in(\varphi_1-\Psi_n)} \rangle \langle e^{in(\varphi_2-\Psi_n)} \rangle \langle e^{-in(\varphi_3-\Psi_n)} \rangle \langle e^{-in(\varphi_4-\Psi_n)} \rangle \rangle. \end{aligned} \quad (2.4.0.10)$$

Since sine terms vanish, each average in the right hand side of above equation is equal to one power of flow harmonic (v_n). Therefore we can express the above equation as

$$\langle\langle 4 \rangle\rangle = \langle v_n^4 \rangle. \quad (2.4.0.11)$$

If we follow the same steps and use the same assumption, higher order relations can be constructed as in the following equations:

$$\langle\langle 6 \rangle\rangle = \langle v_n^6 \rangle, \langle\langle 8 \rangle\rangle = \langle v_n^8 \rangle, \text{ etc.} \quad (2.4.0.12)$$

As we stated before, even if in perfect scenario (only collective flow exist) above equation is biased due to statistical fluctuation: $\langle v_n^k \rangle \neq \langle v_n \rangle^k$.

Up to now we constructed a method which does not depend on symmetry plane angles, but the method is not feasible in terms of CPU time. For instance the time required to run the algorithm of eight particle correlation technique last a few billion years because of nested loops for a dataset corresponding to real heavy-ion collisions collected at LHC. In the next section we will focus on this obstacle.

2.5 Q-vector

Q-vector plays a central role in flow analysis. We start with definition of the Q-vector, afterwards we will show how to implement Q-vector into two and multi-particle correlation technique. Finally, we will see how one gets rid of the nested loops with this implementation. As a result, it will be clear how sharply CPU time will decrease and the correlation technique will become feasible.

2.5.1 Q-vector and Two-Particle Correlations

If φ is the transverse plane angle of the emitted particles in fixed laboratory frame, M_n is the multiplicity of the n th event, Q-vector in n th harmonic for an event will be denoted as Q_n and evaluated in the following way:

$$Q_n = \sum_{i=1}^{M_n} e^{in\varphi_{n,i}}. \quad (2.5.1.1)$$

In order to avoid any confusion, one has to be careful with n th harmonic and n th event, for instance M_n is the multiplicity of n th event but Q_n is the Q-vector of n th harmonic.

As it can be seen from above equation Q-vector is a complex number. Obviously square of an absolute value of a complex number can be expressed as below:

$$|Q_n|^2 = Q_n Q_n^* = \sum_{i=1}^{M_n} e^{in\varphi_i} \sum_{i=1}^{M_n} e^{-in\varphi_i} = \sum_{i=1}^{M_n} \sum_{j=1}^{M_n} e^{in(\varphi_{n,i}-\varphi_{n,j})}. \quad (2.5.1.2)$$

The last term in above equation is exactly the same with the last part of the Eq. (2.3.0.15) except the extraction of the autocorrelation. To be able to implement above equation into straight average of the two-particle correlations, we need to find out the contribution of autocorrelation to above equation. In that purpose we can write the above equation like below with help of two constrains ($i = j$) and ($i \neq j$) which exclude each other:

$$|Q_n|^2 = \sum_{i=1}^{M_n} \sum_{j=1}^{M_n} e^{in(\varphi_{n,i}-\varphi_{n,j})} = \sum_{i=1}^{M_n} \sum_{\substack{j=1 \\ j \neq i}}^{M_n} e^{in(\varphi_{n,i}-\varphi_{n,j})} + \sum_{i=1}^{M_n} \sum_{\substack{j=1 \\ j=i}}^{M_n} e^{in(\varphi_{n,i}-\varphi_{n,j})}. \quad (2.5.1.3)$$

We are familiar with the first term in the most right hand side of above equation. But what is the second term? For two-particle correlation it is relatively easy to answer but it is going to be a real challenge for higher orders, as we will see later. So in the second term i first takes value 1 and j has to take the same value since of the constrain ($i = j$), if we extend the equation in this regard we obtain:

$$\sum_{i=1}^{M_n} \sum_{\substack{j=1 \\ j=i}}^{M_n} e^{in(\varphi_{n,i}-\varphi_{n,j})} = 1 + 1 + \dots + 1 = M_n. \quad (2.5.1.4)$$

By inserting this second term as multiplicity of the n th event in previous equation, we reached out:

$$|Q_n|^2 - M_n = \sum_{i=1}^{M_n} \sum_{\substack{j=1 \\ i \neq j}}^{M_n} e^{in(\varphi_{n,i}-\varphi_{n,j})}. \quad (2.5.1.5)$$

By inserting this equality of the nested loop into straight average of two-particle correlation (Eq. (2.3.0.15)), we can write the following equation:

$$\langle\langle 2 \rangle\rangle = \langle\langle e^{in(\varphi_1-\varphi_2)} \rangle\rangle = \frac{1}{\sum_{n=1}^N P(M_n, 2)} \sum_{n=1}^N [|Q_n|^2 - M_n]. \quad (2.5.1.6)$$

Where $k = 1, 2, 3\dots$ above equation can be generalized as,

$$\langle\langle 2 \rangle\rangle_{kn|kn} = \langle\langle e^{ikn(\varphi_1 - \varphi_2)} \rangle\rangle = \frac{1}{\sum_{n=1}^N P(M_n, 2)} \sum_{n=1}^N [|Q_{kn}|^2 - M_n]. \quad (2.5.1.7)$$

So as it has been seen, we get rid of the nested loops for straight average of two-particle correlation technique by implementing the Q-vector. What we only need to do is the calculation of Q-vector for each event.

Now we repeat the same process for weighted average of two-particle correlation in order to remove nested loops. In Eq. (2.3.0.19) we expressed the weighted average where the equation $\langle 2 \rangle_n$ denotes the average of the n th event. If we write it as

$$\langle 2 \rangle_n = \frac{\sum_{i=1}^{M_n} \sum_{\substack{j=1 \\ k \neq j}}^{M_n} e^{in(\varphi_i - \varphi_j)}}{P(M_n, 2)}, \quad (2.5.1.8)$$

and replace the nested loops with Eq. (2.5.1.5), we get the following equation:

$$\langle 2 \rangle_n = \frac{\sum_{n=1}^N [|Q_n|^2 - M_n]}{P(M_n, 2)}. \quad (2.5.1.9)$$

Now average of two-particle equation Eq. (2.3.0.19) is free of nested loops and takes the final form:

$$\langle\langle 2 \rangle\rangle = \frac{\sum_{n=1}^N W_n \langle 2 \rangle_n}{\sum_{n=1}^N W_n}, \quad (2.5.1.10)$$

where W_n 's are the permutations $P(M_n, 2)$.

In two-particle correlation it is relatively straightforward to figure out the contribution of autocorrelation, but it is instructive to grasp and appreciate the role of Q-vector in flow analysis. As we will see in the next and other chapters, Q-vector technique decreases the CPU time tremendously and makes the correlation technique feasible.

Results

In Fig. (2.4), true Monte Carlo simulation, straight and weighted average of two-particle correlation technique with Q-vector for second harmonic are presented. For this simulation 50K events have been run, symmetry plane angles (Ψ_n) have

been sampled from uniform distribution with sample space $[0, 2\pi)$ and multiplicity of an event from uniform distribution with sample space $[50, 500]$. Azimuthal angles (φ) were sampled from probability density function described in Eq. (2.2.0.8). In this function the value of v_2 was given as 0.05, the other harmonics were set to zero. Weight function of two-particle correlation technique with and without Q-vector are the same and it is multiplicity-permutation of two.

In this figure, first we see that inclusion of Q-vector technique has decreased the CPU time tremendously. Straight averages are equal to weight averages with or without Q-vector. Also this is a cross-check of inclusion of Q-vector, as we see inclusion of Q-vector into technique is giving the same result with two-particle correlation.

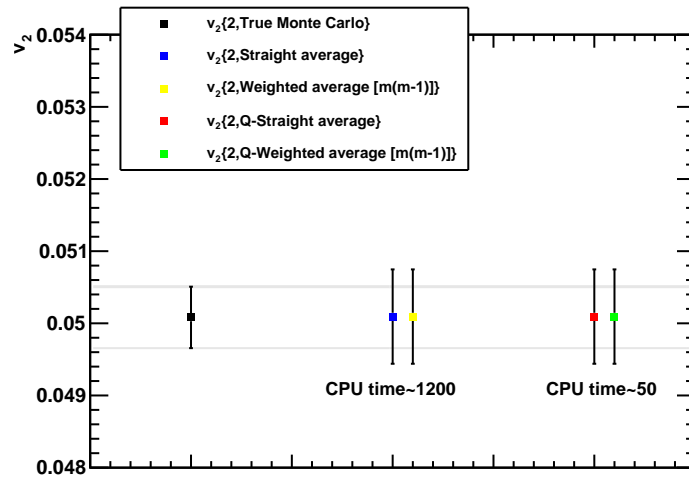


Figure 2.4: Result of straight and weighted average of two and multi particle correlation with Q-vector for second harmonic.

2.5.2 Q-vector and Multi-Particle Correlations

In this section we start with inclusion of Q-vector into four-particle correlation by showing all the steps explicitly and then we will apply the same process to higher orders.

First we write average of four-particle correlation for n th event in a different form,

$$\langle 4 \rangle_{n,n|n,n} = \langle e^{in(\varphi_1 + \varphi_2 - \varphi_3 - \varphi_4)} \rangle = \frac{1}{P(M_n, 4)} \left[\sum_{j,k,l,s}^{M_n} e^{in(\varphi_{n,j} + \varphi_{n,k} - \varphi_{n,l} - \varphi_{n,s})} - A_4 \right]. \quad (2.5.2.1)$$

In above equation, summation term does not exclude any autocorrelation. That is why we subtract A_4 which is the whole contribution from autocorrelations to

summation term. This form let us to write four-particle correlation in terms of Q-vector like in the following equation,

$$\langle 4 \rangle_{n,n|n,n} = \langle e^{in(\varphi_1+\varphi_2-\varphi_3-\varphi_4)} \rangle = \frac{1}{P(M_n, 4)} [|Q_n|^4 - A_4]. \quad (2.5.2.2)$$

Now question is how many autocorrelations we have and what is their contributions. Only two particles might be the same: $4!/(2!2!) = 6$, so we have six combinations ($j = k, j = l, j = s, k = l, k = s, l = s$), each of this combinations corresponds to three different particles. Three of them might be the same: $4!/3! = 4$, hence we have four combinations ($j = k = l, j = k = s, j = l = s, k = l = s$) which is corresponding to two different particles. All particles might be the same ($j = k = l = s$) meaning there is only one particle. One has to be careful here, also we can divide four-particles into two different groups and indexes equal each other in the same group but not equal to other group's index ($j = k \neq l = s, j = l \neq k = s, j = s \neq l = k$), these situations also corresponds to two different particles. So there are three type of autocorrelations and we will examine all these situations and find out their contributions.

There is only one particle:

This is the easiest case obviously, all indices/particles take the same value from one to the multiplicity of the event:

$$\sum_{j=k=l=s=1}^{M_n} e^{in(\varphi_{n,j}+\varphi_{n,k}-\varphi_{n,l}-\varphi_{n,s})} = e^0 + e^0 + \dots + e^0 = M_n. \quad (2.5.2.3)$$

There are two different particles:

These are the combinations we have for two different particles: ($j = k = l, j = k = s, j = l = s, k = l = s$) and ($j = k \neq l = s, j = l \neq k = s, j = s \neq l = k$). We start with first one ($j = k = l$) and write this case as

$$\sum_{j=k=l \neq s}^{M_n} e^{in(\varphi_{n,j}+\varphi_{n,k}-\varphi_{n,l}-\varphi_{n,s})} = P(M_n, 2) \frac{\sum_{j=k=l \neq s}^{M_n} e^{in(\varphi_{n,j}+\varphi_{n,k}-\varphi_{n,l}-\varphi_{n,s})}}{P(M_n, 2)}. \quad (2.5.2.4)$$

In the right hand side of above equation, we divide the summation term with multiplicity-permutation of two, now this term is nothing else but average of two-particle correlation for the n th event. So above equation turns into:

$$\sum_{j=k=l \neq s}^{M_n} e^{in(\varphi_{n,j}+\varphi_{n,k}-\varphi_{n,l}-\varphi_{n,s})} = P(M_n, 2) \langle 2 \rangle_{n|n}. \quad (2.5.2.5)$$

Rest of the three cases ($j = k = s, j = l = s, k = l = s$) have the same amount of contributions.

The other combinations which create two-particle correlations are ($j = k \neq l = s, j = l \neq k = s, j = s \neq l = k$), contribution from the first combination ($j = k \neq l = s$) might be written as

$$\sum_{j=k \neq l=s}^{M_n} e^{in(2\varphi_{n,j}-2\varphi_{n,s})} = P(M_n, 2) \langle 2 \rangle_{2n|2n}. \quad (2.5.2.6)$$

Contribution of the second combination:

$$\sum_{j=l \neq k=s}^{M_n} e^{in(\varphi_{n,j}+\varphi_{n,k}-\varphi_{n,l}-\varphi_{n,s})} = P(M_n, 2), \quad (2.5.2.7)$$

and it is the same for third combination. Finally we can write all contribution for the case of two different particles like below,

$$4P(M_n, 2) \langle 2 \rangle_{n|n} + P(M_n, 2) \langle 2 \rangle_{2n|2n} + 2P(M_n, 2). \quad (2.5.2.8)$$

There are three different particles:

The combinations we have for this cases are ($j = k, j = l, j = s, k = l, k = s, l = s$), we start with ($j = k$) and write the following equation,

$$\sum_{j=k \neq l \neq s}^{M_n} e^{in(2\varphi_{n,j}-\varphi_{n,l}-\varphi_{n,s})} = P(M_n, 3) \frac{\sum_{j=k \neq l \neq s}^{M_n} e^{in(2\varphi_{n,j}-\varphi_{n,l}-\varphi_{n,s})}}{P(M_n, 3)} = P(M_n, 3) \langle 3 \rangle_{2n|n,n}. \quad (2.5.2.9)$$

For the combination of ($l = s$), the contribution is

$$\sum_{j \neq k \neq l=s}^{M_n} e^{in(\varphi_{n,j}+\varphi_{n,k}-2\varphi_{n,s})} = P(M_n, 3) \langle 3 \rangle_{n,n|2n}. \quad (2.5.2.10)$$

For the combination of ($j = l$), the contribution is

$$P(M_n, 3) \frac{\sum_{j=l \neq k \neq s}^{M_n} e^{in(\varphi_{n,j}+\varphi_{n,k}-\varphi_{n,j}-\varphi_{n,s})}}{P(M_n, 3)} = P(M_n, 3) \langle e^{\varphi_1+\varphi_2-\varphi_1-\varphi_3} \rangle. \quad (2.5.2.11)$$

In above equation there are three particles, hence the ‘‘sample space’’ is permutation of three. But two particles cancel each other and two particles are left, that

is why we can not write it directly neither as average of two-particle nor average of three particles but as in the right hand side of above equation. And this term can be decomposed as following,

$$P(M_n, 3) \langle e^{in(\varphi_1+\varphi_2-\varphi_1-\varphi_3)} \rangle = P(M_n, 3) \langle e^{in(\varphi_2-\varphi_3)} \rangle = P(M_n, 3) \langle 2 \rangle_{n|n}. \quad (2.5.2.12)$$

Rest of the combinations ($j = s, k = l, k = s$) contribute with the same amount. Now we can express the total contribution of three different particles as below:

$$P(M_n, 3) \langle 3 \rangle_{2n|n,n} + P(M_n, 3) \langle 3 \rangle_{n,n|2n} + 4P(M_n, 3) \langle 2 \rangle_{n|n}. \quad (2.5.2.13)$$

So we found out all contribution from autocorrelations, now we add them up and write it as,

$$A_4 = P(M_n, 3)[\langle 3 \rangle_{2n|n,n} + \langle 3 \rangle_{n,n|2n} + 4 \langle 2 \rangle_{n|n}] + P(M_n, 2)[4 \langle 2 \rangle_{n|n} + \langle 2 \rangle_{2n|2n} + 2] + M_n. \quad (2.5.2.14)$$

Before we insert the last equation into Eq. (2.5.2.2), average of tree particle correlation has to be expressed in terms of Q-vector. In that regard, average of three particle correlation $\langle 3 \rangle_{2n|n,n}$ is written as

$$\langle 3 \rangle_{2n|n,n} = \frac{\sum_{\substack{j \neq l \neq s \\ j \neq l \neq s}}^{M_n} e^{in(2\varphi_{n,j}-\varphi_{n,l}-\varphi_{n,s})}}{P(M_n, 3)} = \frac{1}{P(M_n, 3)} [Q_{2n}Q_n^*Q_n^* - A_3]. \quad (2.5.2.15)$$

So A_3 is the total contribution from autocorrelation which we will construct as below,

$$A_3 = 2P(M_n, 2) \langle 2 \rangle_{n|n} + P(M_n, 2) \langle 2 \rangle_{2n|2n} + M_n. \quad (2.5.2.16)$$

The first term in right hand side of above equation stems from equality of ($j = k$) and ($j = l$), second term from equality of ($k = l$) and the last term from equality of three indexes.

By following the same steps, $\langle 3 \rangle_{n,n|2n}$ is constructed like

$$\langle 3 \rangle_{n,n|2n} = \frac{\sum_{\substack{j \neq k \neq l \\ j \neq k \neq l}}^{M_n} e^{in(\varphi_{n,j}+\varphi_{n,k}-2\varphi_{n,l})}}{P(M_n, 3)} = \frac{1}{P(M_n, 3)} [Q_nQ_nQ_{2n}^* - A_{3b}], \quad (2.5.2.17)$$

as one may expect A_{3b} is giving the same result and it reads:

$$A_{3b} = 2P(M_n, 2) \langle 2 \rangle_{n|n} + P(M_n, 2) \langle 2 \rangle_{2n|2n} + M_n. \quad (2.5.2.18)$$

Now we insert Eq. (2.5.2.18) into Eq. (2.5.2.17), Eq. (2.5.2.16) into Eq. (2.5.2.15). Afterwards Eq. (2.5.2.17) and Eq. (2.5.2.15) will be inserted into Eq. (2.5.2.14). By putting the last equation into Eq. (2.5.2.2) we obtain final form of average of four-particle correlations in terms of Q-vector for n th events:

$$\begin{aligned} \langle 4 \rangle_n &\equiv \langle \cos(n(\varphi_1 + \varphi_2 - \varphi_3 - \varphi_4)) \rangle \\ &= \frac{1}{P(M_n, 4)} \sum_{\substack{i,j,k,l=1 \\ (i \neq j \neq k \neq l)}}^{M_n} e^{in(\varphi_i + \varphi_j - \varphi_k - \varphi_l)} \\ &= \frac{1}{P(M_n, 4)} \times [|Q_n|^4 + |Q_{2n}|^2 - 2 \cdot \Re [Q_{2n} Q_n^* Q_n^*] - 4(M-2) |Q_n|^2 \\ &\quad + 2M(M-3)], \end{aligned} \quad (2.5.2.19)$$

Finally, in terms of Q-vector, weight average of four-particle over all event reads:

$$\langle \langle 4 \rangle \rangle_{n,n|n,n} = \frac{\sum_{n=1}^{M_n} P(M_n, 4) \langle 4 \rangle_n}{\sum_{n=1}^{M_n} P(M_n, 4)}. \quad (2.5.2.20)$$

In case of straight average, permutations in numerator of above equation cancel each other, we add the terms in square brackets of Eq. (2.5.2.19) and divide the addition by summation of permutations.

If we follow the same steps we reached out average of six particle correlation of an event like in the following equation,

$$\begin{aligned} \langle 6 \rangle_n &= \frac{1}{P(M_n, 6)} \sum_{\substack{j,k,l,s,f,t=1 \\ k \neq j \neq l \neq s \neq f \neq t}}^{M_n} e^{in(\varphi_{1,j} + \varphi_{1,k} - \varphi_{1,l} - \varphi_{1,s})} \\ &= \frac{1}{P(M_n, 6)} [|Q_n|^6 + 9|Q_{2n}|^2 |Q_n|^2 - 6 \cdot \Re [Q_{2n} Q_n Q_n^* Q_n^* Q_n^*] \\ &\quad + 4 \cdot \Re [Q_{3n} Q_n^* Q_n^* Q_n^*] - 12 \cdot \Re [Q_{3n} Q_{2n}^* Q_n^*] + 18(M_n - 4) \cdot \Re [Q_{2n} Q_n^* Q_n^*] \\ &\quad + 4|Q_{3n}|^2 - 9(M_n - 4)(|Q_n|^4 + |Q_{2n}|^2) + 18(M_n - 2)(M_n - 5)|Q_n|^2 \\ &\quad - 6(M_n - 4)(M_n - 5)]. \end{aligned} \quad (2.5.2.21)$$

The same procedure might be followed in order to get higher order correlations (further details and results for higher orders can be found in [7]). The

problem with multi-particle correlation is that the method is precisely applicable in the situation when only collective flow exists (actually as we stated before, even if in this ideal scenario method is biased because of statistical fluctuation of harmonics. But we will delay this discussion to Symmetric Cumulant section). We expressed the key assumption of collective flow analysis as “all emitted particles are independent of each other”. But in reality there are correlated particles contribute average calculation we were dealing with. This contribution is called as non-flow and arise from several sources such as resonance decays, jets, quantum correlation between identical particles, global momentum conservation which causes a back to back correlation between particles’ momentum, Coulomb and strong interaction among the particles especially for low relative velocities and possibly some not known sources yet [13] [14] [15]. So multi-particle correlation method is sensitive to non-flow and next section we will try to explain how it is possible to suppress it.

Results

In Fig. (2.5) we run the Monte Carlo simulation with the same settings which have been described in previous two result sections.

First we observe that straight and weight average as permutation are the same for two, four and six particle correlation. These two averages converge to true Monte Carlo value with relatively small error margin. As one can see from this figure, weight function as one and multiplicity are deviating from true Monte Carlo value for higher orders within relatively huge statistical errors. Finally CPU time is recorded as 90 which is less than two minutes in real time. So we clearly see that inclusion of Q-vector by decreasing the CPU time enormously made the method feasible.

2.6 Q-Cumulants

As we stated in previous section multi-particle correlation technique is not quite correct, due to contribution from non-flow. Cumulant is not capable of calculating quantitatively the magnitude of this contribution but can suppress it down to the scale which we are able to ignore [16] [17], it is not feasible with multi-particle correlation technique since of extremely huge CPU time. Implementation of Q-vector in cumulants which is called as Q-Cumulants makes the technique applicable [18]. In this section we try to explain how it is possible to reduce the non-flow and how one can use Q-Cumulants in collective flow analyses.

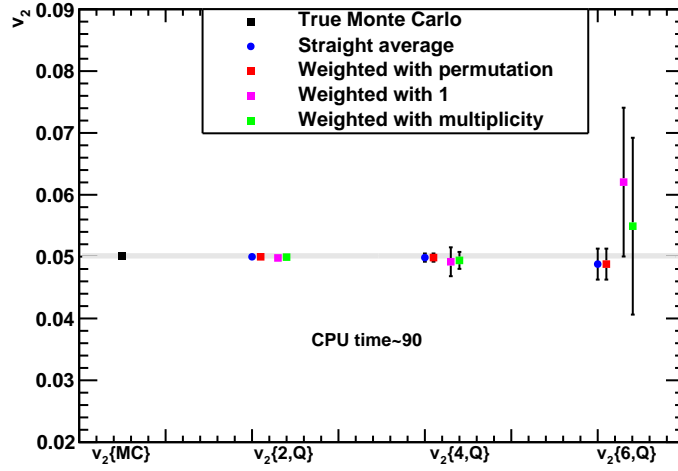


Figure 2.5: Result of straight and weighted average of two and multi-particle correlation with Q-vector for second harmonic. At x axis we sated the order of correlation, y axis is the second flow harmonic.

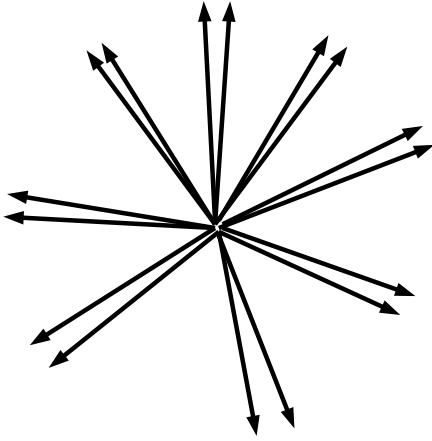


Figure 2.6: Representation of randomly distributed eight correlated pairs; multiplicity is sixteen. .

Due to non-flow correlation, factorization of average is broken; but it is possible to decompose the averages in terms of cumulants. We start with two-particle average and decompose it like in the following way,

$$\langle x_1 x_2 \rangle = \langle x_1 \rangle \langle x_2 \rangle + \langle x_1 x_2 \rangle_c. \quad (2.6.0.22)$$

In above equation x_1 and x_2 are random variables, if they are independent the average on the left side factorizes to $\langle x_1 \rangle \langle x_2 \rangle$; clearly in this case two-particle cumulant is zero. This is a collorary of cumulant: “A cumulant is zero if one of the variables in it is independent of the others. Conversely, a cumulant is not zero if and only if the variables in it are statistically connected. [19]”. Now we set the variables x_1 and x_2 to $e^{in(\varphi_1 - \Psi_n)}$ and $e^{in(\varphi_2 - \Psi_n)}$, respectively:

$$\langle e^{in(\varphi_1 - \varphi_2)} \rangle = \langle e^{in(\varphi_1 - \Psi_n)} \rangle \langle e^{-in(\varphi_2 - \Psi_n)} \rangle + \langle e^{in(\varphi_1 - \varphi_2)} \rangle_c. \quad (2.6.0.23)$$

The term in the left hand side is the two-particle correlation, this is the value we measure. Second term in the right hand side of the equation is two-particle cumulant. It can not be factorized, since it denotes the contribution from correlated particles. For instance ρ meson decays into two pions which are dependent on

each other due to momentum and energy conservation, so the correlation among these pions are measured by cumulant term. Where δ is the two-particle cumulant contribution, previous equation turns into:

$$\langle e^{in(\varphi_1 - \varphi_2)} \rangle = v_n^2 + \delta. \quad (2.6.0.24)$$

In Fig. (2.6) we illustrated a rough picture of Hijing (only non-flow) which is composed of randomly distributed eight-correlated particles pairs. This figure is not a realistic picture of Hijing, simply shows the random distribution of correlated pairs. In this figure closeness of the arrow only represents the correlation among two-particles. In case of Hijing, v_n will vanish since of random distribution of pairs, but two-particle correlations will not and yields a value which comes from non-flow. So Eq. (2.6.0.24) turns into:

$$\langle e^{in(\varphi_1 - \varphi_2)} \rangle = \delta\left(\frac{1}{m}\right). \quad (2.6.0.25)$$

In above equation, if we imagine the average in matrix form at each row there will be one correlated term, at total m rows gives m correlated terms (magnitudes are not clear). Division of uncorrelated terms' addition by sample space ($m(m-1)$) will vanish, this is because of random distribution of pairs. So δ is approximately equal to $\frac{m}{m(m-1)} \sim \frac{1}{m}$. Contribution only comes from correlated particles, that's why simply we can use probabilistic way: probability of a particle matching with its pair, they are dependent on each other, with multiplicity (m) is $\frac{1}{m-1}$. So two-particle cumulant approximately scale as $\frac{1}{m}$. With the same reasoning three-particle cumulant scale as $\frac{1}{m^2}$. More generally, when we have n -particle cumulant, it scale as $\frac{1}{m^{n-1}}$. Unfortunately in Eq. (2.6.0.24) v_n^2 also scale as $\frac{1}{m}$, that is why we can not neglect non-flow contribution.

To be able to understand how it is possible to reduce the non-flow effect, we proceed with decomposition of four-particle correlation average as we explain in Appendix (A). After inserting proper scaling we obtain the final form:

$$\langle e^{in(\varphi_1 + \varphi_2 - \varphi_3 - \varphi_4)} \rangle = v_n^4 + \frac{4v_n^2}{m} + \frac{2}{m^2} + \delta\left(\frac{1}{m^3}\right). \quad (2.6.0.26)$$

With subtraction of Eq. (2.6.0.26) and Eq. (2.6.0.24) like in the following way

$$\begin{aligned} 2 \langle e^{in(\varphi_1 - \varphi_2)} \rangle^2 - \langle e^{in(\varphi_1 + \varphi_2 - \varphi_3 - \varphi_4)} \rangle &= 2v_n^4 + \frac{4v_n^2}{m} + \frac{2}{m^2} \\ &- \left[v_n^4 + \frac{4v_n^2}{m} + \frac{2}{m^2} + \delta\left(\frac{1}{m^3}\right) \right] \\ &= v_n^4 + \delta\left(\frac{1}{m^3}\right), \end{aligned} \quad (2.6.0.27)$$

two-particle cumulant contribution has canceled. Three-particle cumulant contribution has vanished because any three-particle correlator evaluated for three same harmonics is non-isotropic. In above equation first term v_n^4 scales as $\frac{1}{m^2}$, on the other hand second term δ is of order $\frac{1}{m^3}$; relative to the first term non-flow contribution is reduced by factor of $1/m$. Thus, we neglect the second term and write the subtraction as,

$$2 \langle 2 \rangle^2 - \langle 4 \rangle = v_n^4. \quad (2.6.0.28)$$

It is straightforward to show that by definition above equation is equal to four-particle cumulant. We set the variables x_1, x_2, x_3, x_4 in Eq. (A.0.3.1) to $e^{in\varphi_1}, e^{in\varphi_2}, e^{-in\varphi_3}$ and $e^{-in\varphi_4}$, respectively. Non-isotropic terms vanish over all events since we have a “perfect” detector which means its azimuthal acceptance is uniform. In the next result section one may see the distributions of the azimuthal angle, indeed, they are uniform for all centralities. So after defining new variables and removing non-isotropic terms from four-particle average decomposition, we reached out the equation:

$$-\langle 4 \rangle_c = 2 \langle 2 \rangle^2 - \langle 4 \rangle = v_n^4. \quad (2.6.0.29)$$

If $x_1 = e^{in\varphi_1}$ and $x_2 = e^{-in\varphi_2}$ are inserted in Eq. (2.6.0.22), first term of the right hand side of the equation vanish since of nonisotropy and two-particle cumulant becomes:

$$\langle 2 \rangle_c = \langle 2 \rangle. \quad (2.6.0.30)$$

By utilizing the collorary which has been mentioned before (cumulant is zero, only, when there is any independence among its variables), we can state that, two-particle cumulant is sensitive to two and higher order correlations. On the other hand, four-particle cumulant is not sensitive to two or three particle correlation, since there has to be one or two particle which would be independent from the rest and four-particle cumulant becomes zero. More generally, if cumulant order is k and order of correlation is k' ; k -particle cumulant is not sensitive to correlations which have order $k' < k$. Obviously in this regard, six-particle cumulant is less sensitive to non-flow compared to four-particle cumulant. But when we are dealing with higher order cumulants, we are also increasing the statistical uncertainties. That is why, it is the optimal solution to work with four-particle cumulant. In addition to statistical uncertainties, it is clear from the scales of the non-flow correlations, that the most important contribution is coming from two correlated particles which is eliminated by four-particle cumulant, contribution from four or higher order of correlations are negligible, thus the difference of the sensitivity of four and six-particle cumulants is also negligible.

In Eq. (2.6.0.29) and Eq. (2.6.0.30), we use unbiased estimators to be able

to calculate the cumulants as two and four-particle correlation averages with implementation of Q-vector and call it as Q-Cumulants. Now we examine the last two equations for the ideal scenario when statistical fluctuations are absent:

$$v_n\{2\} = \sqrt{\langle 2 \rangle_c} = \sqrt{\langle \langle 2 \rangle \rangle} = v_n, \quad (2.6.0.31)$$

$$v_n\{4\} = \sqrt[4]{-\langle 4 \rangle_c} = \sqrt[4]{2 \langle \langle 2 \rangle \rangle^2 - \langle \langle 4 \rangle \rangle} = \sqrt[4]{2v_n^4 - v_n^4} = v_n. \quad (2.6.0.32)$$

In above equations v_n is flow harmonic, what we measure with Q-Cumulants would be different since of non-flow and statistical fluctuations. Thus we introduce new notations: In the equations above, $v_n\{2\}$ and $v_n\{4\}$ are what we measure with two and four-particle Q-Cumulants, respectively, and they are called as reference flow harmonics.

2.6.1 Data Selection and Results

In this section, we start with data selection criteria and present the results of charged particles in ALICE experiment for flow analysis.

Data have been used for the results in this section collected by ALICE detector in 2010 from Pb–Pb collisions at center-of-mass energy $\sqrt{s_{NN}} = 2.76 \text{ TeV}$ from the runs 137161 and 137162. Particles have been selected from the transverse momentum interval $0.2 < p_T < 5 \text{ GeV}/c$ and pseudorapidity range $|\eta| < 0.8$. The z position of the primary vertex which is found in $|Vertex_z| < 10 \text{ cm}$ has been used to ensure an uniform acceptance (further details might be found in [7]).

First in Fig. (2.7), we present the distribution of azimuthal angle φ over all events for centrality 0 – 5%, 40 – 50% and 70 – 80% (results for other centralities can be found in Appendix (D.1)). We can clearly see that the distribution for all centralities is uniform. This implies that we can regard the detector as a “perfect” one. Now we ensure that, indeed, the average of nonisotropic terms over all events at each centrality vanishes due to uniform distributions.

In Fig. (2.8), distribution of multiplicity for central, midcentral and peripheral collision have been presented (results for the other centralities are in Appendix (D.2)). Most importantly in these figures, we observe that mean value of multiplicity is dropping from central collisions to peripheral collisions. For 70 – 80% centrality, the mean value is around 44. Obviously, for such a small number of particles we may not have reliable results at this centrality, since of high statistical uncertainties.

In Fig. (2.9), we see the results of two and four-particle cumulants for second reference flow harmonic. Elliptic flow characterizes the strength of anisotropy, at

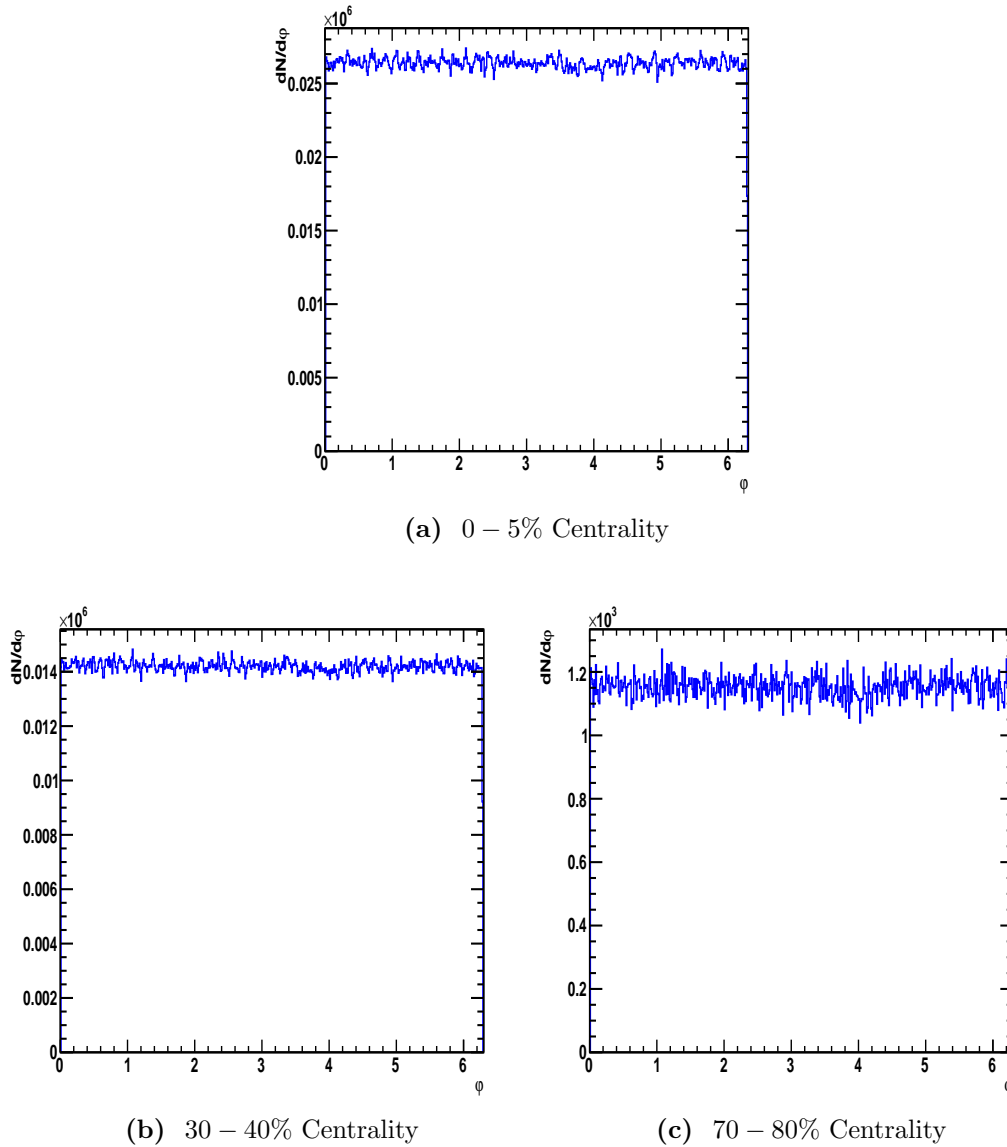


Figure 2.7: Distribution of azimuthal angle φ for central, midcentral and peripheral collisions.

most central collisions because of the collision symmetry v_2 will vanish. In the most central collisions the initial geometry in coordinate space is nearly spherical, and that therefore second harmonic in most central collisions originate solely from fluctuations. At peripheral collisions, due to low multiplicity we expect to see less strong anisotropy compared to midcentral collisions and v_2 reaches its maximum value at midcentral collisions, since of the anisotropy of the collisions and relatively large multiplicity. We see from the figure that four-particle cumulant's result is in agreement with our expectations, but not two-particle cumulant, this is because; as we explained in previous sections, two-particle cumulant is more sensitive to non-flow compared to four-particle cumulant. At centrality 70 – 80% which is regarded as peripheral collision statistical error is in such a magnitude (because of low multiplicity) that it prevents us to compare

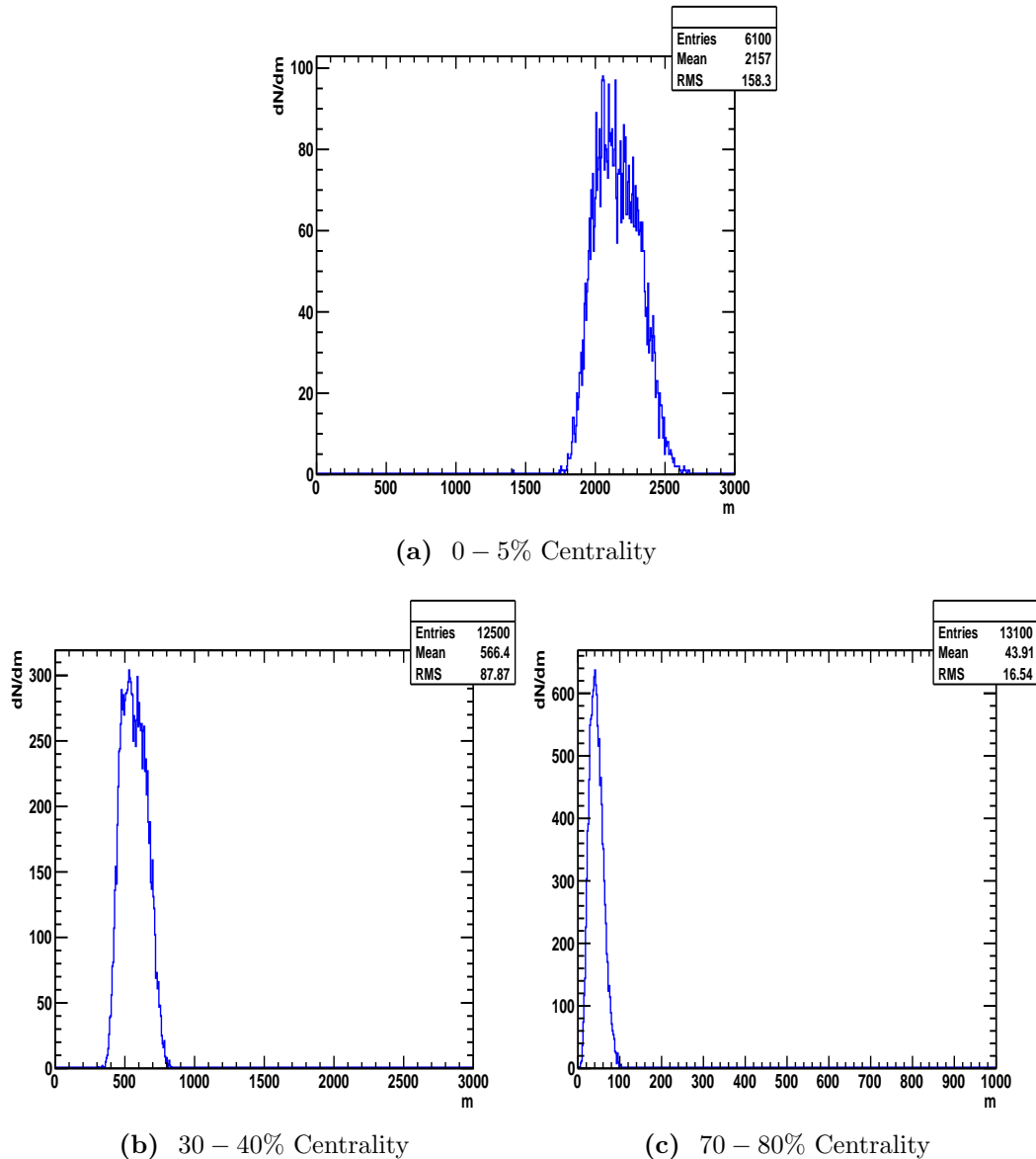


Figure 2.8: Distribution of multiplicity for central, midcentral and peripheral collisions.

the result with other centralities and decide if it increases or decreases. For two-particle cumulant, second harmonic reaches peak values at peripheral collisions. If we remember two-particle correlations of non-flow scale as $\frac{1}{m}$ and two-particle cumulant is sensitive to it, at peripheral collisions flow harmonic contribution will reach its minimum values but non-flow, since of low multiplicity, have its strongest effect. Although both cumulants are seeking for the same quantity, we found out two different results. This difference arises from two different sources. Obviously, first reason is that four-particle cumulant, as we stated before, is suppressing non-flow contribution. Second reason, even if in ideal scenario (there is only flow) two and four-particle cumulants are subject to statistical fluctuation which yields two different results. This will be the topic of the following sections. In the Appendix (E.0.1), we present the code snippets which have been used for

analysis of two and four-particle cumulants (Fig. (2.9)).

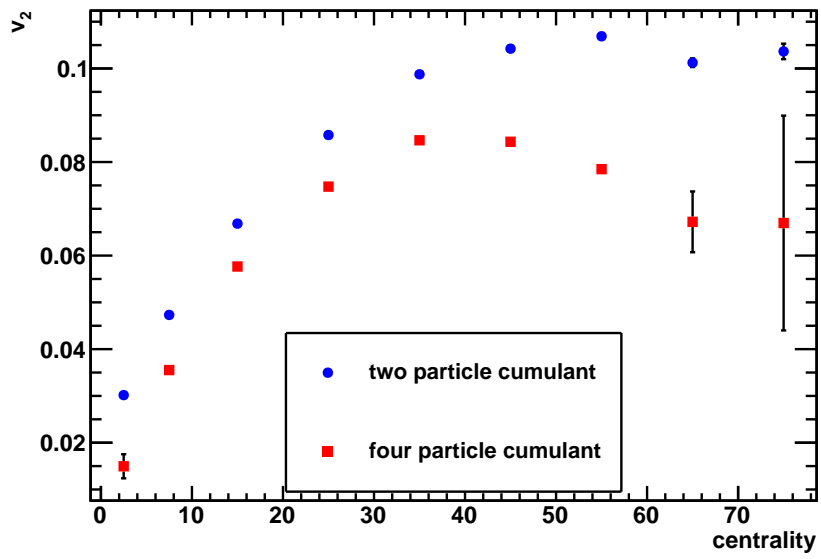


Figure 2.9: Centrality dependence of elliptic flow from two and four-particle cumulants.

Chapter 3

Flow Fluctuations

Anisotropic flow phenomenon was simply defined as transformation of initial anisotropy into transverse plane as anisotropic distribution via interaction of particles. This transformation is responsible for elliptic flow v_2 . On the other hand, fluctuations of initial positions of nucleons inside the collision geometry from event to event is capable of creating any flow harmonics v_n . As it is depicted in Fig. (3.1) distribution of participant nucleons may have contained both elliptic and triangular flow harmonics. In this section we are probing into these fluctuations in terms of correlation of harmonics.

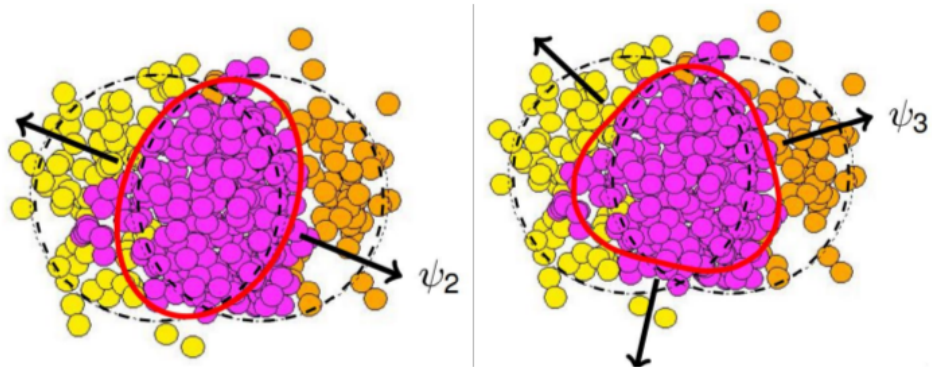


Figure 3.1: Distribution of participant nucleons inside the collision geometry includes both triangular (v_3) (on the right) and elliptic (v_2) (on the left) harmonics.

3.1 Symmetric Cumulants

In previous sections, we stated that even there is no contribution from non-flow, two and multi-particle correlations techniques are biased. Flow fluctuation manifests itself through statistical fluctuation. This fluctuation which we have neglected results in different values for harmonics in each event and are responsible for $\langle v^2 \rangle \neq \langle v \rangle^2$. This bias has been quantified in Appendix (B) and we reached

the following equations:

$$v\{2\} = \langle v \rangle \left(1 + \frac{\sigma_v^2}{\langle v \rangle} \right)^{1/2}, \quad (3.1.0.1)$$

$$v\{4\} = \langle v \rangle \left(1 - 2 \frac{\sigma_v^2}{\langle v \rangle} \right)^{1/4}. \quad (3.1.0.2)$$

The first equation above measures second harmonic via two-particle cumulant; left hand side of the equation is reference harmonic, this is what we are measuring, first term in the right hand side of the equation $\langle v \rangle$ is true value of the harmonic. In the parenthesis, numerator is variance and it is a positive value; denominator is also positive due to correlation of outgoing particles with reaction plane. As a result, we clearly see that what we are measuring with two-particle cumulants is higher than true value. The second equation above measures second harmonic via four-particle cumulant. Examination of this equation shows that what we are measuring is lower than true value. Now we can conclude that in Fig. (2.9), statistical fluctuation is responsible for having two different results or in other words flow fluctuation causes the results of two- and four-particle cumulants to be different from each other.

Now we will quantify the relationship between fluctuations of individual flow harmonics event-by-event. Obviously they might be correlated, anti-correlated or not correlated. We start with setting the variables in Eq. (A.0.3.1) x_1, x_2, x_3 and x_4 to $e^{im\varphi_1}, e^{im\varphi_2}, e^{-in\varphi_3}$ and $e^{-in\varphi_4}$ respectively. All nonisotropic terms vanish and we get:

$$\begin{aligned} \langle \langle \cos(m\varphi_1 + n\varphi_2 - m\varphi_3 - n\varphi_4) \rangle \rangle_c &= \langle \langle \cos(m\varphi_1 + n\varphi_2 - m\varphi_3 - n\varphi_4) \rangle \rangle \\ &\quad - \langle \langle \cos[m(\varphi_1 - n\varphi_2)] \rangle \rangle \langle \langle \cos[n(\varphi_3 - n\varphi_4)] \rangle \rangle \\ &= \langle v_m^2 v_n^2 \rangle - \langle v_m^2 \rangle \langle v_n^2 \rangle. \end{aligned} \quad (3.1.0.3)$$

Left hand side of above equation is four-particle cumulant with two different and symmetric harmonics. This new variable is called as Symmetric Cumulant $SC(m, n)$ [20]. Double angular brackets in above equation represent the average over all events as we carried out before. The last line in above equation is valid in the absence of non-flow, but here we are calculating four-particle cumulant and it has been proven that four-particle cumulant is sensitive to non-flow with scale of $1/m^3$, where m is the multiplicity. Thus, we neglect the non-flow contribution.

The observable in Eq. (3.1.0.3) $SC(m, n)$ is free of symmetry plane angles Ψ_n ; since the observable has two and symmetric harmonics $(m, n, -m, -n)$, dependence on symmetry planes has been canceled. $SC(m, n)$ is zero if any of flow harmonic is absent or constant. In addition to these situations, it is obvious that

if flow harmonics are independent of each other, $SC(m, n)$ is zero; but opposite is not supposedly correct.

v_m and v_n are calculated according to their harmonic index as in Eq. (2.5.1.10). Previously we have calculated four-particle correlation with the same harmonic, this time we have two different harmonics and state the analytic result for four-particle average of the event n in terms of Q -vector as in the following equation [7]:

$$\begin{aligned} \langle 4 \rangle_n &= \langle \cos(m\varphi_1 + n\varphi_2 - m\varphi_3 - n\varphi_4) \rangle = \frac{1}{P(M_n, 4)} [|Q_m|^2 |Q_n|^2 \\ &\quad - 2\Re[Q_{m+n} Q_m^* Q_n^*] - 2\Re[Q_m Q_{m-n}^* Q_n^*] + |Q_{m+n}|^2 + |Q_{m-n}|^2 \\ &\quad - (M_n - 4)(|Q_m|^2 + |Q_n|^2) + M_n(M_n - 6)]. \end{aligned} \quad (3.1.0.4)$$

In above equation subindex of $\langle 4 \rangle_n$ represents the event n . Now by implementing Eq. (2.5.1.10) for different harmonics and Eq. (3.1.0.4) into Eq. (3.1.0.3), it is possible to find out the symmetric cumulant.

3.1.1 Monte Carlo Simulations

Multiplicity has been sampled from uniform distribution [50,500], 50K events has been run and v_2 was distributed uniformly from [0.04, 0.1] for the all following simulations.

First in Fig. (3.2a) we set a positive correlation between fluctuations of fourth and second harmonics: $v_4 = v_2 + d$ and d is 0.15, one has to be careful with assignment of d and with distribution of v_2 ; harmonics should have positive values with these assignments. Now v_2 is positive since of its sample space and for each simulation we give a value to d which makes v_4 a positive harmonic, so that the Fourier series decomposition in Eq. (2.2.0.1), when interpreted as p.d.f, is always positive definite. As a result we see on the figure, $SC(4, 2)$ is positive and consistent with analytic result for $SC(4, 2)$ for this particular Monte Carlo study, which is shown with the blue marker.

In Fig. (3.2b) negative correlation has been created among the harmonics with equation $v_4 = -v_2 + d$. As it can be seen from the graph, symmetric cumulant has a negative value and consistent with analytic result, which is shown with the blue marker, within statistical uncertainty.

The same process can be applied to the correlation among v_3 and v_2 . For this simulation d is set to 0.13. As we see from Fig. (3.3a), we created a positive correlation between fluctuations of the harmonics v_3 and v_2 , as we expect $SC(3, 2)$ has a positive value. In Fig. (3.3b) a negative correlation has been created and as a result $SC(3, 2)$ has a negative value. Both of the numerical results are in

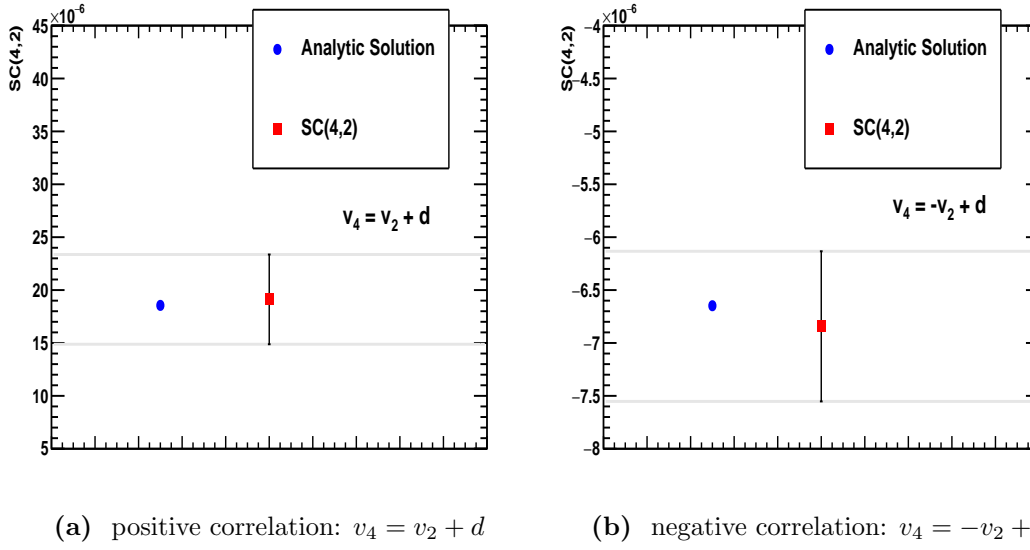


Figure 3.2: Analytic and SC(4,2) results for positive and negative correlations of v_4 and v_2 .

agreement with their analytical results. All analytical results in this thesis were

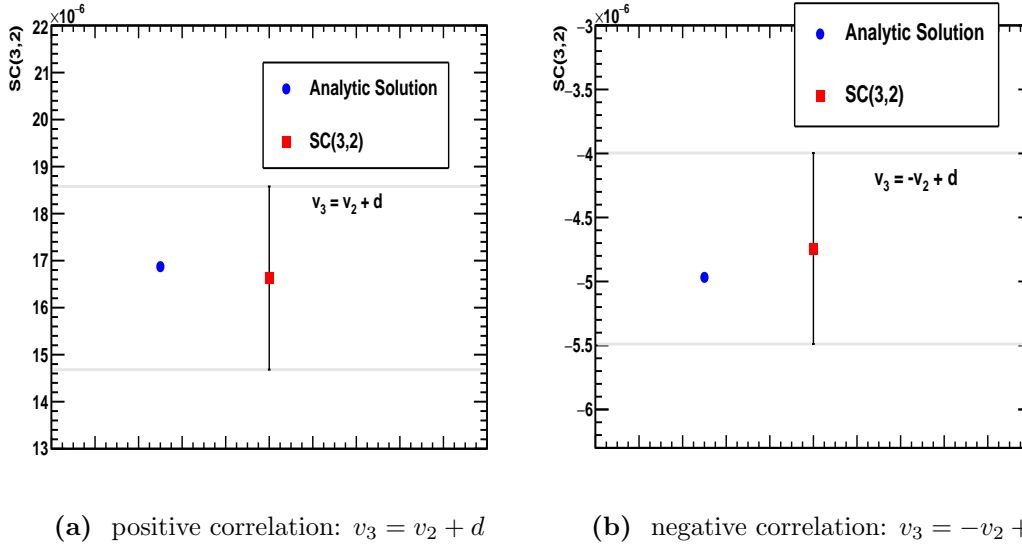


Figure 3.3: Analytic and SC(3,2) results for positive and negative correlations of v_3 and v_2 .

calculated by Mathematica.

3.1.2 Results

Now we present results from data collected by ALICE detector in 2010 from Pb–Pb collisions at center-of-mass energy $\sqrt{s_{NN}} = 2.76 \text{ TeV}$ with momentum interval $0.2 < p_T < 5 \text{ GeV}/c$ and pseudorapidity range $|\eta| < 0.8$.

Unlike in Q-Cumulant analysis, now we need to run over all 2010 data (90 runs in total) which passed all central quality assurance criteria in ALICE, e.g.

we plot two-particle correlation evaluated in second harmonic vs. run number for centrality 10 – 20%. In Fig. (3.4) we see the results, on x -axis we have 90 run numbers and on y -axis two-particle correlation evaluated in second harmonic with its statistical error. Results in all runs for two-particle correlations evaluated in second harmonic are consistent within their statistical errors, otherwise the particular run which has different result would need to be excluded from the further analysis. We have developed the analysis task, which was carried out on the Worldwide LHC Computing Grid (WLCG), a part of it is presented in Appendix (E.0.2).

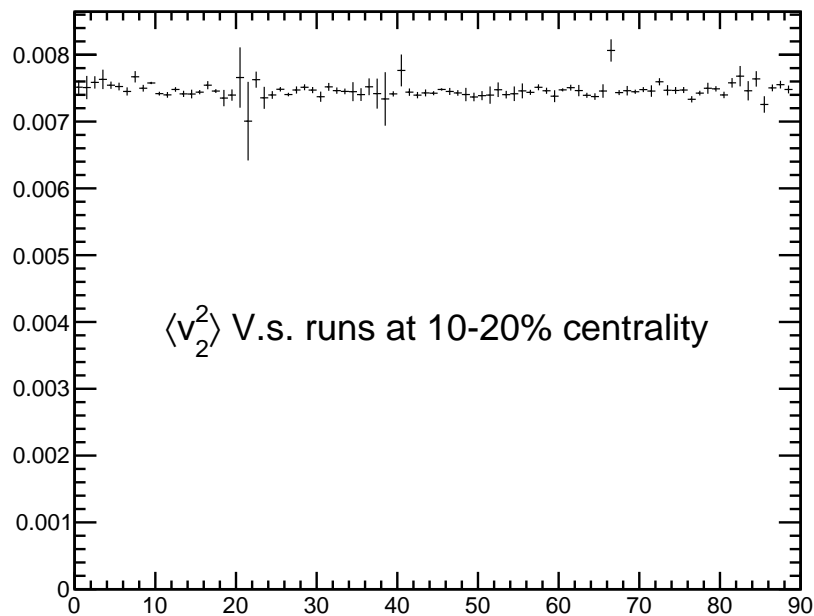
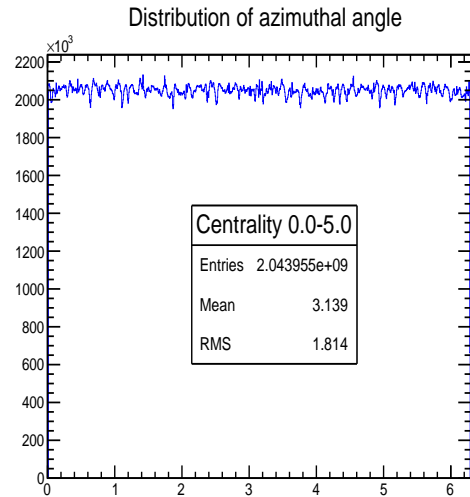


Figure 3.4: Trending

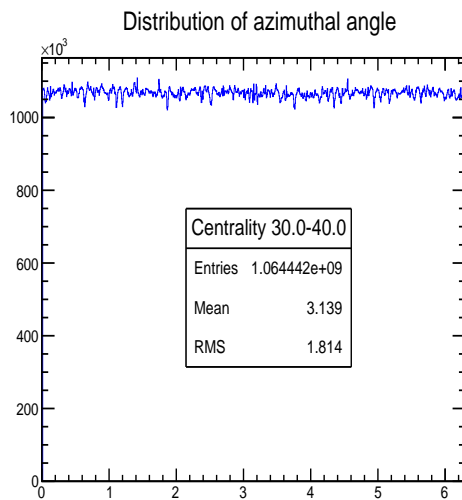
In Fig. (3.5), we see azimuthal angle distribution for central, mid-central and peripheral collisions. The uniform distributions at each centrality ensure that we have an uniform azimuthal acceptance in each of the runs which were analyzed.

In Fig. (3.6), multiplicity distributions for central, mid-central and peripheral collisions are presented. Most importantly we observe that mean value of multiplicity is dropping from central (around 2000) to peripheral collisions (around 75).

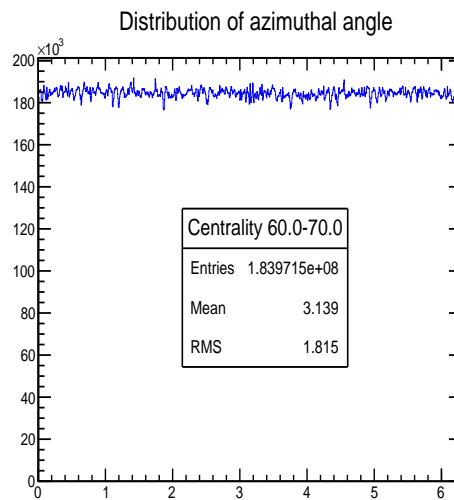
Finally, in Fig. (3.7) red square markers represent $SC(4, 2)$ and blue circle markers represent $SC(3, 2)$. On the other hand, the open markers are result of ALICE Collaboration paper [21] and full markers are results of our research. For each centrality we have positive value of $SC(4, 2)$ and negative value of $SC(3, 2)$. Positive correlation among the harmonics v_4 and v_2 implies that both harmonics



(a) 0 – 5% Centrality



(b) 30 – 40% Centrality



(c) 60 – 70% Centrality

Figure 3.5: Distribution of azimuthal angle φ for central, mid-central and peripheral collisions.

either tend to be larger or smaller than their own averages in a given event. Negative correlation of v_3 and v_2 means that if one of the harmonic has a tendency to be larger or smaller than its own average the other harmonic has an opposite tendency in an event.

3.2 Generalized Symmetric Cumulants

3.2.1 Introduction

Symmetric Cumulants are new flow observables introduced recently to quantify the strength of correlation between the fluctuations of magnitudes of two different flow harmonics v_m and v_n . By design, they should satisfy the following

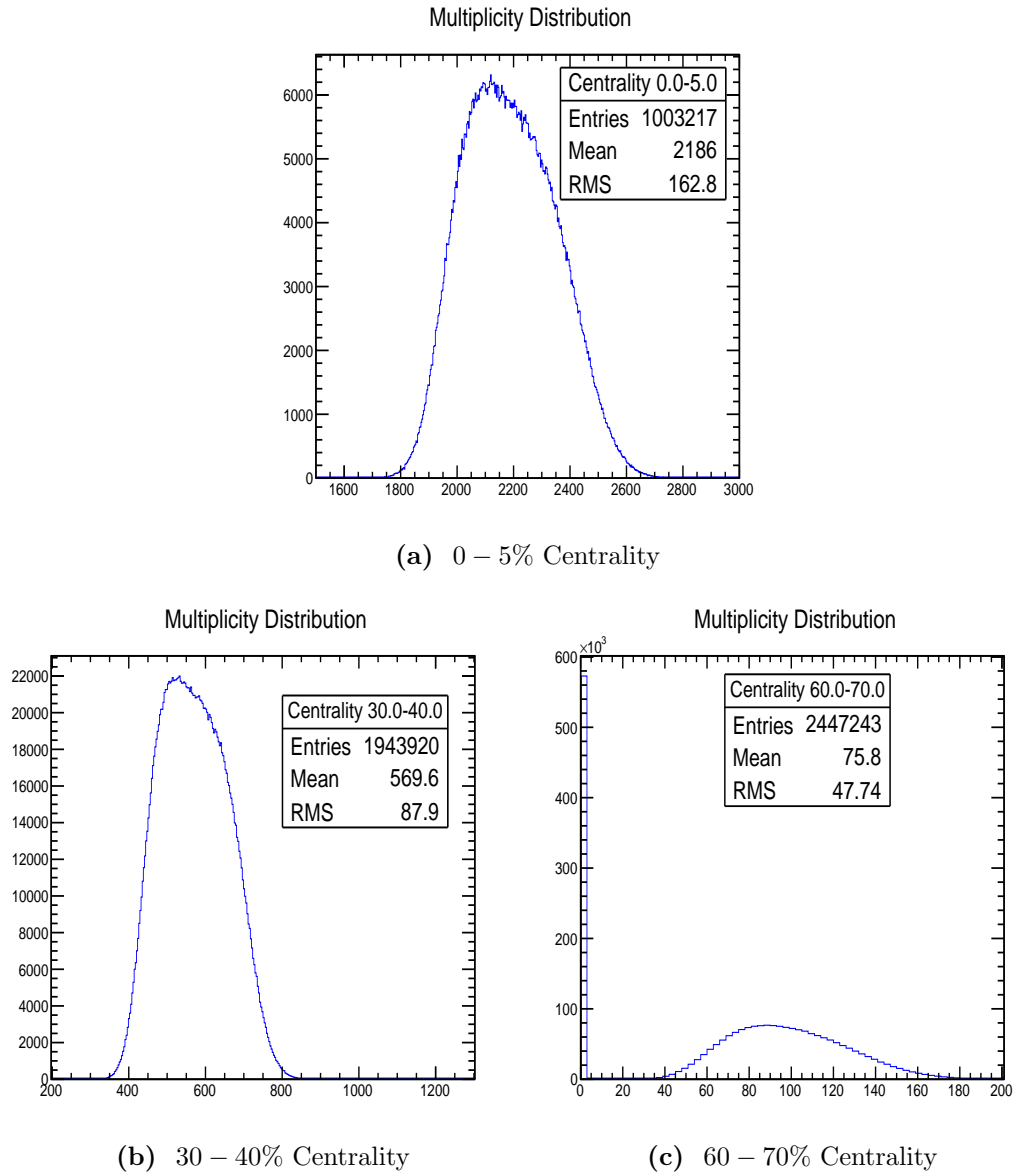


Figure 3.6: Distribution of multiplicity for central, mid-central and peripheral collisions.

requirements:

1. In the absence of fluctuations, i.e. for the fixed values of harmonics v_n in each event, SC are identically 0;
2. All terms in SC are isotropic;
3. Any dependence on the symmetry planes is canceled by definition;
4. If fluctuations of harmonics v_m and v_n are uncorrelated, SC are identically 0;
5. SC should be consistent with 0 for a system containing only non-flow correlations (e.g. HIJING).

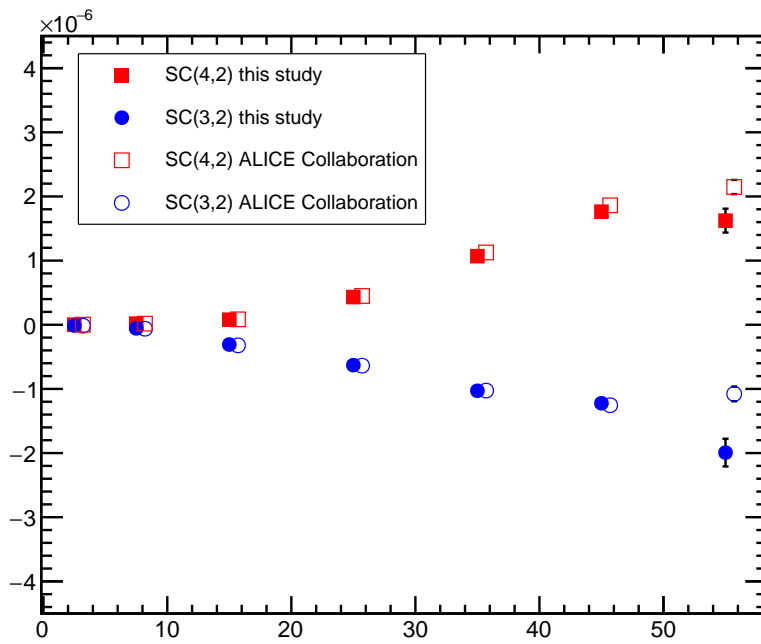


Figure 3.7: Centrality dependence of $SC(4,2)$ and $SC(3,2)$.

All these requirements were met with 2-harmonic Symmetric Cumulants, $SC(m, n)$. Now we investigate to what extent this idea can be generalized for the case of 3 different harmonics.

3.2.2 $SC(k, l, m)$

The general 3-particle cumulant is defined, for any three random observables X_1 , X_2 and X_3 , as follows:

$$\begin{aligned}
 \langle X_1 X_2 X_3 \rangle_c &= \langle X_1 X_2 X_3 \rangle \\
 &- \langle X_1 X_2 \rangle \langle X_3 \rangle - \langle X_1 X_3 \rangle \langle X_2 \rangle - \langle X_2 X_3 \rangle \langle X_1 \rangle \\
 &+ 2 \langle X_1 \rangle \langle X_2 \rangle \langle X_3 \rangle .
 \end{aligned} \tag{3.2.2.1}$$

We now make a specific choice, namely:

$$\begin{aligned}
 X_1 &\equiv \exp[ik(\varphi_1 - \varphi_2)] , \\
 X_2 &\equiv \exp[il(\varphi_3 - \varphi_4)] , \\
 X_3 &\equiv \exp[im(\varphi_5 - \varphi_6)] .
 \end{aligned}$$

It follows, after extending the averaging to all events:

$$\begin{aligned}
\text{SC}(k, l, m) &= \langle\langle \cos[k\varphi_1 + l\varphi_2 + m\varphi_3 - k\varphi_4 - l\varphi_5 - m\varphi_6] \rangle\rangle & (3.2.2.2) \\
&- \langle\langle \cos[k\varphi_1 + l\varphi_2 - k\varphi_3 - l\varphi_4] \rangle\rangle \langle\langle \cos[m(\varphi_5 - \varphi_6)] \rangle\rangle \\
&- \langle\langle \cos[k\varphi_1 + m\varphi_2 - k\varphi_5 - m\varphi_6] \rangle\rangle \langle\langle \cos[l(\varphi_3 - \varphi_4)] \rangle\rangle \\
&- \langle\langle \cos[l\varphi_3 + m\varphi_4 - l\varphi_5 - m\varphi_6] \rangle\rangle \langle\langle \cos[k(\varphi_1 - \varphi_2)] \rangle\rangle \\
&+ 2 \langle\langle \cos[k(\varphi_1 - \varphi_2)] \rangle\rangle \langle\langle \cos[l(\varphi_3 - \varphi_4)] \rangle\rangle \langle\langle \cos[m(\varphi_5 - \varphi_6)] \rangle\rangle ,
\end{aligned}$$

i.e.

$$\begin{aligned}
\text{SC}(k, l, m) &= \langle v_k^2 v_l^2 v_m^2 \rangle - \langle v_k^2 v_l^2 \rangle \langle v_m^2 \rangle - \langle v_k^2 v_m^2 \rangle \langle v_l^2 \rangle \\
&- \langle v_l^2 v_m^2 \rangle \langle v_k^2 \rangle + 2 \langle v_k^2 \rangle \langle v_l^2 \rangle \langle v_m^2 \rangle . & (3.2.2.3)
\end{aligned}$$

Any dependence on symmetry planes is canceled out by definition, as can easily be checked for each term separately in Eq. (3.2.2.3). For instance,

$$\begin{aligned}
\langle v_k^2 v_l^2 \rangle &= \langle\langle \cos(k(\varphi_1 - \Psi_k) + l(\varphi_2 - \Psi_l) - k(\varphi_3 - \Psi_k) - l(\varphi_4 - \Psi_l)) \rangle\rangle \\
&= \langle\langle \cos[k\varphi_1 + l\varphi_2 - k\varphi_3 - l\varphi_4] \rangle\rangle & (3.2.2.4)
\end{aligned}$$

As a result of symmetric harmonics $(k, l, -k, -l)$ in above equation, symmetry plane angles canceled each other. Since all correlators in Eq. (3.2.2.3) are composed of symmetric harmonics, we can conclude that $SC(k, l, m)$ is free of symmetry planes.

3.2.3 Toy Monte Carlo Studies for $SC(k, l, m)$

Now we perform few Monte Carlo studies in order to illustrate the desired properties of 3-harmonic symmetric cumulants $SC(k, l, m)$. In order to evaluate each correlator in Eq. (3.2.2.3), we will use *recursion formula*, the code snippets can be found in Appendix (E.0.3).

Three Constant Harmonics

If harmonics v_k , v_l and v_m are constant in each event, obviously mean value of a constant is equal to itself $\langle c \rangle = c$, Eq. (3.2.2.3) becomes zero:

$$\begin{aligned}
\text{SC}(k, l, m) &= v_k^2 v_l^2 v_m^2 - v_k^2 v_l^2 v_m^2 - v_k^2 v_m^2 v_l^2 \\
&- v_l^2 v_m^2 v_k^2 + 2v_k^2 v_l^2 v_m^2 \\
&= 0 . & (3.2.3.1)
\end{aligned}$$

In the first toy MC study we demonstrate that $SC(k, l, m)$ defined in Eq. (3.2.2.3) is consistent with zero when three harmonics are constant in each event. We implement in ROOT the Fourier like p.d.f as,

$$f(\varphi) = \frac{1}{2\pi}(1 + 2v_1 \cos \varphi + 2v_2 \cos 2\varphi + 2v_3 \cos 3\varphi). \quad (3.2.3.2)$$

and parametrize it only with fixed harmonics $v_1 = 0.05$, $v_2 = 0.1$ and $v_3 = 0.15$. We have run nine hundreds million events with a fixed multiplicity of a thousand and we see the results in Fig. (3.8). In this figure correlators corresponds to terms in Eq. (3.2.2.3), for instance $\langle\langle \cos[\varphi_1 + 2\varphi_2 + 3\varphi_3 - \varphi_4 - 2\varphi_5 - 3\varphi_6] \rangle\rangle = \langle v_1^2 v_2^2 v_3^2 \rangle$ is represented by $\langle \cos(1, 2, 3) \rangle$ and the same representation structure is valid for the rest of the correlators. It is clear that non of them is zero, on the other hand as we expect $SC(1, 2, 3)$ is consistent with zero within statistical uncertainty.

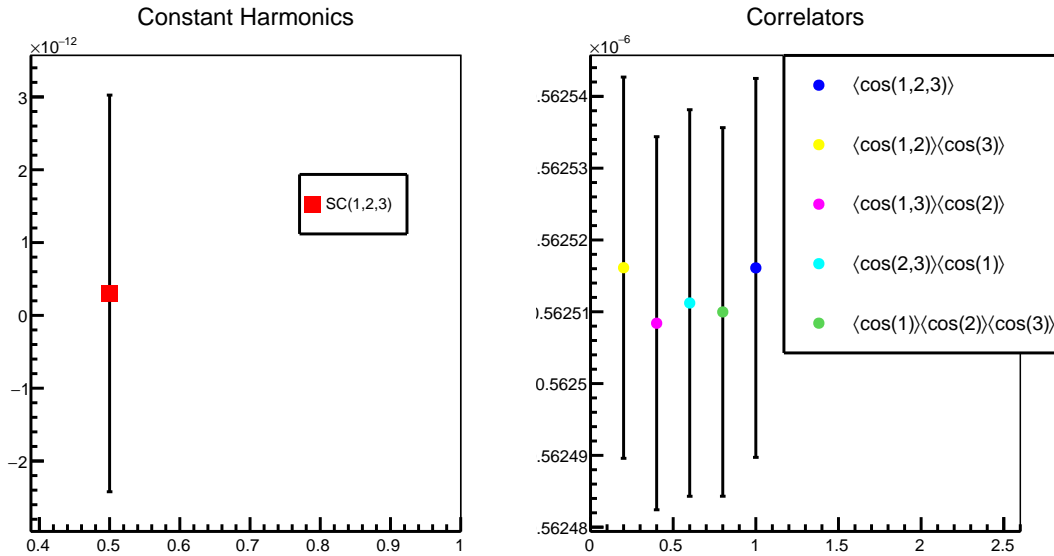


Figure 3.8: Results of generalized symmetric cumulants ($SC(1, 2, 3)$) and correlators for constant harmonics.

Fluctuations of Three Independent Harmonics

We can easily see that when event-by-event fluctuations of v_k , v_l and v_m are uncorrelated, this symmetric cumulant is identically zero, since then

$$\begin{aligned} SC(k, l, m) &= \langle v_k^2 \rangle \langle v_l^2 \rangle \langle v_m^2 \rangle - \langle v_k^2 \rangle \langle v_l^2 \rangle \langle v_m^2 \rangle - \langle v_k^2 \rangle \langle v_m^2 \rangle \langle v_l^2 \rangle \\ &\quad - \langle v_l^2 \rangle \langle v_m^2 \rangle \langle v_k^2 \rangle + 2 \langle v_k^2 \rangle \langle v_l^2 \rangle \langle v_m^2 \rangle \\ &= 0. \end{aligned} \quad (3.2.3.3)$$

We sample now values of three harmonics, v_1 , v_2 and v_3 from 3-variate p.d.f, which explicitly factorizes for all three observables:

$$f(v_1, v_2, v_3) \equiv e^{v_1+v_2+v_3} = e^{v_1}e^{v_2}e^{v_3}. \quad (3.2.3.4)$$

Such a functional dependence ensures that three harmonics are independent observables by definition. We implement in ROOT Eq. (3.2.3.4) as TF3 object:

```
TF3 *pdf3D = new TF3("pdf3Ds", "exp(x+y+z)", 0.01, 0.15, 0.01, 0.15, 0.01, 0.15);
```

As we see from above 3-variate p.d.f sample space of all three harmonics is the same and it is $[0.01, 0.15]$. After we have run the code over all events with two hundred million events and a thousand fixed multiplicity, we got results in Fig. (3.9). In this figure all markers represent the same variables as we described in previous section. As it is expected all of the correlators are nonzero and $SC(1, 2, 3)$ which depends on three independent harmonics is consistent with zero.

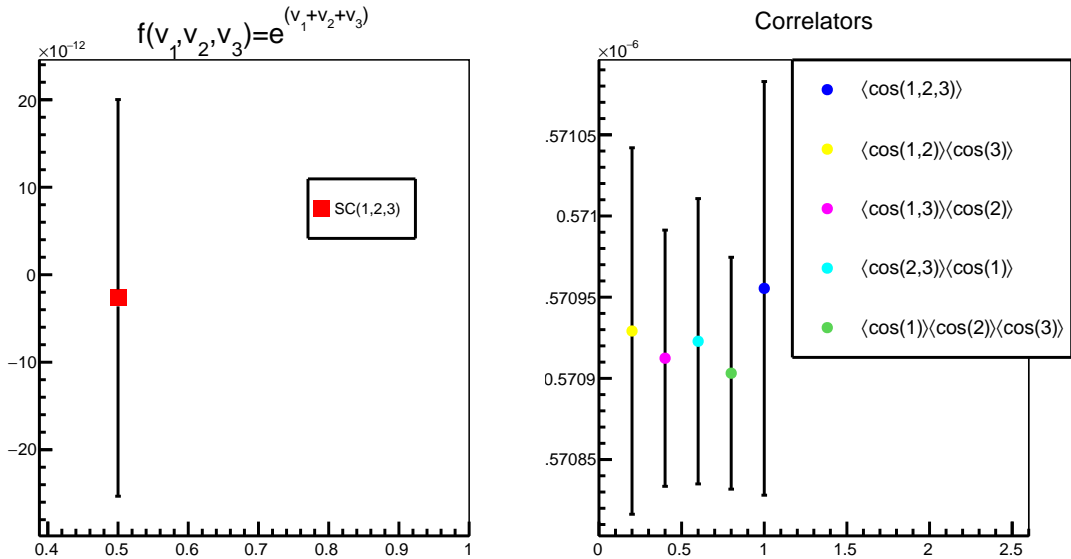


Figure 3.9: Results of generalized symmetric cumulants ($SC(1, 2, 3)$) and correlators for independent harmonics.

Fluctuations of Two Correlated Harmonics

Same as in previous example, we sample the values of harmonics from the following 3D p.d.f:

$$f(v_1, v_2, v_3) \equiv e^{v_1v_2+v_3} = e^{v_1v_2}e^{v_3}. \quad (3.2.3.5)$$

This kind of functional dependence ensures that correlation exists among two harmonics, in this case v_1 and v_2 are dependent and both are independent of v_3 .

In this regard Eq. (3.2.2.3) becomes zero:

$$\begin{aligned}
 SC(k, l, m) &= \langle v_k^2 v_l^2 \rangle \langle v_m^2 \rangle - \langle v_k^2 v_l^2 v_m^2 \rangle - \langle v_k^2 \rangle \langle v_m^2 \rangle \langle v_l^2 \rangle \\
 &\quad - \langle v_l^2 \rangle \langle v_m^2 \rangle \langle v_k^2 \rangle + 2 \langle v_k^2 \rangle \langle v_l^2 \rangle \langle v_m^2 \rangle \\
 &= 0.
 \end{aligned} \tag{3.2.3.6}$$

Implementation in ROOT of Eq. (3.2.3.5) goes as follows:

```
TF3 *pdf3D = new TF3("pdf3Ds", "exp(xy+z)", 0.01, 0.15, 0.01, 0.15, 0.01, 0.15);
```

Everything else is the same as in previous simulation. After we have run over all events, we observe in Fig. (3.10) that each individual correlator is non-zero in Eq. (3.2.2.3) and $SC(1, 2, 3)$ is consistent with zero.

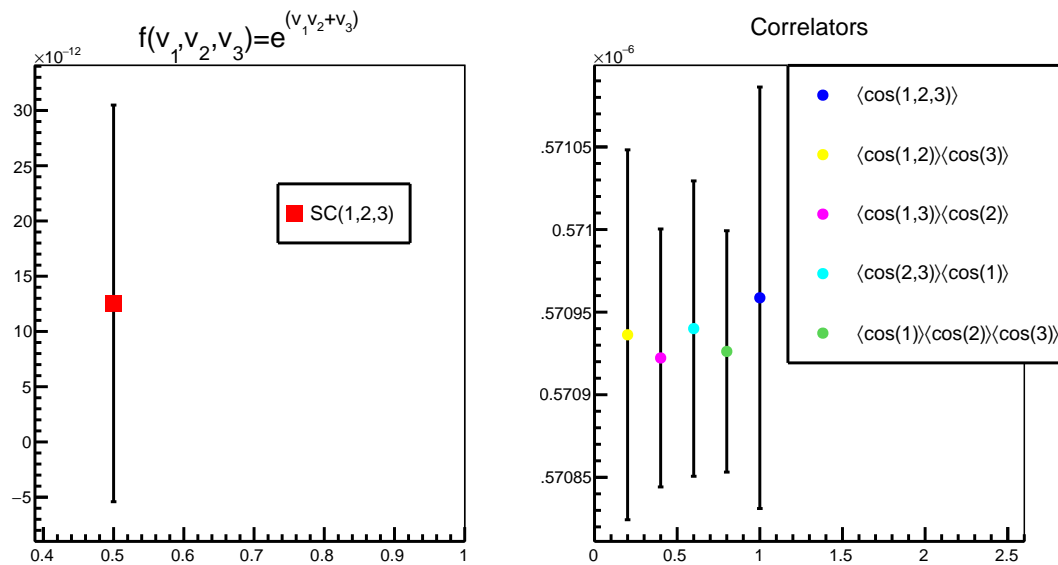


Figure 3.10: Results of generalized symmetric cumulants ($SC(1, 2, 3)$) and correlators for two correlated harmonics (v_1 and v_2).

Fluctuations of Three Correlated Harmonics

We sample the values of harmonics from the following 3D p.d.f:

$$f(v_1, v_2, v_3) \equiv e^{v_1 v_2 v_3}. \tag{3.2.3.7}$$

Such a functional dependence ensures that correlation exists among all three harmonics and $SC(k, l, m)$ is not zero. Implementation in ROOT of Eq. (3.2.3.7) goes as follows:

```
TF3 *pdf3D = new TF3("pdf3Ds", "exp(xyz)", 0.01, 0.15, 0.01, 0.15, 0.01, 0.15);
```

We have run the code over twenty one billion events with fixed multiplicity of a thousand. In Fig. (3.11), we see the results: All correlators have nonzero values and $SC(1,2,3)$ is in agreement with its theoretical result which is also a nonzero value. Theoretical value for this particular model of flow fluctuations was obtained with Mathematica

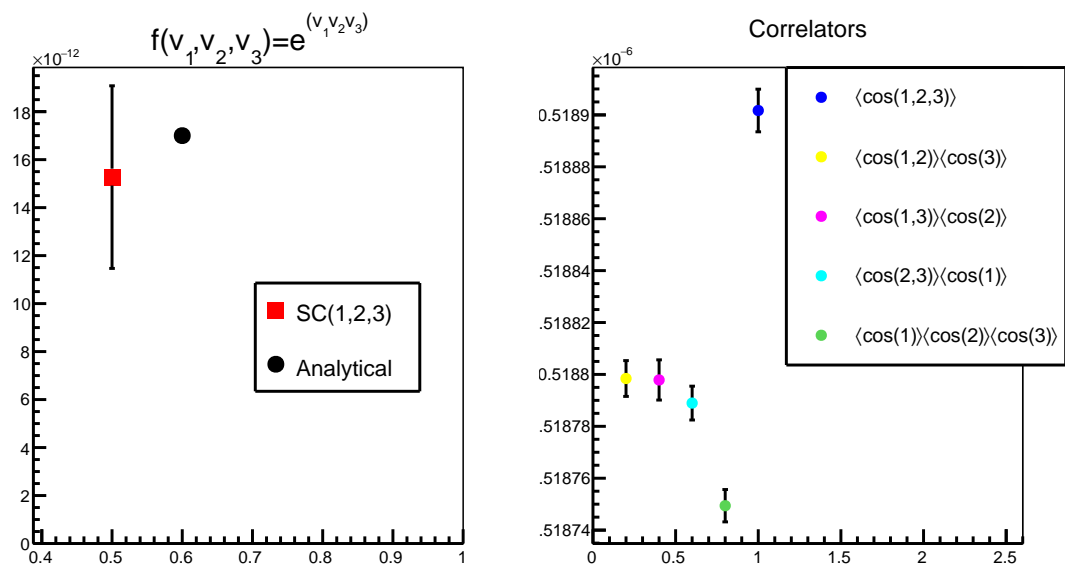


Figure 3.11: Results of generalized symmetric cumulant ($SC(1, 2, 3)$) and correlators for three correlated harmonics.

Summary

We started with characterizing distribution of outgoing particles with Fourier series and developed two and multi particle correlations techniques which do not depend on symmetry planes angle. Optimum weight functions and straight averages of two and multi particle correlations techniques are described and Monte Carlo simulations are presented. Due to nested loops which are needed to eliminate autocorrelations, techniques are not feasible; implementations of Q-vector overcome the obstacle and tremendously decreases CPU time. Two and three correlated particles contributions from non-flow are eliminated by four particle Q-cumulants and result are presented with local data set which is collected by ALICE detector in 2010 from Pb–Pb collisions at center-of-mass energy $\sqrt{s_{NN}} = 2.76 \text{ TeV}$. Fluctuations of nucleons inside the collision geometries are responsible for emerging of any type of flow harmonics and different statistics at each events which results in fluctuations of flow harmonics. As a new observable Symmetric Cumulants $SC(m, n)$ are described to investigate correlations of flow harmonics. Monte Carlo simulations of $SC(3, 2)$ and $SC(4, 2)$ are constructed; analysis task is carried out on the Worldwide LHC Computing Grid (WLCG) over all 2010 data (90 runs in total), which passed all central quality assurance criteria in ALICE, from Pb–Pb collisions at center-of-mass energy $\sqrt{s_{NN}} = 2.76 \text{ TeV}$ with momentum interval $0.2 < p_T < 5 \text{ GeV}/c$ and pseudorapidity range $|\eta| < 0.8$. Finally, SC are extended to the case of 3 different harmonics $SC(1, 2, 3)$ and presented Monte Carlo simulations meet the requirements set for generalized symmetric cumulants.

Bibliography

- [1] D. B. Lichtenberg and Simon Peter Rosen, editors. *DEVELOPMENTS IN THE QUARK THEORY OF HADRONS. VOL. 1. 1964 - 1978.* 1980.
- [2] David J Griffiths. *Introduction to elementary particles; 2nd rev. version.* Physics textbook. Wiley, New York, NY, 2008.
- [3] L. Yi. *Study of Quark Gluon Plasma By Particle Correlations in Heavy Ion Collisions.* Springer Theses. Springer New York, 2016.
- [4] E. Iancu. QCD in heavy ion collisions. *ArXiv e-prints*, May 2012.
- [5] S. Sarkar, H. Satz, and B. Sinha. *The Physics of the Quark-Gluon Plasma: Introductory Lectures.* Lecture Notes in Physics. Springer Berlin Heidelberg, 2009.
- [6] Elliptic flow of charged particles in pb-pb collisions at $\sqrt{s_{NN}} = 2.76$ TeV. *Phys. Rev. Lett.*, 105:252302, Dec 2010.
- [7] A. Bilandzic. Anisotropic flow measurements in alice at the large hadron collider. *Ph.d thesis, Utrecht University*, 2011.
- [8] Georges Aad et al. Observation of a new particle in the search for the Standard Model Higgs boson with the ATLAS detector at the LHC. *Phys. Lett.*, B716:1–29, 2012.
- [9] Serguei Chatrchyan et al. Observation of a new boson at a mass of 125 GeV with the CMS experiment at the LHC. *Phys. Lett.*, B716:30–61, 2012.
- [10] The ALICE Collaboration and K Aamodt et al. The alice experiment at the cern lhc. *Journal of Instrumentation*, 3(08):S08002, 2008.
- [11] S. Voloshin and Y. Zhang. Flow study in relativistic nuclear collisions by fourier expansion of azimuthal particle distributions. *Zeitschrift für Physik C Particles and Fields*, 70(4):665–671, 1996.
- [12] P. Danielewicz and G. Odyniec. Transverse momentum analysis of collective motion in relativistic nuclear collisions. *Physics Letters, Section B: Nuclear, Elementary Particle and High-Energy Physics*, 157(2-3):146–150, 7 1985.
- [13] Nicolas Borghini, Phuong Mai Dinh, and Jean-Yves Ollitrault. Is the analysis of flow at the cern super proton synchrotron reliable? *Phys. Rev. C*, 62:034902, Aug 2000.
- [14] Phuong Mai Dinh, Nicolas Borghini, and Jean-Yves Ollitrault. Effects of {HBT} correlations on flow measurements. *Physics Letters B*, 477(1–3):51 – 58, 2000.
- [15] N. Borghini and J.-Y. Ollitrault. Azimuthally sensitive correlations in nucleus-nucleus collisions. *Phys. Rev. C*, 70(6):064905, December 2004.

-
- [16] Nicolas Borghini, Phuong Mai Dinh, and Jean-Yves Ollitrault. Flow analysis from multiparticle azimuthal correlations. *Phys. Rev. C*, 64:054901, Sep 2001.
 - [17] Nicolas Borghini, Phuong Mai Dinh, and Jean-Yves Ollitrault. New method for measuring azimuthal distributions in nucleus-nucleus collisions. *Phys. Rev. C*, 63:054906, Apr 2001.
 - [18] Ante Bilandzic, Raimond Snellings, and Sergei Voloshin. Flow analysis with cumulants: Direct calculations. *Phys. Rev. C*, 83:044913, Apr 2011.
 - [19] Ryogo Kubo. Generalized cumulant expansion method. *Journal of the Physical Society of Japan*, 17(7):1100–1120, 1962.
 - [20] Ante Bilandzic, Christian Holm Christensen, Kristjan Gulbrandsen, Alexander Hansen, and You Zhou. Generic framework for anisotropic flow analyses with multiparticle azimuthal correlations. *Phys. Rev.*, C89(6):064904, 2014.
 - [21] Jaroslav Adam et al. Correlated event-by-event fluctuations of flow harmonics in Pb-Pb collisions at $\sqrt{s_{NN}} = 2.76$ TeV. *Phys. Rev. Lett.*, 117:182301, 2016.

Appendices

Appendix A

Four Particle Average Decomposition

Where x_1, x_2, x_3 and x_4 are variables, average of their multiplication is decomposed in terms of cumulants as

$$\begin{aligned}
\langle x_1 x_2 x_3 x_4 \rangle &= \langle x_1 \rangle \langle x_2 \rangle \langle x_3 \rangle \langle x_4 \rangle + \langle x_1 x_2 \rangle_c \langle x_3 x_4 \rangle_c + \langle x_1 x_3 \rangle_c \langle x_2 x_4 \rangle_c \\
&+ \langle x_1 x_4 \rangle_c \langle x_2 x_3 \rangle_c + \langle x_1 \rangle \langle x_2 \rangle \langle x_3 x_4 \rangle_c + \langle x_1 \rangle \langle x_3 \rangle \langle x_2 x_4 \rangle_c \\
&+ \langle x_1 \rangle \langle x_4 \rangle \langle x_2 x_3 \rangle_c + \langle x_2 \rangle \langle x_3 \rangle \langle x_1 x_4 \rangle_c + \langle x_2 \rangle \langle x_4 \rangle \langle x_1 x_3 \rangle_c \\
&+ \langle x_3 \rangle \langle x_4 \rangle \langle x_1 x_2 \rangle_c + \langle x_1 x_2 x_3 \rangle_c \langle x_4 \rangle + \langle x_1 x_2 x_4 \rangle_c \langle x_3 \rangle \\
&+ \langle x_1 x_3 x_4 \rangle_c \langle x_2 \rangle + \langle x_2 x_3 x_4 \rangle_c \langle x_1 \rangle + \langle x_1 x_2 x_3 x_4 \rangle_c. \tag{A.0.3.1}
\end{aligned}$$

Now we set the variables x_1, x_2, x_3, x_4 to $e^{in(\varphi_1 - \Psi_n)}, e^{in(\varphi_2 - \Psi_n)}, e^{-in(\varphi_3 - \Psi_n)}$ and $e^{-in(\varphi_4 - \Psi_n)}$, respectively. All non-isotropic terms vanish and previous decomposition turns into

$$\begin{aligned}
\langle e^{in(\varphi_1 + \varphi_2 - \varphi_3 - \varphi_4)} \rangle &= \langle e^{in(\varphi_1 - \Psi_n)} \rangle \langle e^{in(\varphi_2 - \Psi_n)} \rangle \langle e^{-in(\varphi_3 - \Psi_n)} \rangle \langle e^{-in(\varphi_4 - \Psi_n)} \rangle \\
&+ \langle e^{in(\varphi_1 - \varphi_3)} \rangle_c \langle e^{in(\varphi_2 - \varphi_4)} \rangle_c + \langle e^{in(\varphi_1 - \varphi_4)} \rangle_c \langle e^{in(\varphi_2 - \varphi_3)} \rangle_c \\
&+ \langle e^{in(\varphi_1 - \Psi_n)} \rangle \langle e^{-in(\varphi_3 - \Psi_n)} \rangle \langle e^{in(\varphi_2 - \varphi_4)} \rangle_c \\
&+ \langle e^{in(\varphi_1 - \Psi_n)} \rangle \langle e^{-in(\varphi_4 - \Psi_n)} \rangle \langle e^{in(\varphi_2 - \varphi_3)} \rangle_c \\
&+ \langle e^{in(\varphi_2 - \Psi_n)} \rangle \langle e^{-in(\varphi_3 - \Psi_n)} \rangle \langle e^{in(\varphi_1 - \varphi_4)} \rangle_c \\
&+ \langle e^{in(\varphi_2 - \Psi_n)} \rangle \langle e^{-in(\varphi_4 - \Psi_n)} \rangle \langle e^{in(\varphi_1 - \varphi_3)} \rangle_c \\
&+ \langle e^{in(\varphi_1 + \varphi_2 - \varphi_3 - \varphi_4)} \rangle_c. \tag{A.0.3.2}
\end{aligned}$$

In above equation first term over all event is v_n^4 , second and third terms scale as $1/m$ (both contribute to average $\frac{2}{m}$); fourth, fifth and sixth terms all together contribute $\frac{4v_n^2}{m^2}$ and the last term is four-particle cumulant, it scale as $\frac{1}{m^3}$.

Appendix B

Flow Fluctuation

We start with some basic definitions, where x is a random variable which has probability density function $f(x)$, mean value of x and its variance are expressed like in the following equations, respectively:

$$\langle x \rangle = \int_{-\infty}^{\infty} x f(x) dx. \quad (\text{B.0.3.1})$$

$$\sigma_x^2 = \int_{-\infty}^{\infty} (x - \langle x \rangle)^2 f(x) dx. \quad (\text{B.0.3.2})$$

Where $h(x)$ is a function of x , we expand it into Taylor series up to second order at $\langle x \rangle$:

$$h(x) = h(\langle x \rangle) + h'(\langle x \rangle)(x - \langle x \rangle) + \frac{h''(\langle x \rangle)}{2}(x - \langle x \rangle)^2. \quad (\text{B.0.3.3})$$

If we take the average of both sides,

$$\langle h(x) \rangle = h(\langle x \rangle) + h'(\langle x \rangle)(\langle x \rangle - \langle x \rangle) + \frac{h''(\langle x \rangle)}{2} \langle (x - \langle x \rangle)^2 \rangle. \quad (\text{B.0.3.4})$$

In above equation, second term in the right hand side of the equation is zero. Average value in the last term is variance of x . So the equation takes the final form as,

$$\langle h(x) \rangle = h(\langle x \rangle) + \frac{h''(\langle x \rangle)}{2} \sigma_x^2. \quad (\text{B.0.3.5})$$

We found out reference flow harmonics with two-particle correlation as (for the simplicity we drop the subindex n),

$$v\{2\} = \langle v^2 \rangle^{1/2}, \quad (\text{B.0.3.6})$$

variance of harmonic is written as

$$\langle v^2 \rangle = \langle v \rangle^2 + \sigma_v^2, \quad (\text{B.0.3.7})$$

by using equality ($h(v) = v^2$) in Eq. (B.0.3.5), of course we get,

$$\begin{aligned} v\{2\} &= (\langle v \rangle^2 + \sigma_v^2)^{1/2} \\ &= \langle v \rangle \left(1 + \frac{\sigma_v^2}{\langle v \rangle^2} \right)^{1/2}. \end{aligned} \quad (\text{B.0.3.8})$$

In above equation, left hand side is what we are measuring with two-particle correlation. First

argument in the right hand side is true value.

For four-particle cumulant, reference flow harmonic is

$$v\{4\} = (-\langle v \rangle^4 + 2\langle v^2 \rangle^2)^{1/4}. \quad (\text{B.0.3.9})$$

We expand the term $\langle v \rangle^4$ into Taylor series (Eq. (B.0.3.5)) and insert Eq. (B.0.3.7) into above equation like in the following way:

$$\begin{aligned} v\{4\} &= \left(-\langle v \rangle^4 + -6\sigma_v^2 \langle v \rangle^2 + 2\langle v \rangle^4 + 4\langle v \rangle^2 \sigma_v^2 + \sigma_v^4 \right)^{1/4} \\ &= \langle v \rangle \left(1 - 2\frac{\sigma_v^2}{\langle v \rangle^2} \right)^{1/4}. \end{aligned} \quad (\text{B.0.3.10})$$

Left side of the above equation is reference harmonic and it is what we are measuring compared to real value which is the first term of the right hand side of the equation.

Appendix C

Statistical Errors

For statistical uncertainty which we have utilized in Fig. (2.9), Fig. (2.3), Fig. (2.4) and Fig. (2.5) we follow the same structure in [7]. Now it will be briefly explained in this section.

If variable x is sampled from a p.d.f, its mean value μ_x and variance σ_x^2 (or $V[x]$) are expressed like below

$$\mu_x = E[x] = \int_{-\infty}^{\infty} x f(x) dx. \quad (\text{C.0.3.1})$$

$$\sigma_x^2 = V[x] = E[(x - \mu_x)^2] = \int_{-\infty}^{\infty} (x - \mu_x)^2 f(x) dx. \quad (\text{C.0.3.2})$$

We use an unbiased estimator for variance which is denoted as s_x^2 like in the following equation

$$s_x^2 = \frac{\sum_{i=1}^N w_i (x_i - \langle x \rangle)^2}{\sum_{i=1}^N w_i} \times \frac{1}{1 - \frac{\sum_{i=1}^N w_i^2}{[\sum_{i=1}^N w_i]^2}}. \quad (\text{C.0.3.3})$$

In above equation x_i is mean value of i -th event, w_i is the corresponding weight function, $\langle x \rangle$ is average over all events and N is number of events.

Results with statistical errors will be presented as

$$\langle x \rangle \pm V(\langle x \rangle). \quad (\text{C.0.3.4})$$

Variance $V(\langle x \rangle)$ can be written as

$$V(\langle x \rangle) = \frac{\sum_{i=1}^N w_{x,i}^2}{[\sum_{i=1}^N w_{x,i}]^2} \sigma_x^2. \quad (\text{C.0.3.5})$$

By using unbiased estimator of σ_x^2 in above equation as s_x^2 described in Eq. (C.0.3.3), final results will be reported as

$$\langle x \rangle \pm \frac{\sqrt{\sum_{i=1}^N w_i^2}}{\sum_{i=1}^N w_i} s_x. \quad (\text{C.0.3.6})$$

If h is a function of two variables x and y , mean value of $h(x, y)$ is to first order given by

$$\mu_h = E[h(x, y)] \approx h(\mu_x, \mu_y), \quad (\text{C.0.3.7})$$

and variance of h is to first order

$$\begin{aligned}\sigma_h^2 &= V[h] = E[h^2(x, y) - E[h(x, y)]]^2 \\ &\approx \left[\left(\frac{\partial h}{\partial x} \right) \Big|_{x=\mu_x, y=\mu_y} \right]^2 \sigma_x^2 + \left[\left(\frac{\partial h}{\partial y} \right) \Big|_{x=\mu_x, y=\mu_y} \right]^2 \sigma_y^2 \\ &\quad + 2 \left(\frac{\partial h}{\partial x} \frac{\partial h}{\partial y} \right) \Big|_{x=\mu_x, y=\mu_y} V_{xy}.\end{aligned}\quad (\text{C.0.3.8})$$

In above equation V_{xy} is the covariance of variables x and y and its unbiased estimator $Cov(x, y)$ is given by

$$Cov(x, y) = \frac{\frac{\sum w_{x,i} w_{y,i} x_i y_i}{\sum w_{x,i} w_{y,i}} - \frac{\sum w_{x,i} x_i}{\sum w_{x,i}} \frac{\sum w_{y,i} y_i}{\sum w_{y,i}}}{1 - \frac{\sum w_{x,i} w_{y,i}}{\sum w_{x,i} \sum w_{y,i}}}.\quad (\text{C.0.3.9})$$

In above equation and from now on all summations run from one to number of events. For multivariate function h final results will be reported as

$$\langle h \rangle \pm s_{\langle h \rangle} \quad (\text{C.0.3.10})$$

An unbiased estimator for $\langle h \rangle$ was given in Eq. (C.0.3.7). An unbiased estimator for the variance of $\langle h \rangle$ might be derived from Eq. (C.0.3.8) like in the following equation

$$\begin{aligned}V[\langle h \rangle] &\approx \left[\left(\frac{\partial h}{\partial x} \right) \Big|_{x=\mu_x, y=\mu_y} \right]^2 V[\langle x \rangle] + \left[\left(\frac{\partial h}{\partial y} \right) \Big|_{x=\mu_x, y=\mu_y} \right]^2 V[\langle y \rangle] \\ &\quad + 2 \left(\frac{\partial h}{\partial x} \frac{\partial h}{\partial y} \right) \Big|_{x=\mu_x, y=\mu_y} V_{\langle x \rangle \langle y \rangle}.\end{aligned}\quad (\text{C.0.3.11})$$

Due to,

$$V_{\langle x \rangle \langle y \rangle} = \frac{\sum w_{x,i} w_{y,i}}{\sum w_{x,i} \sum w_{y,i}} V_{xy} \quad (\text{C.0.3.12})$$

The unbiased estimator for $V[\langle h \rangle]$:

$$\begin{aligned}s_{\langle h \rangle}^2 &\approx \left[\left(\frac{\partial h}{\partial x} \right) \Big|_{x=\langle x \rangle, y=\langle y \rangle} \right]^2 \frac{\sum w_{x,i}^2}{[\sum w_{x,i}]^2} s_x^2 + \left[\left(\frac{\partial h}{\partial y} \right) \Big|_{x=\langle x \rangle, y=\langle y \rangle} \right]^2 \frac{\sum w_{y,i}^2}{[\sum w_{y,i}]^2} s_y^2 \\ &\quad + 2 \left(\frac{\partial h}{\partial x} \frac{\partial h}{\partial y} \right) \Big|_{x=\langle x \rangle, y=\langle y \rangle} \times \frac{\sum w_{x,i} w_{y,i}}{\sum w_{x,i} \sum w_{y,i}} Cov(x, y).\end{aligned}\quad (\text{C.0.3.13})$$

For the average multi-particle azimuthal correlations final results will be presented as

$$\begin{aligned}\langle \langle 2 \rangle \rangle &\pm \frac{\sqrt{\sum w_{\langle 2 \rangle, i}^2}}{\sum w_{\langle 2 \rangle, i}} s_{\langle 2 \rangle} \\ \langle \langle 4 \rangle \rangle &\pm \frac{\sqrt{\sum w_{\langle 4 \rangle, i}^2}}{\sum w_{\langle 4 \rangle, i}} s_{\langle 4 \rangle} \\ \langle \langle 6 \rangle \rangle &\pm \frac{\sqrt{\sum w_{\langle 6 \rangle, i}^2}}{\sum w_{\langle 6 \rangle, i}} s_{\langle 6 \rangle}.\end{aligned}\quad (\text{C.0.3.14})$$

For the reference flow harmonics final results reported like in the following form

$$\begin{aligned} \langle v_n \{2\} \rangle \pm s_{\langle v_n \{2\} \rangle} \\ \langle v_n \{4\} \rangle \pm s_{\langle v_n \{4\} \rangle} \\ \langle v_n \{6\} \rangle \pm s_{\langle v_n \{6\} \rangle}. \end{aligned} \quad (\text{C.0.3.15})$$

Two-particle estimate:

We start with

$$\langle v_n \{2\} \rangle \approx \sqrt{\langle \langle 2 \rangle \rangle}. \quad (\text{C.0.3.16})$$

For above equation, function h depends on one variable. With this restriction Eq.(C.0.3.13) turns into

$$s_{\langle v_n \{2\} \rangle} = \frac{1}{2\sqrt{\langle \langle 2 \rangle \rangle}} \frac{\sqrt{\sum w_{\langle 2 \rangle, i}^2}}{\sum w_{\langle 2 \rangle, i}} s_{\langle 2 \rangle}. \quad (\text{C.0.3.17})$$

Four-particle estimate:

We start from

$$\langle v_n \{4\} \rangle \approx \sqrt[4]{2 \cdot \langle \langle 2 \rangle \rangle^2 - \langle \langle 4 \rangle \rangle}. \quad (\text{C.0.3.18})$$

This time function h depends on two variable, from Eq.(C.0.3.13) it follows that

$$\begin{aligned} s_{\langle v_n \{4\} \rangle}^2 = \frac{1}{[2 \cdot \langle \langle 2 \rangle \rangle^2 - \langle \langle 4 \rangle \rangle]^{3/2}} \times \left[\langle \langle 2 \rangle \rangle^2 \frac{\sum w_{\langle 2 \rangle, i}^2}{[\sum w_{\langle 2 \rangle, i}]^2} s_{\langle 2 \rangle}^2 \right. \\ \left. + \frac{1}{16} \frac{\sum w_{\langle 4 \rangle, i}^2}{[\sum w_{\langle 4 \rangle, i}]^2} s_{\langle 4 \rangle}^2 - \frac{1}{2} \langle \langle 2 \rangle \rangle \frac{\sum w_{\langle 2 \rangle, i} w_{\langle 4 \rangle, i}}{\sum w_{\langle 2 \rangle, i} \sum w_{\langle 4 \rangle, j}} \text{Cov}(\langle 2 \rangle, \langle 4 \rangle) \right]. \end{aligned} \quad (\text{C.0.3.19})$$

Six-particle estimate:

We start from

$$\langle v_n \{4\} \rangle \approx 2^{-1/3} \sqrt[6]{\langle \langle 6 \rangle \rangle - 9 \cdot \langle \langle 2 \rangle \rangle \langle \langle 4 \rangle \rangle + 12 \cdot \langle \langle 2 \rangle \rangle^3}. \quad (\text{C.0.3.20})$$

The function h depends on three variables, thus we extend the Eq.(C.0.3.13) for three random variables and obtain the following equation

$$\begin{aligned} s_{\langle v_n \{6\} \rangle}^2 = \frac{1}{2 \cdot 2^{2/3} [\langle \langle 6 \rangle \rangle - 9 \cdot \langle \langle 4 \rangle \rangle \langle \langle 2 \rangle \rangle + 12 \cdot \langle \langle 2 \rangle \rangle^3]^{5/3}} \times \\ \left[\frac{9}{2} \cdot [4 \cdot \langle \langle 2 \rangle \rangle^2 - \langle \langle 4 \rangle \rangle]^2 \frac{\sum w_{\langle 2 \rangle, i}^2}{[\sum w_{\langle 2 \rangle, i}]^2} s_{\langle 2 \rangle}^2 \right. \\ + \frac{9}{2} \cdot \langle \langle 2 \rangle \rangle \frac{\sum w_{\langle 4 \rangle, i}^2}{[\sum w_{\langle 4 \rangle, i}]^2} s_{\langle 4 \rangle}^2 + \frac{1}{18} \frac{\sum w_{\langle 6 \rangle, i}^2}{[\sum w_{\langle 6 \rangle, i}]^2} s_{\langle 6 \rangle}^2 \\ - 9 \cdot [4 \cdot \langle \langle 2 \rangle \rangle^2 - \langle \langle 4 \rangle \rangle] \frac{\sum w_{\langle 2 \rangle, i} w_{\langle 4 \rangle, i}}{\sum w_{\langle 2 \rangle, i} \sum w_{\langle 4 \rangle, j}} \text{Cov}(\langle 2 \rangle, \langle 4 \rangle) \\ + [4 \cdot \langle \langle 2 \rangle \rangle^2 - \langle \langle 4 \rangle \rangle] \frac{\sum w_{\langle 2 \rangle, i} w_{\langle 6 \rangle, i}}{\sum w_{\langle 2 \rangle, i} \sum w_{\langle 6 \rangle, j}} \text{Cov}(\langle 2 \rangle, \langle 6 \rangle) \\ \left. - \langle \langle 2 \rangle \rangle \frac{\sum w_{\langle 4 \rangle, i} w_{\langle 6 \rangle, i}}{\sum w_{\langle 4 \rangle, i} \sum w_{\langle 6 \rangle, j}} \text{Cov}(\langle 4 \rangle, \langle 6 \rangle) \right]. \end{aligned} \quad (\text{C.0.3.21})$$

For the rest of the figures, error analyses are based on bootstrapping. If we denote the

variable under probe as y , the initial sample space, which is utilized to measure y , is divided into ten subsamples $\{x_1, x_2, \dots, x_{10}\}$. If the unbiased estimator of variance is s^2 , we express that as

$$s^2 = \frac{1}{9} \sum_{i=1}^{10} (x_i - \langle x \rangle)^2. \quad (\text{C.0.3.22})$$

At the end, we report the result with estimated standard error like in the following way

$$y \pm \sqrt{\frac{s^2}{10}}. \quad (\text{C.0.3.23})$$

Appendix D

Distributions

D.1 Distribution of Azimuthal Angle

In this section we show the distribution of azimuthal angle in Fig. (D.1) and Fig. (D.2). Now we ensure of having perfect detector whose azimuthal acceptance is uniform. As a result, all nonisotropic terms in equations vanish over all event average at each centrality. Results for the other centralities have been presented in Sec. (2.6.1).

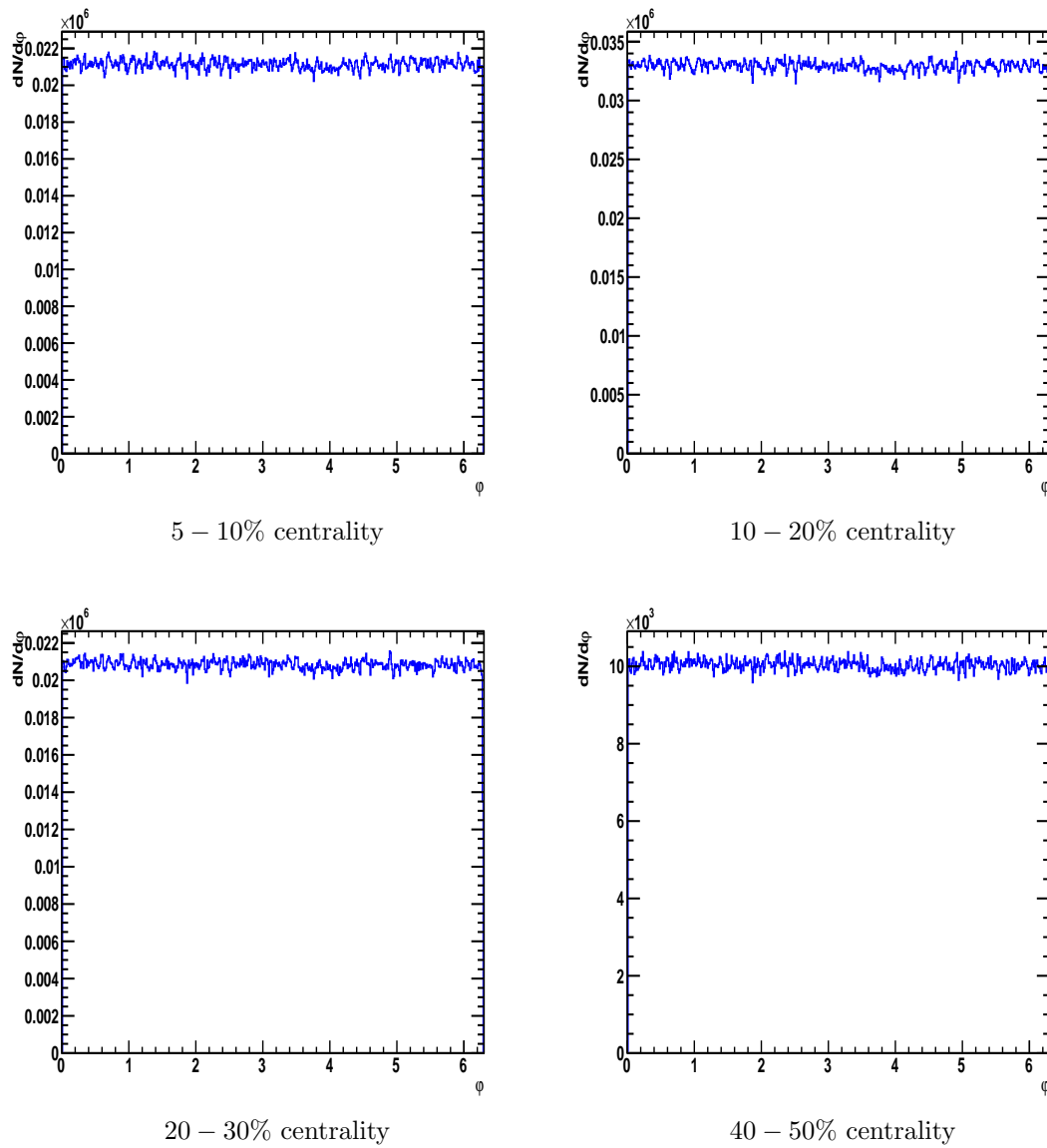


Figure D.1: Distribution of azimuthal angle φ for different centralities.

D.2 Distribution of Multiplicity

In this section, we show the distribution of multiplicity for different centralities in Fig. (D.3),(D.4) and (D.5) . The other centralities have been presented in Sec. (2.6.1).

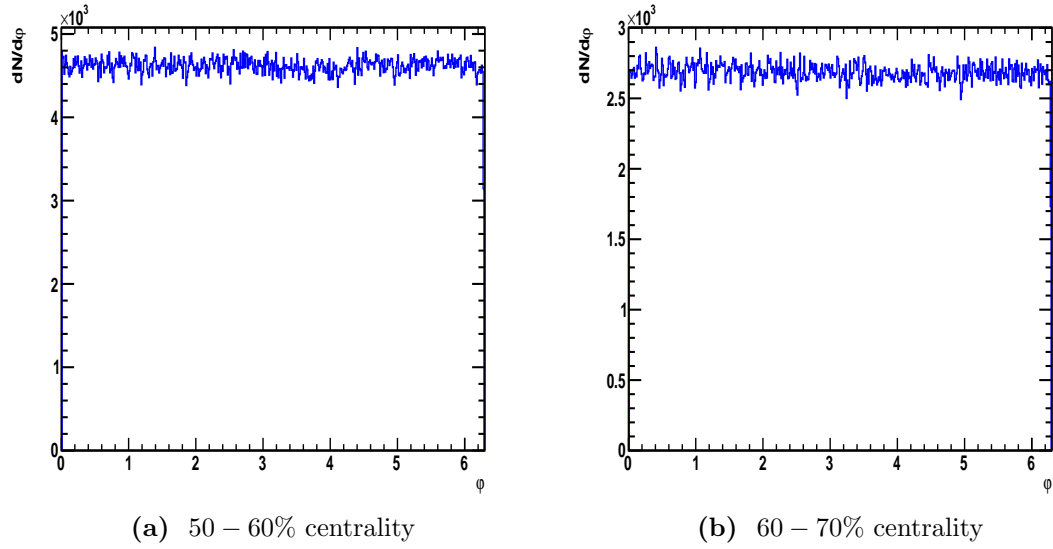


Figure D.2: Distribution of azimuthal angle φ for different centralities.

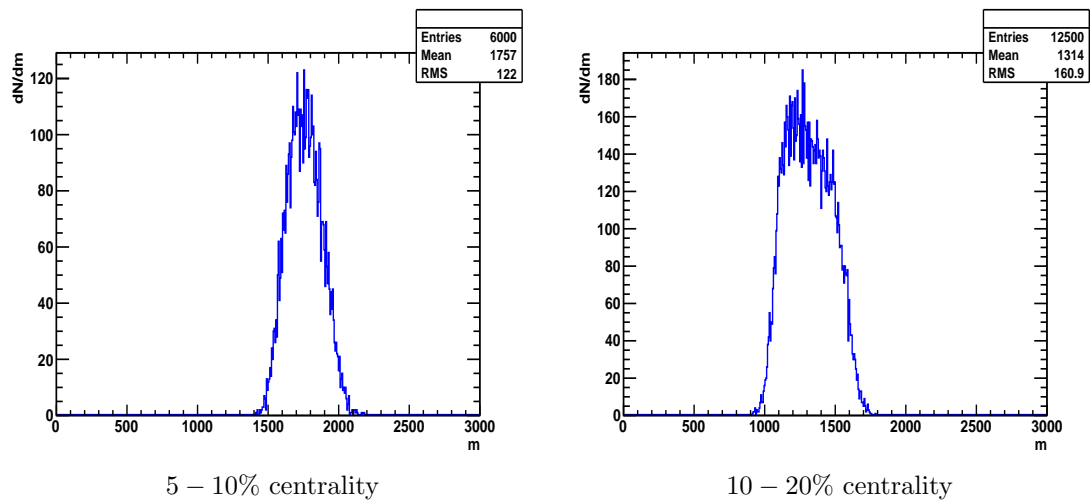


Figure D.3: Multiplicity Distribution for centralities 5-10% and 10-20%.

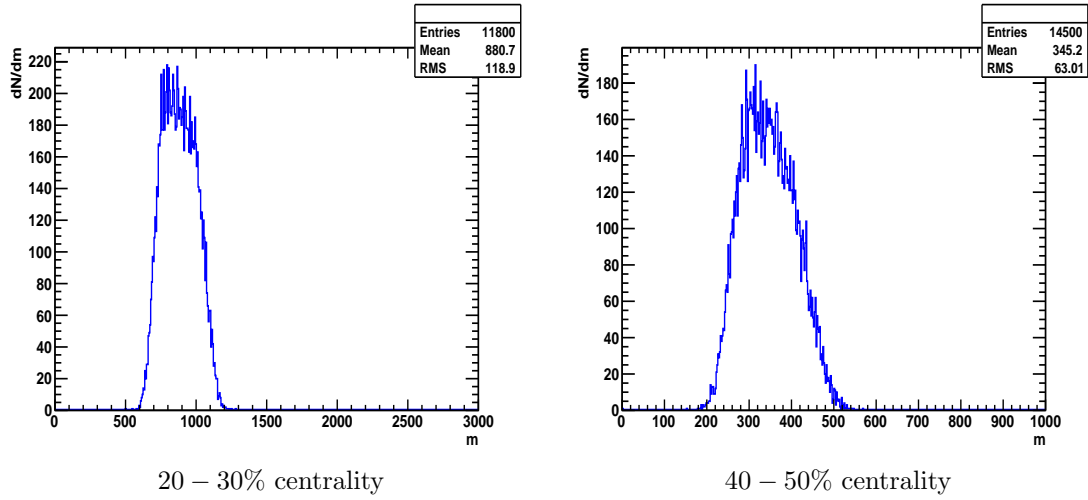


Figure D.4: Multiplicity Distribution for centralities 20-30% and 40-50%.

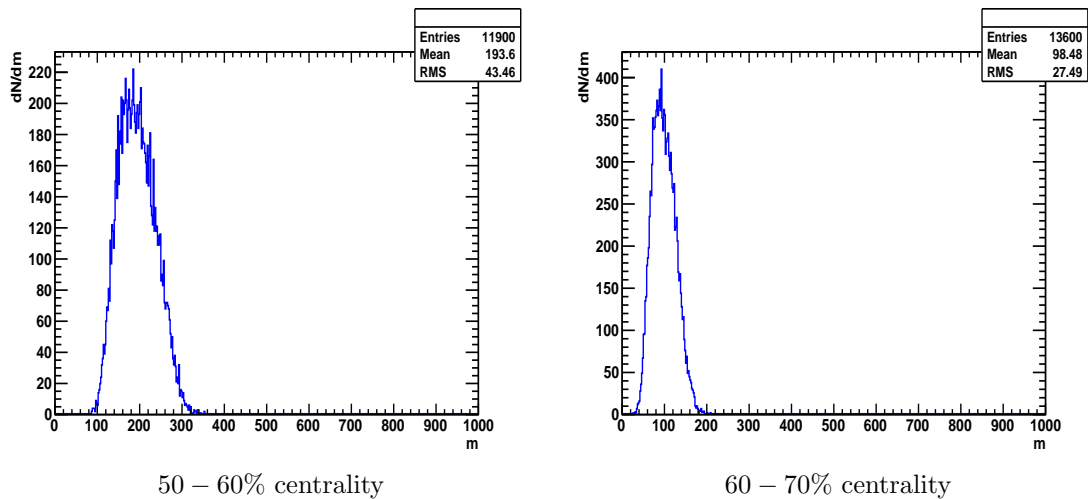


Figure D.5: Multiplicity Distribution for centralities 50-60% and 60-70%.

Appendix E

Code Snippets

In this chapter we present the code snippets of some analysis.

E.0.1 Fig. (2.9)

```
10pt


---


1 #include "Riostream.h"
2 #include <iostream>
3 #include <fstream>
4 using namespace std;
5
6 Int_t counter=0;
7 Int_t counter2=0;
8 Int_t counterb=0;
9 Int_t counter2b=0;
10
11 const Int_t num = 9;
12 Double_t centrality[num] = { 2.5, 7.5, 15.0, 25.0, 35.0, 45.0, 55.0,
    65.0, 75.0};//centrality
13 Double_t v_2[num];//referance flow harmonic v{2}
14 Double_t v_4[num];// reference flow harmonic v{4}
15 Double_t binErrorv_2[num];
16 Double_t binErrorv_4[num];
17
18 void q2_v();
19
20 void main_q2_v () {
21 gROOT->SetStyle("Plain");
22
23 TCanvas *c1 = new TCanvas("c1", "A Graph ", 700, 500);
24 c1->SetTickx(1);
25 c1->SetTicky(1);
26 c1->SetFrameLineWidth(2);
27 gStyle->SetLineWidth(2);
```

```

28
29 q2_v("/home/enes/Documents/mastertez/data2/DATA/0005");
30
31
32 TGraphErrors *gr = new TGraphErrors(num, centrality, v_2, 0, binErrorv_2
    );
33 gr->SetName("gr");
34 gr->SetMarkerColor(4);
35 gr->SetMarkerStyle(8);
36 gr->SetMarkerSize(1);
37 gr->SetLineWidth(2);
38
39 TGraphErrors *gr3 = new TGraphErrors(num, centrality, v_4, 0,
    binErrorv_4);
40 gr3->SetName("gr3");
41 gr3->SetMarkerColor(2);
42 gr3->Draw("AP");
43
44 TMultiGraph *mg = new TMultiGraph();
45 mg->Add(gr);
46 mg->Add(gr3);
47 mg->Draw("AP");
48
49 c1->Update();
50 mg->GetYaxis()->SetTitleOffset(1.2);
51 mg->GetXaxis()->SetTitle("centrality");
52 mg->GetYaxis()->SetTitle("v- $\{2\}$ ");
53
54 leg_hist = new TLegend(0.3151862, 0.1146497, 0.6848138, 0.373673);
55 leg_hist->AddEntry(gr, "two particle cumulant", "p");
56 leg_hist->AddEntry(gr3, "four particle cumulant", "p");
57 leg_hist->SetLineWidth(2);
58 leg_hist->Draw();
59
60 c1->Modified();
61 c1-> SaveAs("assignmentson.pdf");
62 }
63
64 void q2_v(const char *directory)
65 {
66
67     const char *pattern_0 = "Centrality";
68     const char *pattern_1 = ".dat";
69     Double_t sumper=0., sumpers=0., sumper4=0., sumper4s=0., a1=0., b1
        =0., wall=0., cov=0., d1=0, cov1=0, cov3=0, cov4=0;
70     TProfile *hr1 = new TProfile("hr1", "Profile ", 1, 0., 1.);
71     hr1->Sumw2();

```

```

72  hr1->SetErrorOption("s");
73  TProfile *hr2 = new TProfile("hr2","Profile2",1,0.,1.);
74  hr2->SetErrorOption("s");
75  hr2->Sumw2();
76
77  TStopwatch watch;
78  watch.Start();
79
80  TSystemDirectory *baseDir = new TSystemDirectory(".",directory);
81  TList *listOfFilesInBaseDir = baseDir->GetListOfFiles();
82  Int_t nFiles = listOfFilesInBaseDir->GetEntries();
83
84  for(Int_t iFile=0;iFile<nFiles;iFile++)
85  {
86    TSystemFile *currentFile = (TSystemFile*)listOfFilesInBaseDir->At(
      iFile);
87
88    if(!currentFile || currentFile->IsDirectory() ||
89      strcmp(currentFile->GetName(), ".") == 0 ||
90      strcmp(currentFile->GetName(), "..") == 0) {continue;}
91
92    const char* fileName = currentFile->GetName();
93    if(!(TString(fileName).Contains(pattern_0) && TString(fileName).
      Contains(pattern_1))){continue;}
94
95    const char* file = Form("%s/%s",directory,fileName);
96    cout<<Form("Accessing file: %s",file)<<endl;
97    ifstream in;
98    in.open(file);
99
100   Double_t dPhi = 0., dPt = 0., dEta = 0., c=0., per=0., c2=0., per4
      =0.; //permutation
101   string event, multiplicity;
102   Int_t eventNo = 0, M = 0;
103   Int_t eventCounter = 0;
104   TComplex q1;//q1 is q-vector.
105
106   while(1)
107   {
108     in >> event >> eventNo >> multiplicity >> M;
109     if(!in.good() && !TString(event).EqualTo("End")){cout<<"Corrupted
      line :1'("<<endl; break;}
110     if(TString(event).EqualTo("Event"))
111     {
112       if(eventCounter % 10 == 0){cout<<Form("eventNo = %d, M = %d",
      eventCounter,M)<<endl;} // Notify after each 10th event
113

```

```

114   q1 = TComplex(0.,0.);
115   q2 = TComplex(0.,0.);
116   q4 = TComplex(0.,0.);
117   q  = TComplex(0.,0.);
118
119   if ( M>3) {
120       sumper+=M*(M-1.);
121       sumpers+=pow(M*(M-1.),2);
122       sumper4+=M*(M-1.)*(M-2)*(M-3);
123       sumper4s+=pow(M*(M-1.)*(M-2)*(M-3),2);
124       wall+= M*(M-1.)*(M-2)*(M-3)*M*(M-1.);
125   for (Int_t p=1;p<=M;p++)
126   {
127       in >> dPhi >> dPt >> dEta;
128       if (!in.good()) {cout<<"Corrupted line :'"<<endl; break;}
129
130       q1 += TComplex(cos(2.*dPhi),sin(2.*dPhi)); // Q-Qumulant
131
132       q2 += TComplex(cos(2.*dPhi),sin(2.*dPhi));
133       q4 += TComplex(cos(4.*dPhi),sin(4.*dPhi));
134
135   } // for (Int_t p=1;p<=M;p++)
136   eventCounter++;
137   per=M*(M-1.);
138   c=(q1.Rho2()-M)/per;
139   hr1->Fill(0.5,c,per); //weighted 2-p correlation
140
141   per4=M*(M-1.)*(M-2)*(M-3);
142   q=q4*TComplex::Conjugate(q2)*TComplex::Conjugate(q2);
143   c2=(pow(q2.Rho2(),2) + q4.Rho2() - 2.*q.Re() - 4.*(M-2)*q2.Rho2()
        +2.*M*(M-3))/per4;
144   hr2->Fill(0.5,c2,per4);
145
146   cov1 += M*(M-1.)*(M-2)*(M-3)*M*(M-1.)*c*c2;
147   cov3 += M*(M-1.)*c;
148   cov4 += M*(M-1.)*(M-2)*(M-3)*c2;
149   }
150   } else if (TString(event).EqualTo("End")) {break;}
151 } // while(1) bir eventin bittigi yer. bitince diger evente gecer.
152
153 in.close(); // Close the external file.
154
155 }
156
157 if (hr1->GetBinContent(1))>0.){
158     v_2[counter++] = sqrt(hr1->GetBinContent(1)); // reference flow
        harmonic v{2},

```

```

159     binErrorv_2[counterb++] =(0.5/sqrt(hr1->GetBinContent(1)))*hr1->
        GetBinError(1)*sqrt(sumpers/(1.-sumpers/pow(sumper,2)))/sumper
        ;
160 }
161 else {
162     cout<<endl<<" v_2 < 0 " <<endl;
163     counter++;
164     counterb++;
165 }
166 if((-hr2->GetBinContent(1) + 2.*pow(hr1->GetBinContent(1),2))>0.){
167     v_4[counter2++] = pow(-hr2->GetBinContent(1) + 2.*pow(hr1->
        GetBinContent(1),2), 1./4);
168
169     a1 = pow(hr1->GetBinContent(1),2)*pow(hr2->GetBinError(1),2)*(
        sumpers/(1.-sumpers/pow(sumper,2)))/pow(sumper,2);
170     b1 = (1./16.)*pow(hr2->GetBinError(1),2)*(sumper4s/(1.-sumper4s/
        pow(sumper4,2)))/pow(sumper4,2);
171     cov=(cov1/wall - cov3*cov4/(sumper*sumper4))/(1.-(wall/(sumper*
        sumper4)));
172     d1 = (0.5*hr1->GetBinContent(1)*wall/(sumper*sumper4))*cov;
173
174     binErrorv_4[counter2b++] = sqrt((1/pow(2.*pow(hr1->GetBinContent
        (1),2)-hr2->GetBinContent(1), 3./2))*(a1 + b1 - d1)) ;
175 }
176 else {
177     cout<<endl<<" v_4 < 0 " <<endl;
178     counter2++;
179     counter2b++;
180 }
181
182 watch.Stop();
183 watch.Print();
184 cout<<endl;
185
186 return ;
187 }

```

E.0.2 Fig. (3.7)

```

1 #include "Riostream.h"
2 #include "AliAnalysisTaskForStudents.h"
3 #include "AliLog.h"
4 #include "AliAODEvent.h"
5 #include "AliAODInputHandler.h"
6 #include "AliAnalysisManager.h"
7 #include "AliMultSelection.h"

```

```
8 #include "TLegend.h"
9
10 using std::cout;
11 using std::endl;
12
13 ClassImp(AliAnalysisTaskForStudents)
14
15 AliAnalysisTaskForStudents::AliAnalysisTaskForStudents(const char *
    name, Bool_t useParticleWeights):
16     AliAnalysisTaskSE(name),
17     fHistList(NULL),
18     fControlHistogramsList(NULL),
19     fPtHist(NULL),
20     fNbins(1000),
21     fMinBin(0.),
22     fMaxBin(10.),
23     fCentralityHist(NULL),
24     fNCentralityBins(10),
25     fMinCentrality(0.),
26     fMaxCentrality(100.),
27     fMultHist(NULL),
28     fPhiHist(NULL),
29     fEtaHist(NULL),
30     fhf(NULL),
31     fhf2(NULL),
32     leg_hist(NULL),
33     fFinalResultsList(NULL),
34     num(0),
35     fhr2bin(0),
36     fsize(9),
37     fbignum(0),
38     fcounter1(0),
39     fcounter2(0),
40     fcounter3(0),
41     fmult(0),
42     c2(0.),
43     fhr2min(0.),
44     fhr2max(0.),
45     fper2(0.),
46     fper3(0.),
47     fper4(0.),
48     fvarb(0.),
49     fmu(0.),
50     fymin(0.),
51     fymax(0.),
52     fc4(0.),
53     fc3(0.),
```

```

54  fc22 (0.) ,
55  fc24 (0.) ,
56  fc23 (0.) ,
57  fhr2 (NULL) ,
58  fhr3 (NULL) ,
59  fhrc22 (NULL) ,
60  fhrc23 (NULL) ,
61  fhrc24 (NULL) ,
62  fhrc3 (NULL) ,
63  fhrc4 (NULL) ,
64  fgr (NULL) ,
65  fq6 (0. ,0.) ,
66  fq4 (0. ,0.) ,
67  fq (0. ,0.) ,
68  fq2 (0. ,0.) ,
69  fqq (0. ,0.) ,
70  fq5 (0. ,0.) ,
71  fq3 (0. ,0.) ,
72  fq1 (0. ,0.) ,
73  fq3x (0. ,0.) ,
74  fqq3 (0. ,0.)
75  {
76
77  AliDebug (2, "AliAnalysisTaskForStudents :: AliAnalysisTaskForStudents
      (const char *name, Bool_t useParticleWeights)");
78
79  fHistList = new TList ();
80  fHistList ->SetName ("outputStudentAnalysis");
81  fHistList ->SetOwner (kTRUE);
82  this ->InitializeArrays ();
83  DefineOutput (1, TList :: Class ());
84
85  if (useParticleWeights)
86  {
87  }
88
89 } // AliAnalysisTaskForStudents :: AliAnalysisTaskForStudents (const
      char *name, Bool_t useParticleWeights):
90
91 AliAnalysisTaskForStudents :: AliAnalysisTaskForStudents () :
92  AliAnalysisTaskSE (),
93  fHistList (NULL) ,
94  fControlHistogramsList (NULL) ,
95  fPtHist (NULL) ,
96  // ....
97  // the same structure are presented here
98

```

```

99  {
100  AliDebug(2,"AliAnalysisTaskForStudents::AliAnalysisTaskForStudents
      ()");
101
102  } // AliAnalysisTaskForStudents::AliAnalysisTaskForStudents():
103
104
105  AliAnalysisTaskForStudents::~~AliAnalysisTaskForStudents()
106  {
107
108  if(fHistList) delete fHistList;
109
110  } // AliAnalysisTaskForStudents::~~AliAnalysisTaskForStudents()
111
112  void AliAnalysisTaskForStudents::UserCreateOutputObjects()
113  {
114
115  Bool_t oldHistAddStatus = TH1::AddDirectoryStatus();
116  TH1::AddDirectory(kFALSE);
117  this->BookAndNestAllLists();
118  this->BookControlHistograms();
119  this->BookFinalResultsHistograms();
120  TH1::AddDirectory(oldHistAddStatus);
121  PostData(1,fHistList);
122
123  } // void AliAnalysisTaskForStudents::UserCreateOutputObjects()
124
125  void AliAnalysisTaskForStudents::UserExec(Option_t *)
126  {
127  Int_t im=0, jm=0;
128
129  fq6 = TComplex(0.,0.);
130  fq4 = TComplex(0.,0.);
131  fq2 = TComplex(0.,0.);
132  fq5 = TComplex(0.,0.);
133  fq3 = TComplex(0.,0.);
134  fq1 = TComplex(0.,0.);
135
136  AliAODEvent *aAOD = dynamic_cast<AliAODEvent*>(InputEvent()); //
      from TaskSE
137  if(!aAOD){return;}
138  AliMultSelection *ams = (AliMultSelection*)aAOD->FindListObject("
      MultSelection");
139  if(!ams){return;}
140  if(ams->GetMultiplicityPercentile("VOM") >= fMinCentrality && ams->
      GetMultiplicityPercentile("VOM") < fMaxCentrality)
141  {

```

```

142   fCentralityHist->Fill(ams->GetMultiplicityPercentile("V0M"));
143   }
144   else
145   {
146     return; // this event do not belong to the centrality class
              // specified for this particular analysis
147   }
148
149   Int_t nTracks = aAOD->GetNumberOfTracks(); // number of all tracks
              // in current event
150   for(Int_t iTrack=0;iTrack<nTracks;iTrack++) // starting a loop over
              // all tracks
151   {
152     AliAODTrack *aTrack = dynamic_cast<AliAODTrack*>(aAOD->GetTrack(
              iTrack)); // getting a pointer to a track
153     if(!aTrack){continue;} // protection against NULL pointers
154     if(!aTrack->TestFilterBit(128)){continue;} // filter bit 128
              // denotes TPC-only tracks, use only them for the analysis
155
156     Double_t e = aTrack->E(); // energy
157     Double_t phi = aTrack->Phi(); // azimuthal angle
158     Double_t eta = aTrack->Eta(); // pseudorapidity
159     Double_t pt = aTrack->Pt(); // Pt
160
161     if ( (-0.8 < eta) && (eta < 0.8) && (0.2 < pt) && (pt < 5.0) ) {
162
163         fq2 += TComplex(cos(2.*phi), sin(2.*phi));
164         fq4 += TComplex(cos(4.*phi), sin(4.*phi));
165         fq6 += TComplex(cos(6.*phi), sin(6.*phi));
166         fq1 += TComplex(cos(phi), sin(phi));
167         fq3 += TComplex(cos(3.*phi), sin(3.*phi));
168         fq5 += TComplex(cos(5.*phi), sin(5.*phi));
169         im++;
170         fPtHist->Fill(pt);
171         fPhiHist->Fill(phi);
172         fEtaHist->Fill(eta);
173
174     } // if ( (-0.8 < eta) && (eta < 0.8) && (0.2 < pT) && (pT < 5.0)
              // )
175
176 } // for(Int_t iTrack=0;iTrack<nTracks;iTrack++) // starting a loop
              // over all tracks
177   fmult = im;
178   fMultHist->Fill(fmult);
179
180   if ( fmult > 3) {
181     fper2 = fmult*(fmult-1.);

```

```

182     fper4 = fmult*(fmult-1.)*(fmult-2.)*(fmult-3.);
183     fc22=(fq2.Rho2()-fmult)/fper2;
184     fhr2->Fill(0.1,fc22,fper2);
185     fc24=(fq4.Rho2()-fmult)/fper2;
186     fhr2->Fill(1.1,fc24,fper2);
187     fq=fq6*TComplex::Conjugate(fq2)*TComplex::Conjugate(fq4);
188     fqq=fq4*TComplex::Conjugate(fq2)*TComplex::Conjugate(fq2);
189
190     fc4=(fq2.Rho2()*fq4.Rho2() - 2.*fq.Re() - 2.*fqq.Re() + fq6.
        Rho2()+fq2.Rho2()-(fmult-4.)*(fq2.Rho2()+fq4.Rho2()+fmult
        *(fmult-6.))/fper4;
191     fhr2->Fill(2.1,fc4,fper4);
192     fc23=(fq3.Rho2()-fmult)/fper2;
193     fhr3->Fill(0.1,fc23,fper2);
194     fq3x=fq5*TComplex::Conjugate(fq2)*TComplex::Conjugate(fq3);
195     fqq3=fq3*TComplex::Conjugate(fq1)*TComplex::Conjugate(fq2);
196
197     fc3=(fq2.Rho2()*fq3.Rho2() - 2.*fq3x.Re() - 2.*fqq3.Re() + fq5
        .Rho2()+fq1.Rho2()-(fmult-4.)*(fq2.Rho2()+fq3.Rho2()+fmult
        *(fmult-6.))/fper4;
198     fhr3->Fill(0.6,fc3,fper4);
199     fbinnum = gRandom->Uniform(0,10);
200     fhrc22->Fill(fbinnum,fc22,fper2);
201     fhrc24->Fill(fbinnum,fc24,fper2);
202     fhrc4->Fill(fbinnum,fc4,fper4);
203     fhrc23->Fill(fbinnum,fc23,fper2);
204     fhrc3->Fill(fbinnum,fc3,fper4);
205     } // if ( fmult > 3)
206
207     // d) PostData:
208     PostData(1,fHistList);
209
210 } // void AliAnalysisTaskForStudents::UserExec(Option_t *)
211
212 void AliAnalysisTaskForStudents::Terminate(Option_t *)
213 {
214     Double_t varb4=0., mu4=0., varb3=0., mu3=0., sc42=0., sc32=0.;
215     sc42 = fhr2->GetBinContent(3)-fhr2->GetBinContent(1)*fhr2->
        GetBinContent(2);
216     sc32 = fhr3->GetBinContent(2)-fhr2->GetBinContent(1)*fhr3->
        GetBinContent(1);
217     fhf->SetBinContent(1,sc32);
218     fhf->SetBinContent(2,sc42);
219
220     for (Int_t i=1;i<11;i++) { mu4 +=fhrc4->GetBinContent(i)-fhrc24->
        GetBinContent(i)*fhrc22->GetBinContent(i); }
221     for (Int_t s=1;s<11;s++) {

```

```

222     varb4+= pow(fhrc4->GetBinContent(s)-fhrc24->GetBinContent(s)*
                fhrc22->GetBinContent(s) - mu4/10.,2);
223     }
224     fhf->SetBinError(2, sqrt(varb4/90.));
225
226     for (Int_t i=1;i<11;i++) { mu3 +=fhrc3->GetBinContent(i)-fhrc23->
                GetBinContent(i)*fhrc22->GetBinContent(i); }
227     for (Int_t s=1;s<11;s++) {
228         varb3+= pow(fhrc3->GetBinContent(s)-fhrc23->GetBinContent(s)*
                fhrc22->GetBinContent(s) - mu3/10.,2);
229     }
230     fhf->SetBinError(1, sqrt(varb3/90.));
231     fHistList = (TList*)GetOutputData(1);
232     if(!fHistList){exit(1);}
233
234     TFile *f = new TFile("AnalysisResultsSC.root","RECREATE");
235     fHistList->Write(fHistList->GetName(),TObject::kSingleKey);
236     delete f;
237 } // end of void AliAnalysisTaskForStudents::Terminate(Option_t *)
238
239 void AliAnalysisTaskForStudents::InitializeArrays()
240 {
241     for(Int_t i=0;i<9;i++)
242     {
243         fsc4[i] = 0.;
244         fcentral[i] = 0.;
245         fyerr[i] = 0.;
246     }
247
248 } // void AliAnalysisTaskForStudents::InitializeArrays()
249
250 void AliAnalysisTaskForStudents::BookAndNestAllLists()
251 {
252
253     TString sMethodName = "void AliAnalysisTaskForStudents::
                BookAndNestAllLists()";
254     if(!fHistList){Fatal(sMethodName.Data(),"fHistList is NULL");}
255     fControlHistogramsList = new TList();
256     fControlHistogramsList->SetName("ControlHistograms");
257     fControlHistogramsList->SetOwner(kTRUE);
258     fHistList->Add(fControlHistogramsList);
259     fFinalResultsList = new TList();
260     fFinalResultsList->SetName("FinalResults");
261     fFinalResultsList->SetOwner(kTRUE);
262     fHistList->Add(fFinalResultsList);
263
264 } // void AliAnalysisTaskForStudents::BookAndNestAllLists()

```

```

265
266 void AliAnalysisTaskForStudents::BookControlHistograms()
267 {
268   fPtHist = new TH1F("fPtHist","a\{t\}");
272   fControlHistogramsList->Add(fPtHist);
273
274   fCentralityHist = new TH1F("fCentralityHist","ams->
        GetMultiplicityPercentile("\VOM")",fNCentralityBins,
        fMinCentrality,fMaxCentrality);
275   fCentralityHist->SetFillColor(kBlue-10);
276   fCentralityHist->GetXaxis()->SetTitle("centrality percentile");
277   fControlHistogramsList->Add(fCentralityHist);
278   fMultHist = new TH1F("fMultHist","Multiplicity Distribution"
        ,1000,0,3000);
279   fMultHist->GetXaxis()->SetTitle("m");
280   fMultHist->SetLineColor(4);
281   fControlHistogramsList->Add(fMultHist);
282
283   fPhiHist = new TH1F("fPhiHist","Phi Distribution",1000,0.,6.3);
284   fPhiHist->GetXaxis()->SetTitle("Phi");
285   fPhiHist->SetLineColor(4);
286   fControlHistogramsList->Add(fPhiHist);
287
288   fEtaHist = new TH1F("fEtaHist","Eta Distribution",1000,-1.,1.);
289   fEtaHist->GetXaxis()->SetTitle("Eta");
290   fEtaHist->SetLineColor(4);
291   fControlHistogramsList->Add(fEtaHist);
292
293   fgr = new TGraphErrors(fsize,fcentral,fsc4,0,fyerr);
294   fgr->SetName("gr");
295   fgr->SetMarkerColor(2);
296
297   fhr2 = new TProfile("fhr2","fhr2 ",3,0.,3.);
298   fhr2->Sumw2();
299   fControlHistogramsList->Add(fhr2);
300
301   fhr3 = new TProfile("fhr3","fhr3 ",2,0.,1.);
302   fhr3->Sumw2();
303   fControlHistogramsList->Add(fhr3);
304
305   fhrc22 = new TProfile("fhrc22","fhrc22 ",10,0.,10);
306   fhrc22->Sumw2();
307 // similar declerations of other TProfiles take place here

```

```

308
309 } // void AliAnalysisTaskForStudents::BookControlHistograms()
310
311 void AliAnalysisTaskForStudents::BookFinalResultsHistograms()
312 {
313
314   fhf = new TH1F("fhf","Profil ",2,0.,100);
315   fhf->GetXaxis()->SetTitle(" Centrality percentile");
316   fhf->GetYaxis()->SetTitle("SC(m,n)");
317   fhf->SetStats(0);
318   fhf->SetOption("pex0");
319
320   fFinalResultsList->Add(fhf);
321
322 } // void AliAnalysisTaskForStudents::BookFinalResultsHistograms()

```

E.0.3 Fig. (3.11)

```

1 #include "TComplex.h"
2 #include "TProfile.h"
3 #include "TStopwatch.h"
4 #include "Riostream.h"
5
6 const Int_t nParticles = 1000;
7 Double_t angles[nParticles] ;
8 Double_t weights[nParticles];
9 Bool_t bUseWeights = kFALSE;
10 const Int_t h1=1, h2=2, h3=3, h4=-1, h5=-2, h6=-3;
11
12 const Int_t sum = (h1<0?-1*h1:h1)+(h2<0?-1*h2:h2)+(h3<0?-1*h3:h3)+(
13     h4<0?-1*h4:h4)
14     + (h5<0?-1*h5:h5)+(h6<0?-1*h6:h6);
15 const Int_t maxCorrelator = 6; // We will not go beyond 8-p
16     correlations
17 const Int_t maxHarmonic = sum+1;
18 const Int_t maxPower = maxCorrelator+1;
19 TComplex Qvector[maxHarmonic][maxPower]; // All needed Q-vector
20     components
21
22 TF1 *f1 = new TF1("f1", "(1./TMath::TwoPi())*(1. + 2.*[0]*cos(x) +
23     2.*[1]*cos(2*x) + 2.*[2]*cos(3*x))", 0., TMath::TwoPi());
24 TProfile *correlations[2][maxCorrelator] = {{NULL}};
25 TProfile *hr7 = new TProfile("hr7","Profile77 ",7,0.,7.);
26 hr7->Sumw2();
27 Double_t v1,v2,v3;
28 Int_t nParticles;

```

```

25
26 void particles () {
27 v1=0.05;
28 v2=0.1;
29 v3=0.15;
30
31 f1->SetParameter(0,v1);
32 f1->SetParameter(1,v2);
33 f1->SetParameter(2,v3);
34
35 for (Int_t i=0;i<nParticles;i++) {angles[i] = f1->GetRandom();}
36 }
37 void Cosmetics()
38 {
39     for(Int_t cs=0;cs<2;cs++)
40     {
41         for(Int_t c=0;c<maxCorrelator;c++)
42         {
43
44             correlations[cs][c] = new TProfile("", "", 1, 0., 1.);
45             correlations[cs][c]->Sumw2();
46         } // end of for(Int_t c=0;c<maxCorrelator;c++)
47     } // end of for(Int_t cs=0;cs<2;cs++)
48
49 } // void Cosmetics()
50
51 void CalculateQvectors()
52 {
53     for(Int_t h=0;h<maxHarmonic;h++)
54     {
55         for(Int_t p=0;p<maxPower;p++)
56         {
57             Qvector[h][p] = TComplex(0.,0.);
58         } // for(Int_t p=0;p<maxPower;p++)
59     } // for(Int_t h=0;h<maxHarmonic;h++)
60
61     Double_t dPhi = 0.; // particle angle
62     Double_t wPhi = 1.; // particle weight
63     Double_t wPhiToPowerP = 1.; // particle weight raised to power p
64     for(Int_t i=0;i<nParticles;i++) // loop over particles
65     {
66         dPhi = angles[i];
67         if(bUseWeights){wPhi = weights[i];}
68         for(Int_t h=0;h<maxHarmonic;h++)
69         {
70             for(Int_t p=0;p<maxPower;p++)
71             {

```

```

72     if(bUseWeights){wPhiToPowerP = pow(wPhi,p);}
73     Qvector[h][p] += TComplex(wPhiToPowerP*TMath::Cos(h*dPhi),
74                               wPhiToPowerP*TMath::Sin(h*dPhi));
75 } // for(Int_t p=0;p<maxPower;p++)
76 } // for(Int_t h=0;h<maxHarmonic;h++)
77 } // for(Int_t i=0;i<nParticles;i++) // loop over particles
78 } // void CalculateQvectors()
79
80 TComplex Q(Int_t n, Int_t p)
81 {
82
83     if(n>=0){return Qvector[n][p];}
84     return TComplex::Conjugate(Qvector[-n][p]);
85
86 } // TComplex Q(Int_t n, Int_t p)
87
88 TComplex Recursion(Int_t n, Int_t* harmonic, Int_t mult = 1, Int_t
89                   skip = 0)
90 {
91     // Calculate multi-particle correlators by using recursion (an
92     // improved faster version) originally developed by
93     // Kristjan Gulbrandsen (gulbrand@nbi.dk).
94
95     Int_t nm1 = n-1;
96     TComplex c(Q(harmonic[nm1], mult));
97     if (nm1 == 0) return c;
98     c *= Recursion(nm1, harmonic);
99     if (nm1 == skip) return c;
100
101     Int_t multp1 = mult+1;
102     Int_t nm2 = n-2;
103     Int_t counter1 = 0;
104     Int_t hhold = harmonic[counter1];
105     harmonic[counter1] = harmonic[nm2];
106     harmonic[nm2] = hhold + harmonic[nm1];
107     TComplex c2(Recursion(nm1, harmonic, multp1, nm2));
108     Int_t counter2 = n-3;
109     while (counter2 >= skip) {
110         harmonic[nm2] = harmonic[counter1];
111         harmonic[counter1] = hhold;
112         ++counter1;
113         hhold = harmonic[counter1];
114         harmonic[counter1] = harmonic[nm2];
115         harmonic[nm2] = hhold + harmonic[nm1];
116         c2 += Recursion(nm1, harmonic, multp1, counter2);
117         --counter2;

```

```

116     }
117     harmonic[nm2] = harmonic[counter1];
118     harmonic[counter1] = hhold;
119
120     if (mult == 1) return c-c2;
121     return c-Double_t(mult)*c2;
122
123 } // TComplex AliFlowAnalysisWithMultiparticleCorrelations::
124     Recursion(Int_t n, Int_t* harmonic, Int_t mult = 1, Int_t skip =
125     0)
126
127 TComplex Q(Int_t n, Int_t p)
128 {
129     if(n>=0){return Qvector[n][p];}
130     return TComplex::Conjugate(Qvector[-n][p]);
131 } // TComplex Q(Int_t n, Int_t p)
132
133 TComplex Two(Int_t n1, Int_t n2)
134 {
135     TComplex two = Q(n1,1)*Q(n2,1)-Q(n1+n2,2);
136     return two;
137 } // TComplex Two(Int_t n1, Int_t n2)
138
139 void scgha()
140 {
141     TStopwatch timerRecursion;
142     Double_t mu=0., varb=0., wTwoRecursion, wFourRecursion,
143     wSixRecursion, wTwo ;
144     Int_t N=10;
145
146     const Int_t nvec = 1;
147     const Int_t harmv = 2;
148     const Int_t harmvb = 4;
149     const Int_t harmvc = 6;
150     Double_t xans[nvec]={0.5}, yans[nvec], yerr[nvec], xans2[nvec
151     ]={1.}, xans3[nvec]={0.2}, xans4[nvec]={0.4}, xans5[nvec]={0.6},
152     xans6[nvec]={0.8} yans2[nvec], yerr2[nvec], yans3[nvec], yerr3[
153     nvec], yans4[nvec], yerr4[nvec], yans5[nvec], yerr5[nvec], yans6[
154     nvec], yerr6[nvec];
155     Int_t harmonics_Two_Num[harmv], harmonics_Two_Den[harmv]={0,0},
156     harmonics_Four_Num[harmvb], harmonics_Four_Den[harmvb
157     ]={0,0,0,0,0,0}, harmonics_Six_Num[harmvc], harmonics_Six_Den[

```

```

    harmvc]={0,0,0,0};
154
155 TComplex twoRecursion , fourRecursion , sixRecursion , two;
156 TProfile *hrb1 = new TProfile("hrb1","Profile1 ",10,0.,N);
157 hrb1->Sumw2();
158 TProfile *hrb2 = new TProfile("hrb2","Profile2 ",10,0.,N);
159 hrb2->Sumw2();
160 // other TProfiles are declared in the same way here.
161
162 for (Int_t ne=0;ne<N;ne++) {
163
164   particles ();
165   CalculateQvectors ();
166   timerRecursion.Start ();
167
168   harmonics_Two_Num [0] = h1; //1-1
169   harmonics_Two_Num [1] = h4;
170
171   twoRecursion = Recursion (2,harmonics_Two_Num)/Recursion (2,
        harmonics_Two_Den).Re ();
172   wTwoRecursion = Recursion (2,harmonics_Two_Den).Re ();
173   hr7->Fill (0.,twoRecursion.Re (),wTwoRecursion); // <<cos(h1*phi1+h2
        *phi2)>>
174   hrb1->Fill (ne,twoRecursion.Re (),wTwoRecursion);
175
176   harmonics_Two_Num [0] = h2; // 2-2
177   harmonics_Two_Num [1] = h5;
178
179   twoRecursion = Recursion (2,harmonics_Two_Num)/Recursion (2,
        harmonics_Two_Den).Re ();
180   wTwoRecursion = Recursion (2,harmonics_Two_Den).Re ();
181   hr7->Fill (1.,twoRecursion.Re (),wTwoRecursion); // <<cos(h1*phi1+h2*
        phi2)>>
182   hrb2->Fill (ne,twoRecursion.Re (),wTwoRecursion);
183
184   harmonics_Two_Num [0] = h3; // 3-3
185   harmonics_Two_Num [1] = h6;
186
187   twoRecursion = Recursion (2,harmonics_Two_Num)/Recursion (2,
        harmonics_Two_Den).Re ();
188   wTwoRecursion = Recursion (2,harmonics_Two_Den).Re ();
189   hr7->Fill (2.,twoRecursion.Re (),wTwoRecursion); // <<cos(h1*phi1+h2*
        phi2)>>
190   hrb3->Fill (ne,twoRecursion.Re (),wTwoRecursion);
191
192   harmonics_Four_Num [0] = h1 ; //1 2 -1 -2
193   harmonics_Four_Num [1] = h2 ;

```

```

194 harmonics_Four_Num [2] = h4 ;
195 harmonics_Four_Num [3] = h5 ;
196
197 fourRecursion = Recursion (4, harmonics_Four_Num) / Recursion (4,
    harmonics_Four_Den) . Re() ;
198 wFourRecursion = Recursion (4, harmonics_Four_Den) . Re() ;
199 hr7->Fill (3., fourRecursion . Re() , wFourRecursion) ; // <<cos(h1*phi1+
    h2*phi2+h3*phi3+h4*phi4)>>
200   hrb4->Fill (ne, fourRecursion . Re() , wFourRecursion) ;
201
202 harmonics_Four_Num [0] = h1 ; //1 3 -1 -3
203 harmonics_Four_Num [1] = h3 ;
204 harmonics_Four_Num [2] = h4 ;
205 harmonics_Four_Num [3] = h6 ;
206
207 fourRecursion = Recursion (4, harmonics_Four_Num) / Recursion (4,
    harmonics_Four_Den) . Re() ;
208 wFourRecursion = Recursion (4, harmonics_Four_Den) . Re() ;
209 hr7->Fill (4., fourRecursion . Re() , wFourRecursion) ; // <<cos(h1*phi1+
    h2*phi2+h3*phi3+h4*phi4)>>
210   hrb5->Fill (ne, fourRecursion . Re() , wFourRecursion) ;
211
212 harmonics_Four_Num [0] = h2 ; //2 3 -2 -3
213 harmonics_Four_Num [1] = h3 ;
214 harmonics_Four_Num [2] = h5 ;
215 harmonics_Four_Num [3] = h6 ;
216
217 fourRecursion = Recursion (4, harmonics_Four_Num) / Recursion (4,
    harmonics_Four_Den) . Re() ;
218 wFourRecursion = Recursion (4, harmonics_Four_Den) . Re() ;
219 hr7->Fill (5., fourRecursion . Re() , wFourRecursion) ; // <<cos(h1*phi1+
    h2*phi2+h3*phi3+h4*phi4)>>
220   hrb6->Fill (ne, fourRecursion . Re() , wFourRecursion) ;
221
222 harmonics_Six_Num [0] = h1 ; // 1 2 3 -1 -2 -3
223 harmonics_Six_Num [1] = h2 ;
224 harmonics_Six_Num [2] = h3 ;
225 harmonics_Six_Num [3] = h4 ;
226 harmonics_Six_Num [4] = h5 ;
227 harmonics_Six_Num [5] = h6 ;
228
229 sixRecursion = Recursion (6, harmonics_Six_Num) / Recursion (6,
    harmonics_Six_Den) . Re() ;
230 wSixRecursion = Recursion (6, harmonics_Six_Den) . Re() ;
231 hr7->Fill (6., sixRecursion . Re() , wSixRecursion) ; // <<cos(h1*phi1+h2*
    phi2+h3*phi3+h4*phi4+h5*phi5+h6*phi6)>>
232   hrb7->Fill (ne, sixRecursion . Re() , wSixRecursion) ;

```

```

233 }
234 yans[0] = hr7->GetBinContent(7) - hr7->GetBinContent(4)*hr7->
    GetBinContent(3) - hr7->GetBinContent(5)*hr7->GetBinContent(2) -
    hr7->GetBinContent(6)*hr7->GetBinContent(1) + 2.*hr7->
    GetBinContent(1)*hr7->GetBinContent(2)*hr7->GetBinContent(3);
235
236 for (Int_t i=1;i<11;i++) { mu +=hrb7->GetBinContent(i) - hrb4->
    GetBinContent(i)*hrb3->GetBinContent(i) - hrb5->GetBinContent(i)
    *hrb2->GetBinContent(i) - hrb6->GetBinContent(i)*hrb1->
    GetBinContent(i) + 2.*hrb1->GetBinContent(i)*hrb2->GetBinContent
    (i)*hrb3->GetBinContent(i); }
237
238 for (Int_t i=1;i<11;i++) {
239     varb+= pow(hrb7->GetBinContent(i) - hrb4->GetBinContent(i)*hrb3
    ->GetBinContent(i) - hrb5->GetBinContent(i)*hrb2->
    GetBinContent(i) - hrb6->GetBinContent(i)*hrb1->GetBinContent
    (i) + 2.*hrb1->GetBinContent(i)*hrb2->GetBinContent(i)*hrb3->
    GetBinContent(i) - mu/10.,2);
240 }
241 yerr[0]=sqrt(varb/90.);
242
243 mu=0.;
244 varb=0.;
245 yans2[0] = hr7->GetBinContent(7);
246
247 for (Int_t i=1;i<11;i++) { mu +=hrb7->GetBinContent(i) ; }
248
249 for (Int_t i=1;i<11;i++) {
250     varb+= pow(hrb7->GetBinContent(i) - mu/10.,2);
251 }
252
253 yerr2[0]=sqrt(varb/90.);
254 mu=0.;
255 varb=0.;
256 yans3[0] = hr7->GetBinContent(4)*hr7->GetBinContent(3);
257
258 for (Int_t i=1;i<11;i++) { mu += hrb4->GetBinContent(i)*hrb3->
    GetBinContent(i) ; }
259
260 for (Int_t i=1;i<11;i++) {
261     varb+= pow( hrb4->GetBinContent(i)*hrb3->GetBinContent(i) - mu
    /10.,2);
262 }
263
264 yerr3[0]=sqrt(varb/90.);
265
266 mu=0.;

```

```

267  varb=0.;
268  yans4[0] = hr7->GetBinContent(5)*hr7->GetBinContent(2);
269
270  for (Int_t i=1;i<11;i++) { mu += hrb5->GetBinContent(i)*hrb2->
    GetBinContent(i) ; }
271
272  for (Int_t i=1;i<11;i++) {
273      varb+= pow( hrb5->GetBinContent(i)*hrb2->GetBinContent(i) - mu
    /10.,2);
274  }
275
276  yerr4[0]=sqrt(varb/90.);
277
278  mu=0.;
279  varb=0.;
280  yans5[0] = hr7->GetBinContent(6)*hr7->GetBinContent(1);
281
282  for (Int_t i=1;i<11;i++) { mu += hrb6->GetBinContent(i)*hrb1->
    GetBinContent(i) ; }
283
284  for (Int_t i=1;i<11;i++) {
285      varb+= pow( hrb6->GetBinContent(i)*hrb1->GetBinContent(i) - mu
    /10.,2);
286  }
287
288  yerr5[0]=sqrt(varb/90.);
289
290  mu=0.;
291  varb=0.;
292  yans6[0] = hr7->GetBinContent(1)*hr7->GetBinContent(2)*hr7->
    GetBinContent(3);
293
294  for (Int_t i=1;i<11;i++) { mu += hrb1->GetBinContent(i)*hrb2->
    GetBinContent(i)*hrb3->GetBinContent(i) ; }
295
296  for (Int_t i=1;i<11;i++) {
297      varb+= pow( hrb1->GetBinContent(i)*hrb2->GetBinContent(i)*hrb3->
    GetBinContent(i) - mu/10.,2);
298  }
299
300  yerr6[0]=sqrt(varb/90.);
301  TCanvas *can = new TCanvas("can","A Graph",800,450);
302  can->SetTickx(1);
303  can->Divide(2,1,0.0001,0.001);
304
305  can->cd(1);
306  TGraphErrors *gr3 = new TGraphErrors(nvec,xans,yans,0,yerr);

```

```

307  gr3->SetName("gr3");
308  gr3->SetTitle("Constant Harmonics");
309  gr3->Draw();
310  leg_hist = new TLegend(0.6,0.6,0.8,0.7);
311  leg_hist->AddEntry(gr3,"SC(1,2,3)","p");
312
313  leg_hist->SetLineWidth(2);
314  leg_hist->Draw("Same");
315
316  can->cd(2);
317
318  TGraphErrors *gra = new TGraphErrors(nvec,xans3,yans3,0,yerr3);
319  gra->SetName("gra");
320  gra->SetMarkerColor(5);
321  TGraphErrors *grb = new TGraphErrors(nvec,xans4,yans4,0,yerr4);
322  grb->SetName("grb");
323  grb->SetMarkerColor(6);
324  TGraphErrors *grc = new TGraphErrors(nvec,xans5,yans5,0,yerr5);
325  grc->SetName("grc");
326  grc->SetMarkerColor(7);
327  TGraphErrors *grd = new TGraphErrors(nvec,xans6,yans6,0,yerr6);
328  grd->SetName("grd");
329  grd->SetMarkerColor(8);
330  TGraphErrors *gr = new TGraphErrors(nvec,xans2,yans2,0,yerr2);
331  gr->SetName("gr");
332  gr->SetMarkerColor(4);
333  gr->SetMarkerStyle(8);
334
335  TMultiGraph *mg = new TMultiGraph();
336  mg->Add(gr);
337  mg->Add(gra);
338  mg->Add(grb);
339  mg->Add(grc);
340  mg->Add(grd);
341  mg->SetTitle("Correlators");
342  mg->Draw("AP");
343  mg->GetXaxis()->SetLimits(0.,2.6);
344
345  TLegend *leg_hist2 = new TLegend(0.46,0.4,0.98,0.9);
346  leg_hist2->AddEntry(gr,"#LTCos(1,2,3)#GT","p");
347  leg_hist2->SetLineWidth(2);
348  leg_hist2->SetTextSize(.04);
349  leg_hist2->Draw( );
350 }

```
